

**LIBRARY
Michigan State
University**

This is to certify that the
dissertation entitled

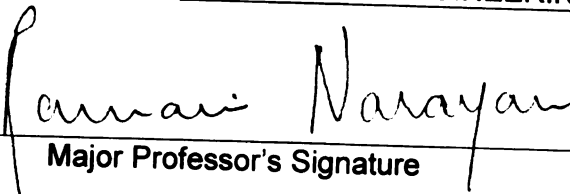
**ENGINEERED SOY OILS FOR NEW VALUE ADDED
APPLICATIONS**

presented by

PHUONG T. TRAN

has been accepted towards fulfillment
of the requirements for the

Ph.D. degree in CHEMICAL ENGINEERING


Major Professor's Signature

May 12th, 2005

Date

PLACE IN RETURN BOX to remove this checkout from your record.
TO AVOID FINES return on or before date due.
MAY BE RECALLED with earlier due date if requested.

DATE DUE	DATE DUE	DATE DUE
JUN 21 2007		

ENGINEERED SOY OILS FOR NEW VALUE ADDED APPLICATIONS

By

Phuong T. Tran

A DISSERTATION

**Submitted to
Michigan State University
in partial fulfillment of the requirements
for the degree of**

DOCTORATE IN PHILOSPOHY

Department of Chemical Engineering and Material Science

2005

ABSTRACT
ENGINEERED SOY OILS FOR NEW VALUE ADDED APPLICATIONS

By

Phuong T. Tran

Soybean oil is an abundant annually renewable resource. It is composed of triglycerides with long chain saturated and unsaturated fatty acids. The presence of unsaturated fatty acids allows for chemical modification to introduce new functionalities to soybean oil. A portfolio of chemically modified soy oil with suitable functional groups has been designed and engineered to serve as the starting material in applications such as polyamides, polyesters, polyurethanes, composites, and lubricants. Anhydride, hydroxyl, and silicone functionalities were introduced to soy oil. Anhydride functionality was introduced using a single-step free radical initiated process, and the chemically modified soy oils were evaluated for potential applications as a composite and lubricant. Hydroxyl functionalities were introduced in a single-step catalytic ozonolysis process recently developed in our labs, which proceeds rapidly and efficiently at room temperature without solvent. The transformed soy oil was used to successfully prepare bio-lubricants with good thermal/oxidative stability and bio-plastics such as polyamides, polyesters, and polyurethanes. A new class of organic-inorganic hybrid materials was prepared by curing vinyltrimethoxysilane functionalized soy oil. This hybrid material could have potential as biobased sealant through a moisture initiated room temperature cure. These new classes of soy-based materials are competitive both in cost and performance to petroleum based materials, but offer the advantage of being biobased.

ACKNOWLEDGEMENTS

I would like to first thank my advisor, Dr. Ramani Narayan, for the opportunity to work on such an interesting project both in the lab and in the business world. For giving me guidance with numerous aspects of the project, I would like to thank Dr. Daniel Graiver and Ken Farminer. For help in the lab, I would like to thank Dr. Yogaraj Nabar, Dr. Jean-Marie Raquez, Dr. Sunder Balakarishnan and Madhu Srinivasan. For their valuable comments and suggestions during the course of this work, I would like to thank my guidance committee members. I would also like to thank all of my friends in the department for helping me in the many ways that you did, especially Laura, Christina, Madhu, Sharad, Guoren, Steve, and Ty. And finally I would like to thank my family for all of the support they have provided.

TABLE OF CONTENTS

List of Tables	vii
List of Figures.....	viii
List of Abbreviations	xiii
Chapter 1: Introduction to Soybean Oil Based Feedstocks	1
1.1 BACKGROUND AND RATIONALE.....	1
1.1.1 Agricultural Based Feedstock	1
1.1.2 Carbon Cycle	1
1.1.3 Soy Oil as a Feedstock.....	2
1.1.4 Soy Oil Statistics.....	2
1.2 PROBLEM DESCRIPTION.....	5
1.2.1 Variability in Soy Oil.....	5
1.2.2 Fatty Acid Distribution in Soy Oil.....	6
1.3 SPECIFIC GOAL	6
1.4 RESEARCH OBJECTIVE	8
1.5 ORGANIZATION OF THESIS	9
Chapter 2: Maleic Anhydride Modified Soy Oil.....	10
2.1 LITERATURE REVIEW	10
2.1.1 Research on Maleic Anhydride Modified Soy Oil	10
2.2 EXPERIMENTAL PROCEDURES	15
2.2.1 Materials and Methods.....	15
2.2.2 Analysis Equipment	15
2.3 RESULTS AND DISCUSSION	16
2.3.1 Investigation of Processing Conditions	16
2.3.2 Diels-Alder Addition to Maleic Anhydride to Soy Oil.....	18
2.3.3 Characterization of Maleated Soy Oil.....	19
2.4 CONCLUSIONS.....	24
2.5 REFERENCES	25
Chapter 3: Biocomposites from Modified Soy-Oil and Biofibers.....	26
3.1 LITERATURE REVIEW	26
3.1.1 Research in Soy-based Polymers	26
3.2 EXPERIMENTAL PROCEDURES	29
3.2.1 Reagents and Equipment.....	29
3.2.2 Synthesis Methods	29
3.3 RESULTS AND DISCUSSION	33
3.3.1 Characterization of Soy-based Thermosets	33
3.3.2 Mechanical Properties of Soy-based Composites.....	35
3.3.3 Silane Surface Treatment of Biofibers.....	37
3.4 CONCLUSIONS.....	39
3.5 REFERENCES	40

Chapter 4: Ozone Mediated Polyol Synthesis	42
4.1 INTRODUCTION	42
4.1.1 Properties of Ozone.....	42
4.1.2 Ozone Generation	43
4.1.3 Ozone Chemistry	44
4.2 LITERATURE REVIEW	47
4.2.1 Methods of Polyol Preparation from Vegetable Oils.....	47
4.3 EXPERIMENTAL PROCEDURES	49
4.3.1 Materials and Methods.....	49
4.3.2 Catalytic Ozonolysis	49
4.3.3 Characterization Procedures	50
4.4 RESULTS AND DISCUSSION	51
4.4.1 Reactions with Ozone	51
4.4.2 Composition of Ozone Treated Soy Oil.....	53
4.4.3 Reactions with Heterogeneous Catalysis.....	59
4.5 CONCLUSIONS.....	63
4.6 REFERENCES	64
Chapter 5: Continuous Process for the Catalytic Ozonolysis of Soy Oil.....	65
5.1 INTRODUCTION	65
5.1.1 Soy Polyol Production	65
5.2 REACTOR DESIGN THEORY	67
5.2.1 Batch and Continuous Reactors	67
5.3 REACTOR DESIGN METHODOLOGY	69
5.3.1 Comparison of Reactors.....	69
5.4 RESULTS AND DISCUSSIONS	71
5.4.1 Processing Parameter Considerations	71
5.5 CONTINUOUS REACTOR DESIGN	77
5.5.1 Reactor Selection and Sizing	77
5.5.2 Process Scale-up	79
5.5.3 Process Economics.....	82
Chapter 6: Thermal-Oxidatively Stable Biobased Lubricants	83
6.1 LITERATURE REVIEW	83
6.1.1 Soy Oil Based Lubricants	83
6.2 EXPERIMENTAL PROCEDURES	85
6.2.1 Materials and Methods.....	85
6.2.2 Synthesis Techniques.....	85
6.2.3 Characterization Procedure	87
6.3 RESULTS AND DISCUSSION	90
6.3.1 Transformation of Double Bonds via Maleation	90
6.3.2 Transformation of Double Bonds via Catalytic Ozonolysis	92
6.3.3 Evaluation as a Biobased Lubricant.....	96
6.4 CONCLUSIONS.....	101
6.5 REFERENCES	102

Chapter 7: Silane Functionalized Soybean Oil	103
7.1 LITERATURE REVIEW	103
7.1.1 Silane Addition to Soy Oil.....	103
7.2 EXPERIMENTAL PROCEDURES.....	104
7.2.1 Materials and Methods	
7.2.2 Synthesis Techniques.....	104
7.2.3 Characterization Methods	105
7.3 RESULTS AND DISCUSSION.....	106
7.3.1 Evaluation of Processing Parameters.....	106
7.3.2 Characterization of Silane Functionalized Soy Oil.....	110
7.3.3 Room Temperature Moisture Activated Cure Studies.....	115
7.3.4 Swelling of Soybased Thermosets	116
7.4 CONCLUSIONS.....	121
7.5 REFERENCES	122
Chapter 8: Conclusions and Recommendations	123
8.1 MALEIC ANHYDRIDE FUNCTIONALIZED SOY OIL.....	123
8.2 BIOFIBER REINFORCED SOYBEAN COMPOSITES	123
8.3 SYNTHESIS OF SOY POLYOLS VIA OZONE CHEMISTRY	124
8.4 EVOLUTION SOY POLYOL PRODUCTION.....	125
8.5 SOY OIL BASE OIL LUBRICANT PROPERTIES EVALUATED	127
8.6 SILANE FUNCTIONALIZED SOY OIL.....	127
8.7 RECOMMENDATIONS.....	128
Appendix A: Verification with a Model Compound	129
Appendix B: Ozonolysis in an Alkaline Median	136
Appendix C: Scale-up Process Economics for Polyol Production	139
Appendix D: NMR of Silane Treated Soy Oil.....	141

LIST OF TABLES

Table 1.1: Fatty Acid Profile of Natural Oils	3
Table 3.1: Batch Curing Experiments in the Presence of a Base Catalyst	30
Table 3.2: Batch Curing Experiments in the Presence of a Diamine.....	30
Table 3.3: Soy-based Biofiber Reinforced Natural Composite	31
Table 4.1: Statistical Distribution of Soy Polyol	52
Table 5.1: Hydroxyl and Acid Value of Soy Polyols	74
Table 5.2: Apparent Residence Time.....	79
Table 6.1: Calculated Molecular Weight Distribution.....	93
Table 6.2: Molecular Weight Distribution for Reactions with Methanol.....	93
Table 7.1: Solubility Parameter for Various Solvents	117

LIST OF FIGURES

Figure 1.1: Natural Oilseed Production Worldwide in 2002	3
Figure 1.2: Annual Production of Soybean Oilseeds.....	4
Figure 1.3: Annual Oil Consumption of Natural Oils.....	5
Figure 1.4: Major Fatty Acid Components of Soybean Oil.....	6
Figure 1.5: Theoretical Fatty Acid Distribution of Soy Oil.....	7
Figure 2.1: 1-4 Diels-Alder Adduct	10
Figure 2.2: Peroxide Initiated Conjugation of Double Bonds	11
Figure 2.3: 1,2 Diels-Alder Addition of MA to Oleic Acid.....	12
Figure 2.4: Radical Initiated Addition of MA	12
Figure 2.5: Addition of a Second Mole of MA by a 1,4 Diels-Alder Adduct	13
Figure 2.6: Addition of a second mole of MA by a 1,2 Diels-Alder Adduct	13
Figure 2.7: Crosslinking of SO with MA.....	14
Figure 2.8: Effect of Reaction Time on Acid Value at 150°C using different MA/SO Ratio ▲0.2; ■ 0.6; and ◆ 1.1.....	16
Figure 2.9: Effect of Peroxide Concentration on Acid Value after 60 minutes at 150°C ▲No Initiator; ■ 0.005 wt%; ◆ 0.01 wt%.....	17
Figure 2.10: Change in Viscosity with Increases in MA Concentration	19
Figure 2.11: Effect of Reaction Temperature on Maleation of Soy Oil ▲ 100°C ■ 120°C ◆ 150°C	20
Figure 2.12: Temperature Profile during Maleation (A) 0 wt%, (B) 0.005 wt% and (C) 0.01 wt% L101	22
Figure 2.13: FTIR of Soybean Oil and Maleated Soybean Oil.....	23
Figure 3.1: Preparation of Soy-based Composites by Resin Transfer Molding	32
Figure 3.2: FTIR Spectra of Epoxidized and Maleated Functional Soy Oils	34

Figure 3.3: Tensile Strength of Composites Prepared by Compression Molding	36
Figure 3.4: Tensile Strength of Soy Composites after a Silane Surface Treatment of Kenaf Fibers.....	38
Figure 4.1: Generation of Ozone	42
Figure 4.2: Resonance Structure of Ozone	42
Figure 4.3: Ozone Generation by Corona Discharge.....	43
Figure 4.4: Formation of Primary Ozonide.....	45
Figure 4.5: Ozonolysis Reaction Mechanism.....	45
Figure 4.6: Ozonolysis Products of Methyl Oleate in Methanolic NaOH.....	46
Figure 4.7: Ozonolysis Reaction with a Model Compound.....	51
Figure 4.8: Catalytic Ozonolysis of Alkene with Ethylene Glycol	53
Figure 4.9: Catalytic Ozonolysis Products of Soy Oil with Ethylene Glycol.....	54
Figure 4.10: Statistical Distribution of Soy Polyols	55
Figure 4.11: Average Functionality	55
Figure 4.12: FTIR of Soy Oil (A) and Soy Polyol (B)	57
Figure 4.13: Hydroxyl Number (---) and Double Bonds (—) as a Function of Ozonolysis Time	58
Figure 4.14: Hydroxylation of Soy Oil using CaCO ₃ at Different Ozonolysis Times: (A) t=0; (B) t=0.25; (C) t=0.5; (D) t=1.0; and (E) t=2.0 min/g of soy oil	60
Figure 4.15: ¹³ C-NMR of Soy Oil.....	61
Figure 4.16: ¹³ C-NMR of Soy Polyol	62
Figure 5.1: Competing Reactions of Ozone.....	66
Figure 5.2: General Mole Balance	67
Figure 5.3: Batch Reactor Mole Balance.....	67
Figure 5.4: Batch Reactor Design Equation	67

Figure 5.5: Continuous Stirred Tank Reactor Design Equation	67
Figure 5.6: Plug Flow Reactor Design Equation	68
Figure 5.7: Ozonolysis Mole Balance.....	70
Figure 5.8: Rate of Reactant Disappearance.....	70
Figure 5.9: Rate of Product Formation	70
Figure 5.10: FTIR of Soy Polyol using Different Frit Locations	71
Figure 5.11: FTIR of Soy Polyol for Catalyst Loadings of 1 wt% & 10 wt%.....	73
Figure 5.12: FTIR of Soy Polyols using Different Particle Sizes of CaCO ₃	74
Figure 5.13: Variation of Catalyst Particle Size using a Model Compound.....	75
Figure 5.14: Sensitivity Analysis of Soy Polyol Cost	76
Figure 5.15: Reactor Design Selection	77
Figure 5.16: Continuous Production of Soy Polyol.....	78
Figure 5.17: Process Flow Diagram for Continuous Polyol Production	79
Figure 5.18: Polyol Production Downstream from Soy Oil Extraction.....	80
Figure 5.19: Ozone Injected to a Mixture of Soy Oil and Ethylene Glycol	81
Figure 5.20: Ozone Injected into Ethylene Glycol	81
Figure 5.21: Ozone Injected by Gas Sparging.....	82
Figure 6.1: Soy Oil Maleation and Esterification Apparatus.....	86
Figure 6.2: FTIR of Soybean Oil (A); Maleated Soybean Oil (B); and Esterified Maleated Soybean Oil (C)	90
Figure 6.3: Esterification of Maleated Soybean Oil with an Alcohol.....	91
Figure 6.4: Catalytic Ozonolysis of Soy Oil in the Presence of an Alcohol.....	92
Figure 6.5: Rate of Decomposition of Ozone Treated MEG350 and Soy Oil 0 min reaction (A); 10 min reaction (B); and 30 min reaction (C).....	94

Figure 6.6: Weight Loss of Ozone Treated MEG350 and Soy Oil 0 min reaction (A); 10 min reaction (B); and 30 min reaction (C).....	95
Figure 6.7: FTIR of Soy Oil (A) and Ozonized Soy Oil with Methoxy-PEG350 (B)..	96
Figure 6.8: Deposits Formation of Lubricant Sample	97
Figure 6.9: Cold Flow Properties of Lubricants	98
Figure 6.10: Failure Load for Soy-based Lubricants.....	99
Figure 6.11: Wear Plot of Esterified-Maleated Soy Oil	99
Figure 6.12: Wear Plot of Ozone Modified Soy Oil.....	100
Figure 7.1: Diels-Alder and Ene Addition Product	107
Figure 7.2: Addition of VTMS to SO at 150C with Time (A) no catalyst; (B) L101; (C) BF ₃ -methanol	108
Figure 7.3: Addition of VTMS to SO with No Catalyst for 30 minutes with Increasing Temperature	109
Figure 7.4: Double Bonds Remaining Following the Reactions of VTMS with SO at 150°C for 120 minutes (and other model compounds).....	110
Figure 7.5: FTIR of SO and VTMS Functionalized SO	111
Figure 7.6: FTIR of LA (A); LA/VTMS (B); and LA/VTMS/L101 (C).....	112
Figure 7.7: Room Temperature Cure of VTMS Functionalized Soy Oil	116
Figure 7.8: Degree of Swelling of the Soy Thermoset with Different Solvents.....	118
Figure 7.9: Thermal-Oxidative of Soy Oil and RT Cured Silated Soy Oil.....	120
Figure A1: Ozonolysis of Methyl Soyate in Triethylamine and CH ₃ OH.....	130
Figure A2: GC-MS of Methyl Soyate.....	131
Figure A3: GC-MS of Ozonolysis Products	132
Figure A4: Mass Spectra of C ₉ Ozonolysis Products	133
Figure A5: Mass Spectra of C ₉ Base Fragment	134

Figure A5: Mass Spectra of C ₆ Fragment	135
Figure B1: Formation of Primary Ozonide	136
Figure B2: Ozonolysis Reaction Mechanism	136
Figure B3: Possible Reactions of Carbonyl Oxides.....	137
Figure B4: Ozonolysis of Methyl Oleate	138
Figure B5: Ozonolysis of Methyl Oleate in the Presence of Methanolic NaOH.....	138
Figure D.1: ¹ H – NMR Spectra of Soybean Oil.....	141
Figure D2: ¹ H – NMR of Silylated Soybean Oil	142
Figure D3: ¹³ C – NMR Spectra of Silylated Soybean Oil	143
Figure D4: HMBC Correlation Spectrum of Silated Soy Oil	144

LIST OF ABBREVIATIONS

4-DMAP	4-Dimethylamino Pyridine
BF ₃	Boron Trifluoride
CD	Corona Discharge
CDCl ₃	Deuterated Chloroform
CSTR	Continuous Stirred Tank Reactor
ESO	Epoxidized Soybean Oil
FTIR	Fourier Transform Infrared Spectroscopy
HMD	Hexamethylene Diamine
L101	2,5-Bis(tert-butylperoxy)-2,5-dimethylhexane
LA	Linoleic Acid
MA	Maleic Anhydride
MMS	Maleated Methyl Soyate
M _n	Number Average Molecular Weight
MSO	Maleated Soybean Oil
M _w	Weight Average Molecular Weight
NMR	Nuclear Magnetic Resonance
OA	Oleic Acid
PFR	Plug Flow Reactor
RT	Room Temperature
RTD	Residence Time Distribution
RTM	Resin Transfer Molding
SO	Soybean Oil
SSO	Silated Soybean Oil
TAG	Triacylglycerol
UV	Ultraviolet
VTMS	Vinyltrimethoxysilane

Chapter 1: Introduction to Soybean Oil Based Feedstock

1.1 BACKGROUND AND RATIONALE

1.1.1 Agricultural Based Feedstock

A growing awareness of the environment has led to the emergence of biodegradability and/or the usage of renewable resources as being an important design criterion. Issues such as sustainability, industrial ecology, biodegradability, and recyclability are becoming major considerations in a company's product. Agricultural based chemicals are one of the most attractive alternatives because they are a sustainable source of development.

1.1.2 Carbon Cycle

As the demand for petroleum exceeds production, alternative feedstock will have to be found. In contrast to petroleum based materials, agricultural based materials are not depleted and are readily regenerated by photosynthesis. Materials based on annually renewable agricultural feedstock can form the basis for a portfolio of sustainable, eco-efficient products that is an environmentally preferable, sustainable alternative to current materials based exclusively on petroleum feedstock. The use of annually renewable biomass, as the feedstock for the production of polymers, chemicals, and fuels/lubricants can be rationalized from a global carbon cycle perspective. Carbon is present in the atmosphere as CO₂. Plants fix this carbon by photosynthesis using sunlight as the energy source. Over geological time frames (>10⁶ years) these plant materials are fossilized to provide petroleum/natural gas. These fossil resources are used to make polymers, chemicals and fuels/lubricants which release carbon back into the atmosphere as CO₂ in a short time frame of 1-10 years. The CO₂ emissions problem is a kinetic rate issue. The

rate at which biomass is converted to fossil resources is not in balance with the rate at which they are consumed and liberated ($>10^6$ years vs. 1-10 years). Alternatively, the use of annually renewable crops as feedstock maintains/balances the global carbon cycle as the rate at which CO_2 is fixed is equal to or greater than (if more biomass is planted than harvested) the rate at which it is consumed and liberated. Thus, the use of annually renewable crop feedstock to produce the polymers, chemicals, and fuels/lubricants as an adjunct to fossil resources would begin to move the rate of CO_2 release more in balance with the rate at which CO_2 is fixed.

Thus, the use of renewable crop/biomass feedstock allows for:

- Sustainable development of carbon based polymer materials
- Control and even reduce CO_2 emissions

1.1.3 Soy Oil as a Feedstock

One potential agriculture feedstock is soybean oil (SO). Soybean oil is an abundant renewable resource composed of a mixture of triglycerides consisting of glycerin and saturated and unsaturated long chain fatty acids. Some typical natural oil fatty acid compositions are presented in **Table 1.1**.

Fatty Acid	Canola	Corn	Linseed	Sunflower	Soybean
Myristic - C14:0	0.04	-	0.03	0.06	0.1
Palmitic - C16:0	4.1	10.8	5.5	5.6	11
Palmitoleic - C16:1	0.21	0.11	0.06	0.1	0.1
Margaric - C17:0	0.1	0.09	0.06	0.06	-
Stearic - C18:0	1.9	1.9	1.9	4.5	4
Oleic - C18:1	60.9	28.2	20.2	23.2	23.4
Linoleic - C18:2	21.4	57.5	16.3	64.9	51.4
Linolenic - C18:3	8.5	0.7	54.1	0.5	7.8
Arachidic - C20:0	0.6	0.3	0.12	0.3	0.3
Eicosatrienoic - C20:3	0.1	-	-	-	-
Behenic - C22:0	0.2	0.03	0.41	0.4	0.1

Table 1.1: Fatty Acid Profile of Natural Oils

1.1.3 Soy Oil Statistics

The annual production of soybean worldwide reached over 400 billion pounds in 2002 (Figure 1.1).

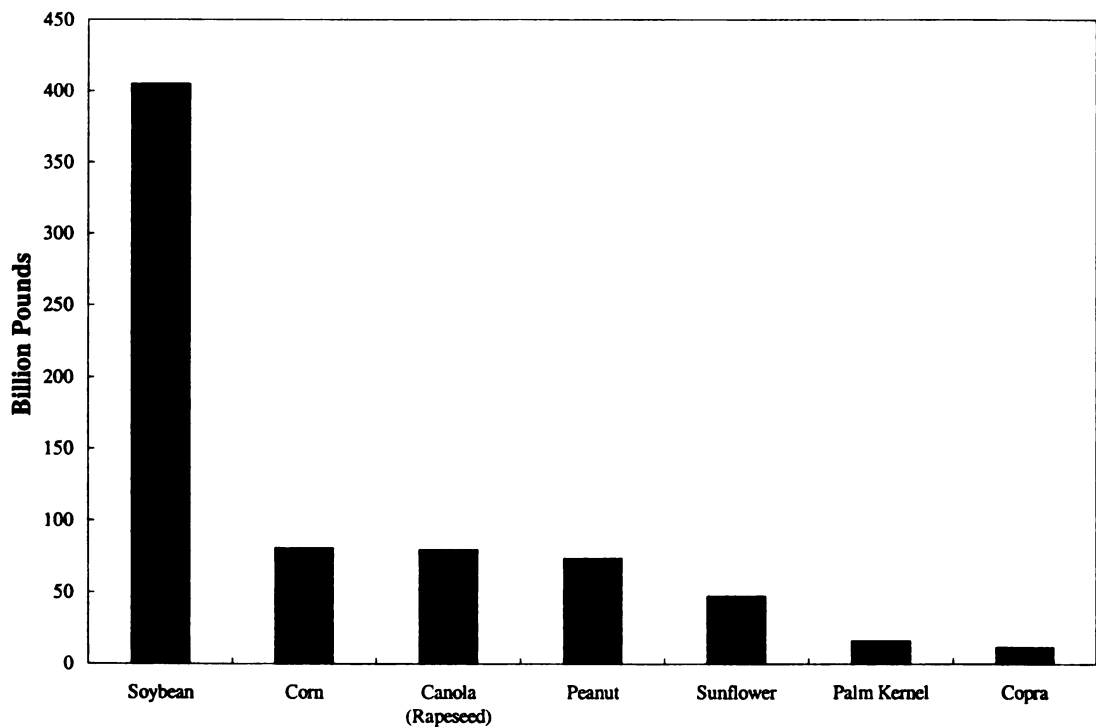


Figure 1.1: Natural Oilseed Production Worldwide in 2002

Of the annual production of soybean oilseeds, the United States is the world's largest producer as seen in **Figure 1.2**. Nearly 1/2 of the world's soybean oilseed production is by the United States.

The annual production of soybean oilseed in the United States is over 170 billion pounds. Soybean oilseeds contain about 30-35% oil by mass, amounting to about 120 billion pounds of soybean oil annually produced globally. Of the nearly 120 billions pounds, only 63 billion pounds are currently being consumed as presented in **Figure 1.3**.

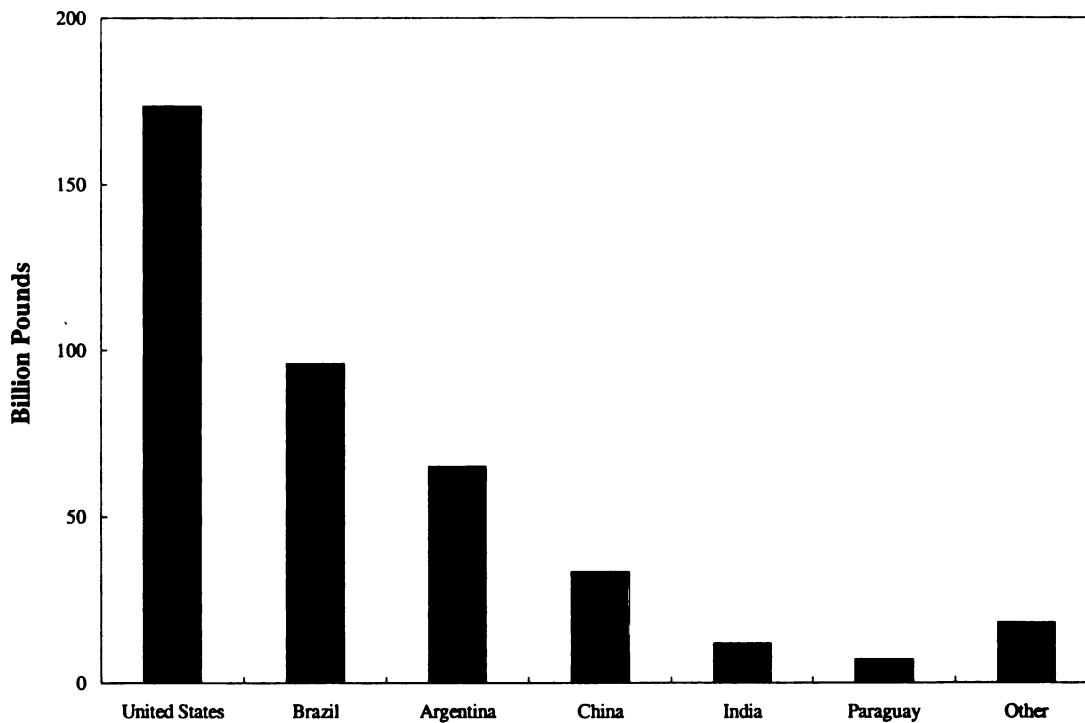


Figure 1.2: Annual Production of Soybean Oilseeds

The net result is a surplus of over 57 billion pounds of soybean oil. The most common usage of soybean oil is for edible applications such as salad/cooking oils, baking/frying fats, and margarine. These applications make up nearly 98%. Currently, only 2% of the total soybean oil usage is for application such as resins/plastics,

paints/varnishes, and fuels/lubricants. The development of new value-added applications of soy oil is beneficial both environmentally and economically.

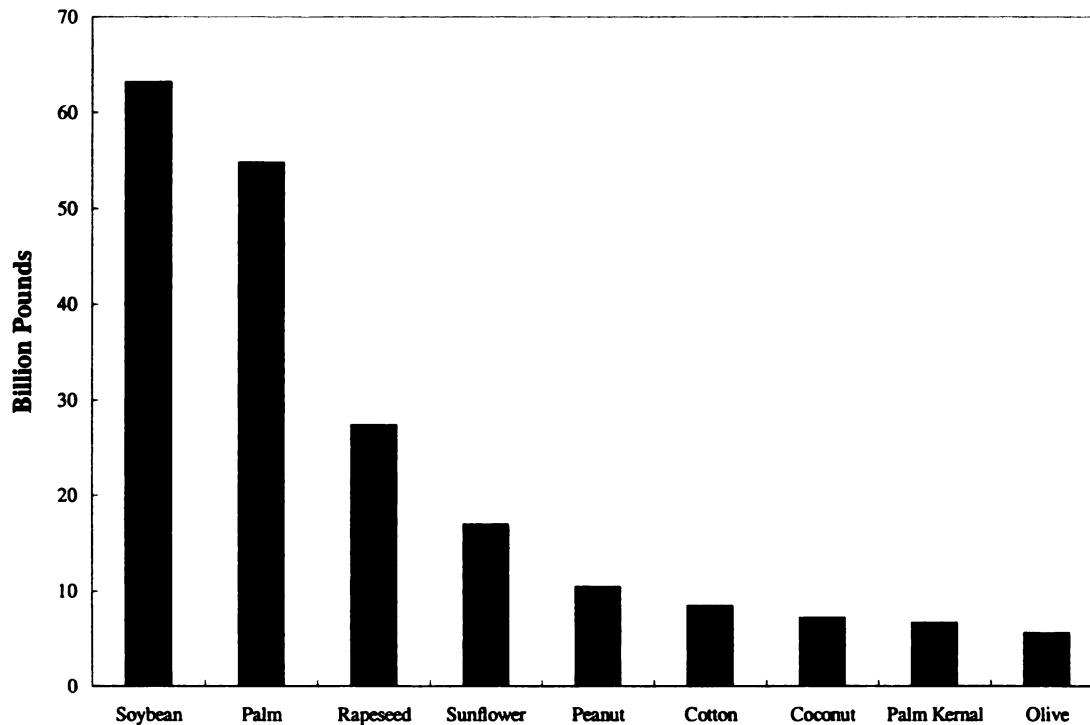


Figure 1.3: Annual Oil Consumption of Natural Oils

1.2 PROBLEM DESCRIPTION

1.2.1 Variability among Soy Oil

Soybean oil is a complex mixture of primarily fatty acids, which can vary from region-to-region and from season-to-season. Typically, soybean oil contains 4.3-4.6 “cis” double bonds per mole depending on the origin of the seed (Figure 1.4). To develop new value added applications for soy oil, chemical modification is used to incorporate reactive groups in the soy oil molecules. The presence of unsaturation allows for modifications through specific reactions with these double bonds and the introduction of reactive functional groups.

		R=	Palmitic acid (16:0) -- 11% Stearic acid (18:0) -- 4% Oleic acid (18:1, 9C) -- 23% Linoleic acid (18:2; 9C, 12C) -- 51% Linolenic acid (18:3 9C,12C,15C) -- 7%
Carbons	Common Name	IUPAC Name	Double Bonds
16	Palmitic Acid	hexadecanoic acid	0
18	Stearic Acid	octadecanoic acid	0
18	Oleic	<i>cis</i> -9-octadecenoic acid	1
18	Linoleic Acid	<i>cis,cis</i> -9,12-octadecadienoic acid	2
18	Linolenic Acid	<i>cis,cis,cis</i> -9,12,15-octadecatrienoic acid	3

Figure 1.4: Major Fatty Acid Components of Soybean Oil

1.2.2 Fatty Acid Distribution of Soy Oil

The statistical distribution of fatty acids within soy oil suggests about 71% of all triacylglycerol (TAG) species contain at least one linoleic acid chain (**Figure 1.5**). Furthermore, 25% contain only 1 linoleic acid, while 32% and 14% contain 2 and 3 linoleic acid chains, respectively. Additionally, it can be seen that 29% of the TAG species contain only 1 polyunsaturated fatty acid (linoleic or linolenic).

The successful application of soy oil as an alternative to petroleum based products depends on the cost competitiveness and end-use performance. Additionally, any proposed chemical modification must be robust enough to account for the inherent variability among soy oil.

1.3 SPECIFIC GOAL

The goal of this research is to design and engineer a portfolio of chemically modified soy oil with reactive groups that can serve as the starting material for applications such as polyesters, polyamides, polyurethanes, composites, and lubricants.

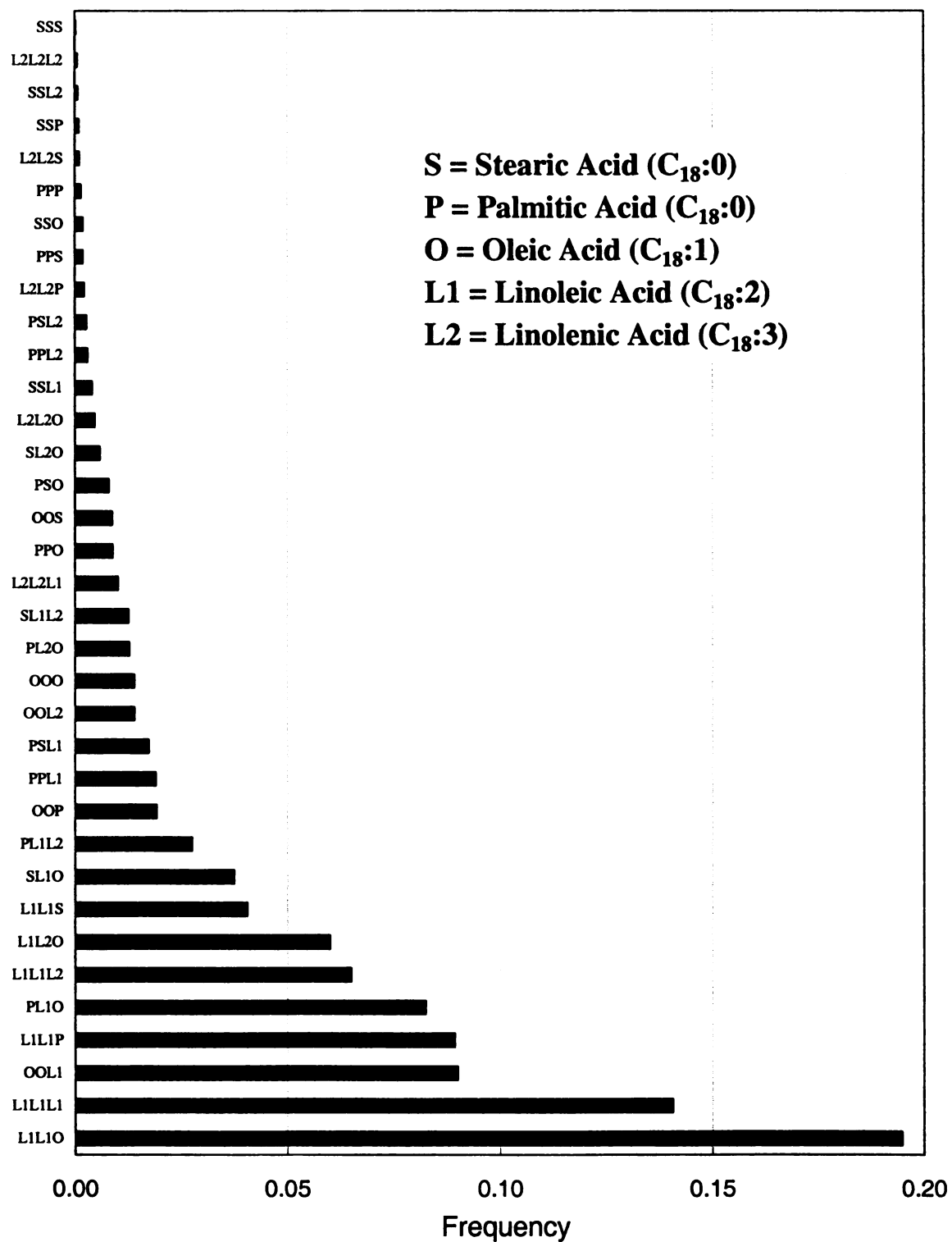


Figure 1.5: Theoretical Fatty Acid Distribution of Soy Oil

1.4 RESEARCH OBJECTIVE:

- I. Preparation of maleic anhydride functionalized soy oil
 - A. Optimizing of processing parameters (time, temperature, catalyst type, and catalyst concentration)
 1. Structural determination of maleated soy oil
 - B. Prepare a soy-based resin matrix by reacting maleated soy oil with a commercially available epoxidized soy oil
 - C. Create a structurally strong thermoset by increasing the cross-link densities by using a spacer molecule
 - D. Curing in the presence of biofibers to create an all natural composite
 1. Optimization of process parameters
 2. Enhancement of mechanical properties by a silane surface treatment of the biofibers
 - E. Develop soy-based lubricants
 1. Esterification with a series of alcohols to enhance stability
 2. Determine base oil lubricant properties
- II. Develop a process to synthesize primary soy-based polyols using ozone chemistry
 - A. Develop a novel single step catalytic ozonolysis to prepare polyols
 1. Effects of catalysts type and concentration
 2. Effects of processing parameters (time and temperature)
 3. Structural determination using model compound
 - B. Prepare rigid polyurethane foams using soy polyols
 - C. Develop soy polyols for flexible foam applications
 1. Variation of molecular architecture of soy polyol
 - a. Synthesize polyols with increased molecular weight
 - b. Prepare polyols with varying hydroxyl content
 - D. Prepare thermal-oxidatively stable lubricants
 1. Variation of molecular architecture by using different alcohols
 2. Determine base oil lubricant properties
 - E. Establish proof-of-concept for the continuous production of soy polyols
- III. Synthesize a silane functionalized soy oil
 - A. Develop a fast efficient process to functionally modify soy oil with vinyltrimethoxysilane
 1. Optimizing processing parameters (time, temperature, and catalyst type, and catalyst concentration)
 2. Structural determination of silylated soy oil
 - B. Prepare a soy-based thermoset by a moisture activated curing of the silane functionalized soy oil at room temperature
 1. Investigate effects of cure time and catalyst type on the sol-gel properties of the thermoset

1.5 ORGANIZATION OF THESIS

The thesis is divided into three main parts. The first part, Chapter 2, discusses the development of a new process to synthesize maleic anhydride functionalized soy oil, and subsequent chapters discuss applications of the maleated soy oil to prepare all-natural biofiber reinforced soybean oil based composites (Chapter 3) and as a base oil stock for a lubricant (Chapter 6).

The second part, Chapters 4 through 6, details the development of a new ozone mediated synthesis of soy polyols, which were further engineered to have varying hydroxyl functionalities and molecular weight for potential use in polyesters, polyamides, and polyurethanes. Chapter 5 discusses the development of a continuous production of the soy polyols, and Chapter 6 evaluates the lubricating properties of the ozone treated soy oil.

The third part, Chapter 7, discusses the synthesis of silane functionalized soy oil. Soy based thermosets were prepared using a room temperature moisture activated cure of this organic-inorganic hybrid.

In Chapter 8, the overall conclusions and recommendations are presented.

Chapter 2: Maleic Anhydride Modified Soy Oil

2.1 LITERATURE REVIEW:

2.1.1 Research on Maleic Anhydride Modified Soy Oil

There is a great deal of literature on functionalization of vegetable oils using maleic anhydride (MA) to enhance their reactivity. Morrel and Samuels (1) studied the reaction between maleic anhydride and conjugated oil systems using oils from china wood and oiticica containing fatty acids with conjugated double bonds. The reaction was found to follow a typical Diels-Alder addition as seen in **Figure 2.1**.

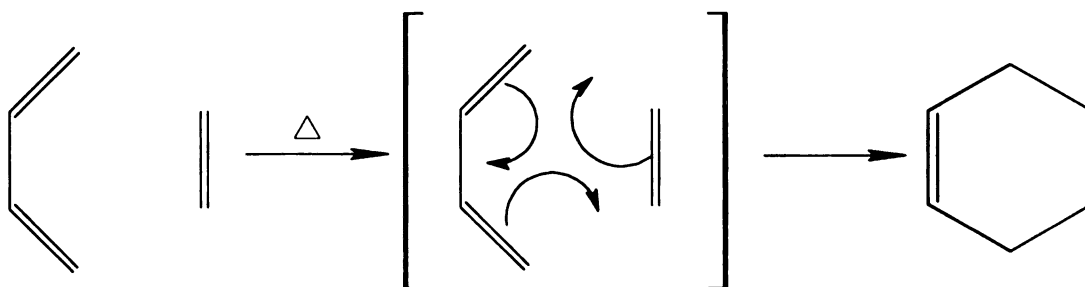


Figure 2.1: 1-4 Diels-Alder Adduct

Root (2) investigated the functionalization of soybean oil with maleic anhydride and described the use of benzoyl peroxide in the maleation reaction. He concluded that the use of benzoyl peroxide as a catalyst was advantageous as it allowed the reaction to proceed at a lower reaction temperature of 110°C as compared 160-190°C when benzoyl peroxide was not used. Root hypothesized that the presence of a peroxide leads to electron delocalization, resulting in conjugation of the double bonds within the unsaturated fatty acids in the soybean oil to form a conjugated system as shown in **Figure 2.2**. However, very little data was provided to support this claim.

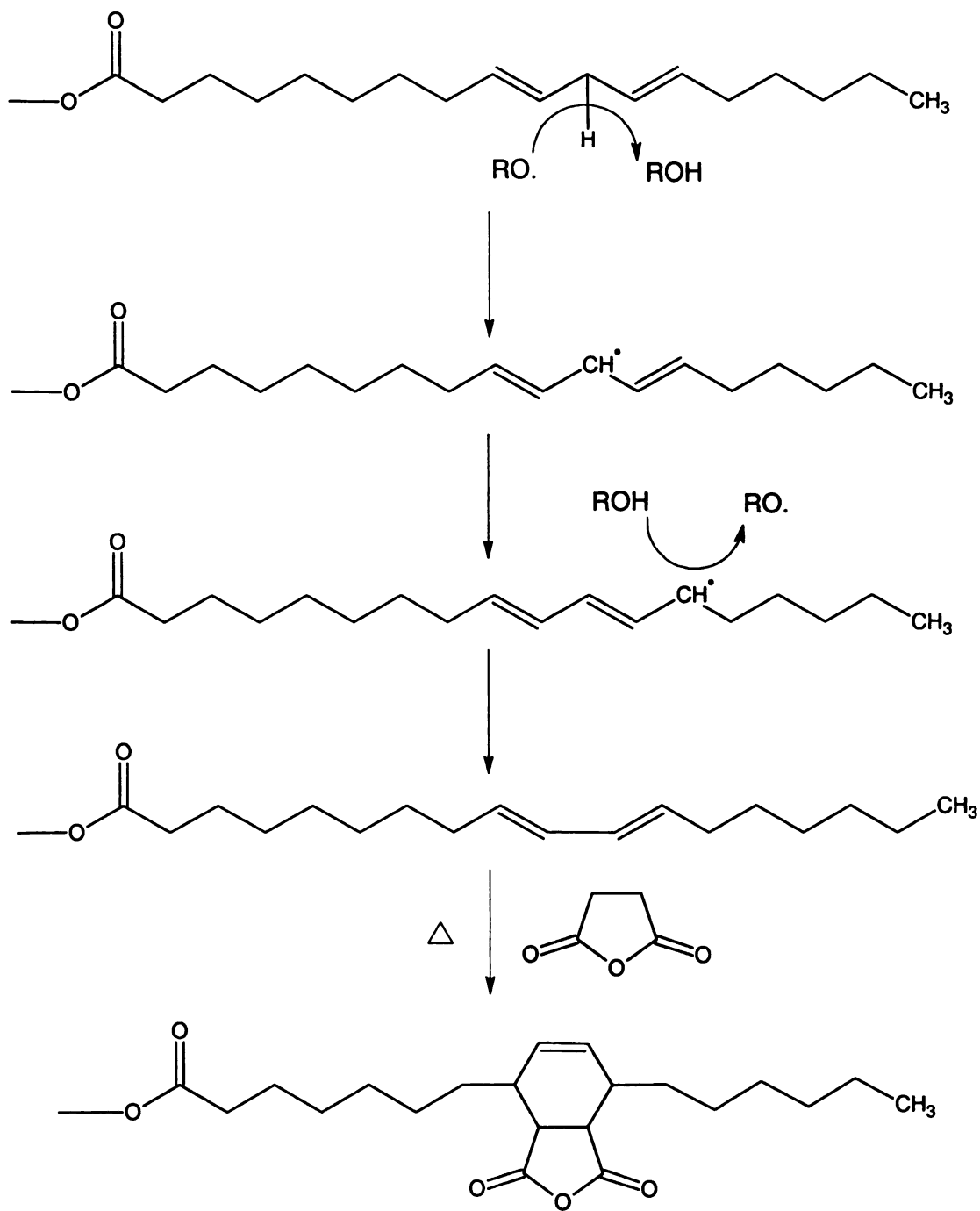


Figure 2.2: Peroxide Initiated Conjugation of Double Bonds

However, the mechanism of MA addition to soy oil and the products of this reaction are still ill defined and are the subject of a great deal of debate in the literature. Clocker (5) postulated a cyclobutane structure for oleic acid adducts (Figure 2.3).

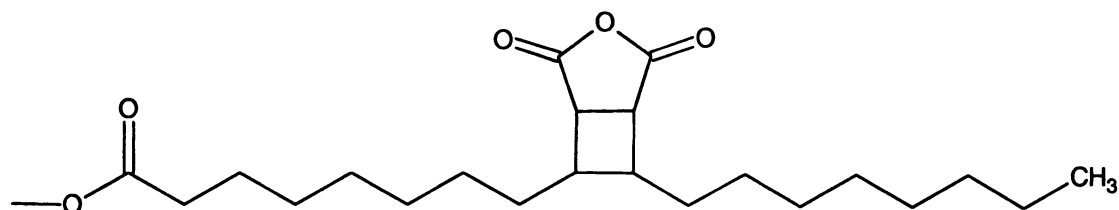
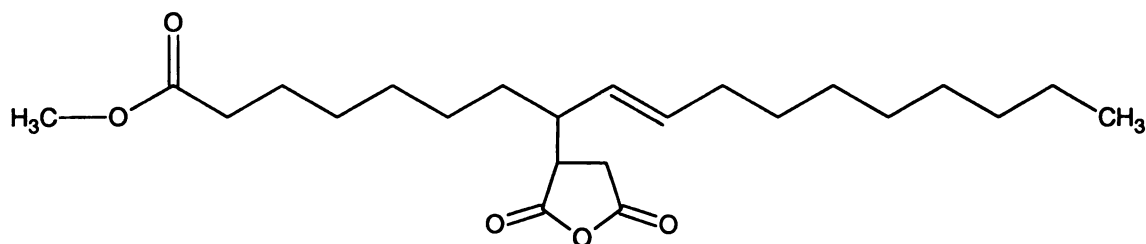
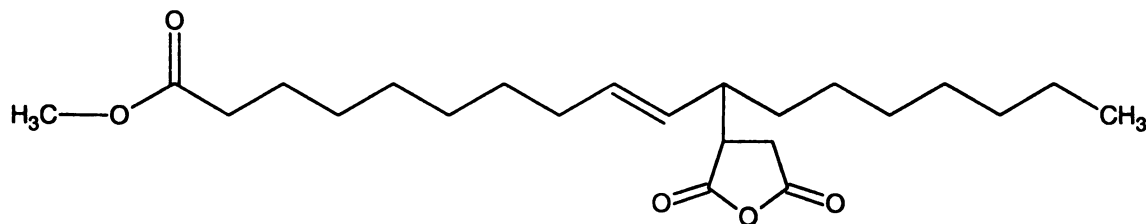


Figure 2.3: 1,2 Diels-Alder Addition of MA to Oleic Acid

Bickford and coworkers (6) studied the reaction between maleic anhydride with methyl oleate and suggested that MA was added at the eighth or eleventh carbon atom (Figure 2.4).



MA Addition to the Eighth Carbon



MA Addition to the Eleventh Carbon

Figure 2.4: Radical Initiated Addition of MA

The results of Teeter (3) and Kappelmeier (4) also support succinic type structures on the basis of model compounds studies using methyl linoleate and methyl linolenate. Accordingly, the reactions with di-unsaturated, nonconjugated double bonds proceeded by the 'ene' reaction mechanism and the succinic type addition occurs at the eighth, eleventh, and fourteenth carbon atoms, with a major addition product at the eleventh carbon. Based on these results, Kappelmeier and Van Den Nuet (5) postulated that conjugation might occur simultaneously with an attack at the methylene carbon by which a second mole of maleic anhydride can be added by a Diels-Alder addition (**Figure 2.5**).

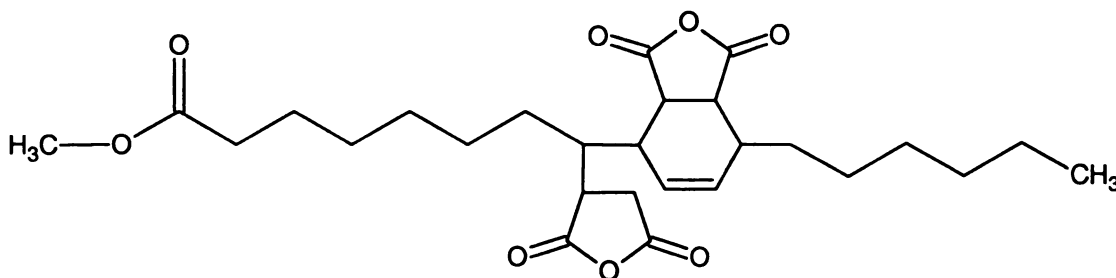


Figure 2.5: Addition of a Second Mole of MA by a 1,4 Diels-Alder Adduct

Somewhat similarly, Plimmer (6) suggested a second mole of maleic anhydride could be added to the hexene ring (**Figure 2.6**).

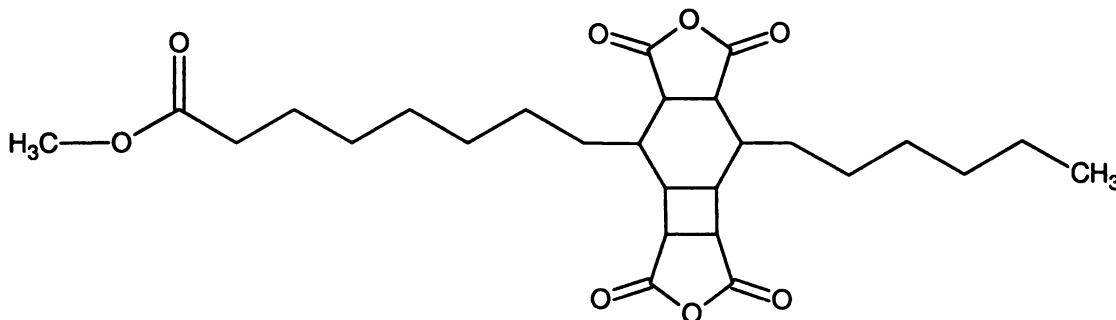


Figure 2.6: Addition of a second mole of MA by a 1,2 Diels-Alder Adduct

Nagakura and Yoshitomi (7), however, suggested the presence of free radicals leads to copolymerization of maleic anhydride with the triglyceride and based their conclusion on the increase in the viscosity of the reaction product (**Figure 2.7**).

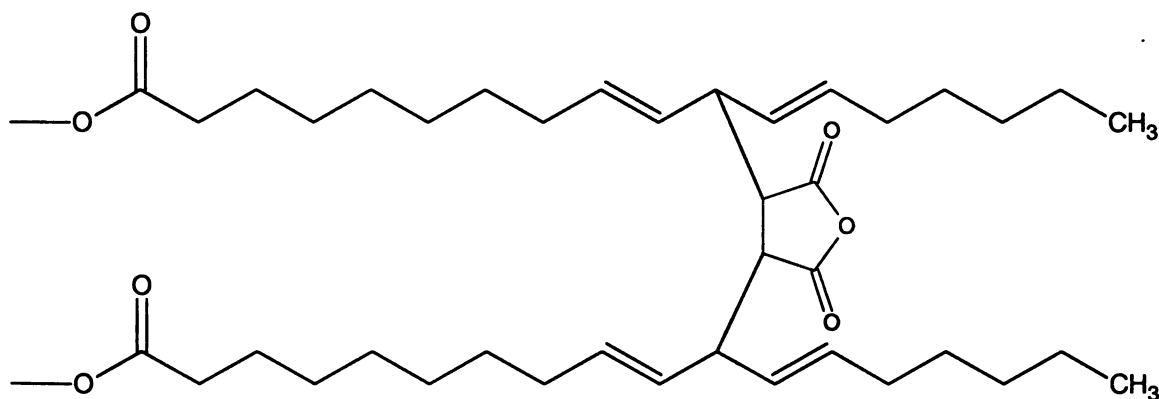


Figure 2.7: Crosslinking of SO with MA

It is apparent that although maleation of soybean oil has been reported previously, most of the work was focused on the mechanism of this reaction and almost no attention was given to process optimization of this free radical initiated reaction. It is therefore our goal in this work, is to asses the process and determines the usefulness of this reaction. Uniquely, the study will focus on maleation within a closed system under elevated temperatures and pressures. The closed system synthesis prevents premature sublimation of the MA, which was a recurring problem in the past and caused lower yields.

2.2 EXPERIMENTAL PROCEDURES:

2.2.1 *Materials and Methods*

Unhydrogenated soybean oil was purchased from Spectrum Chemicals (Gardena, CA). Maleic anhydride, octanol, isopropanol, 2,5-bis(*tert*-butylperoxy)-2,5-dimethylhexane (L101) and di-*tert*-butyl peroxide were purchased from Sigma-Aldrich (Milwaukee, WI).

Reactions were carried out by charging a 2L Parr Reactor equipped with a motorized stirrer, thermocouple, and heating element with MA, SO, and the initiator. The initial reaction time was taken at the time the reactor temperature reached a preset temperature. At the end of each reaction, the reactor was connected to a vacuum pump for 30 minutes and volatile products were collected in a solvent trap immersed in an isopropanol dry ice bath. Acid numbers were determined according to ASTM D1980 (8) and iodine number was measured by ASTM D1959 (9).

2.2.2 *Analysis Equipment*

FTIR analyses were run on a Perkin-Elmer model 1000 with a NaCl window. Viscosity measurements were done using a Brookfield Viscometer model EX100 at 25°C.

2.3 RESULTS AND DISCUSSION:

2.3.1 Investigation of Processing Conditions

The effects of reaction time, initiator concentration, and MA concentration were studied in details using two different initiators, L101 and di-*tert*-butyl peroxide. The degree of maleation was determined using acid value, and the products were further characterized using FTIR spectroscopy and iodine number.

The maleation of soybean oil in a closed system under high temperatures and pressures in the presence of peroxides proceeded relatively fast. In all cases the reaction proceeded to completion within ~30 minutes independent of the MA concentrations in the reaction mixture (MA/SO molar ratio of 0.2, 0.6, and 1.1) as shown in **Figure 2.8**.

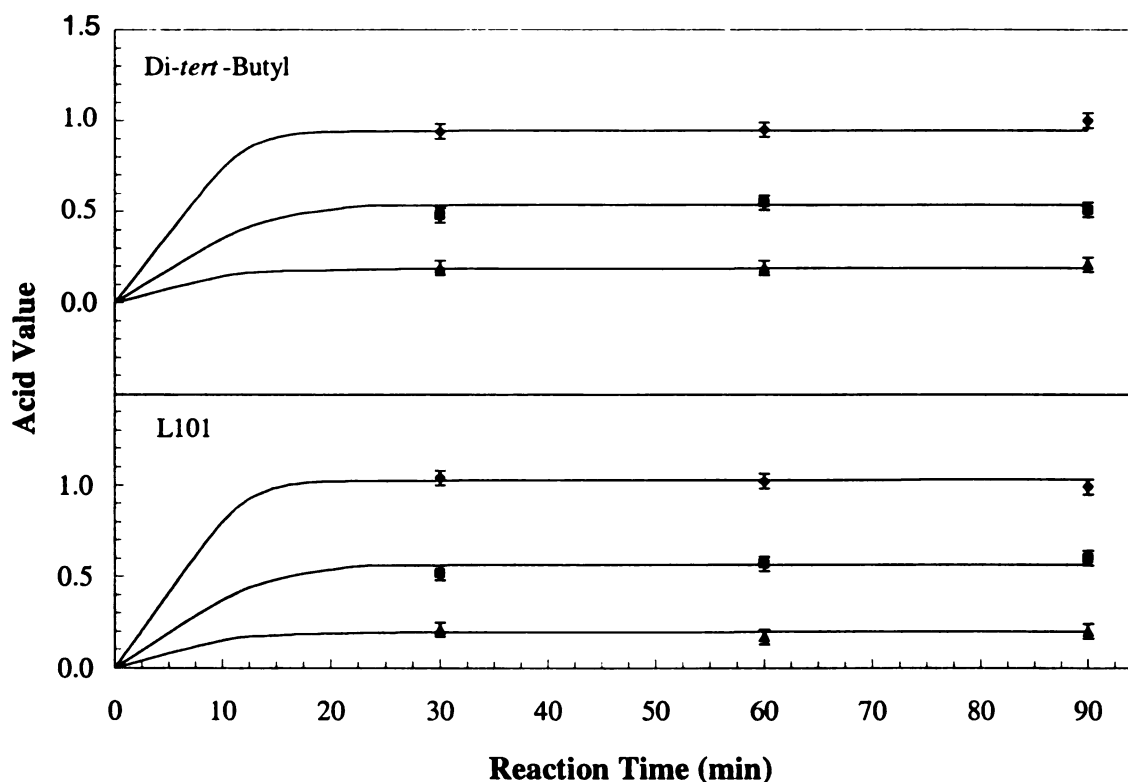


Figure 2.8: Effect of Reaction Time on Acid Value at 150°C using different MA/SO Ratio ▲0.2; ■0.6; and ◆1.1

It is further interesting to note that the type of peroxide had little effect on the progress of the reaction and essentially the same reaction rates were observed for both L101 and di-*tert*-butyl initiators. However, the presence of the initiator in the reaction mixture greatly impacted the progress of the reaction (**Figure 2.9**) and led to acid value of 1.0 compared to acid value of 0.25 when no peroxide initiator was used.

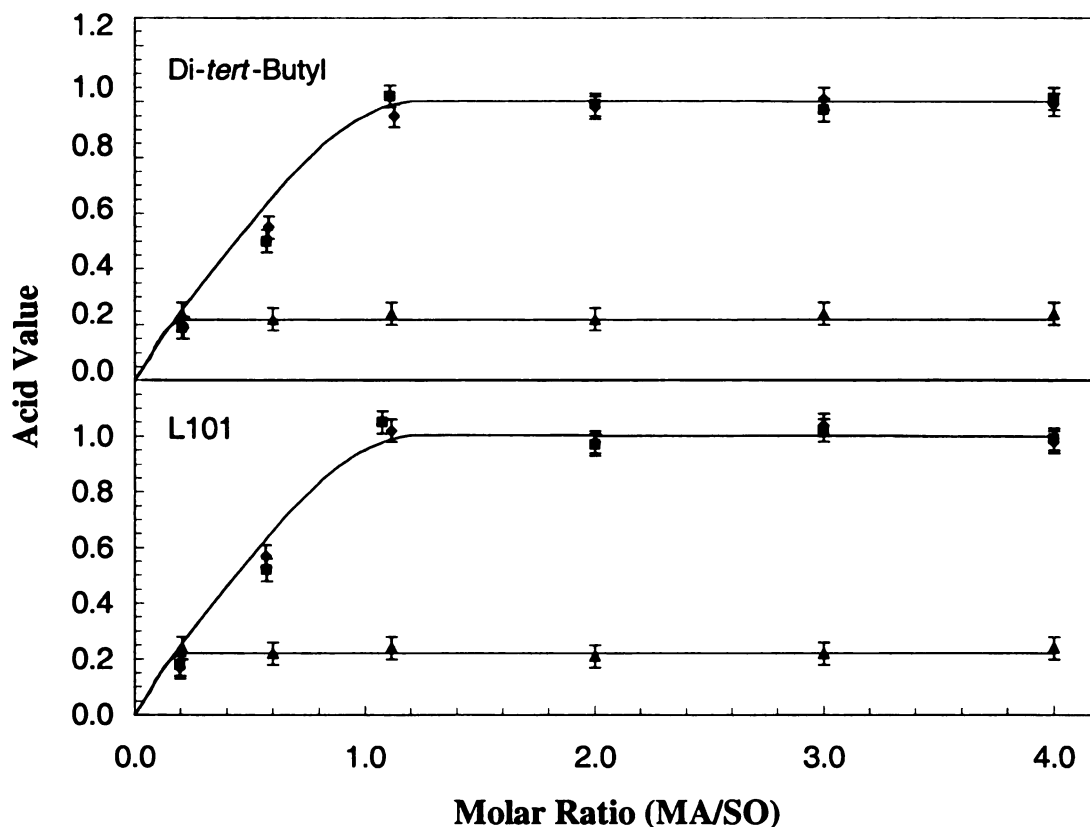


Figure 2.9: Effect of Peroxide Concentration on Acid Value after 60 minutes at 150°C ▲No Initiator; ■ 0.005 wt%; ◆ 0.01 wt%

Yet, doubling of the initiator concentration from 0.005 wt% to 0.01 wt% had no effect on the acid values, which were statistically similar. Furthermore, when the reaction was run with no peroxide, the resulting iodine number indicates the presence of about 4.5 moles double bonds per triglyceride, meaning no net change in the number of double bonds

after the addition of MA. This same number of double bonds suggests that reactions at lower temperatures favor the “ene” addition over Diels Alder addition.

2.3.2 Diels-Alder Addition of Maleic Anhydride to Soy Oil

It is apparent from **Figures 2.2 and 2.3** that even in the presence of a peroxide and large excess MA (up to molar ration of MA/SO=4), the maximum acid value never exceeded ~1. Experimentally, it was observed that when excess MA was used (e.g. reactions containing MA/SO molar ratio of 2:1, 3:1, and 4:1), unreacted MA remained in the reaction mixture and then was accumulated and collected in the solvent trap during the work-up procedure. Attempts to run the reaction for longer times (up to 240 minutes) did not lead to higher acid values and no further increase in the maleation was observed. The iodine number of the products with acid value around 1.0 was always correlated to soy oil having about 3.5 double bonds. This net reduction of 1 double bond from the unmodified soy oil suggests that 1 mole of MA was added to SO by a Diels-Alder addition (**Figure 2.1**). Although, further maleation is theoretically possible, it was found experimentally that only 1 mole of MA had reacted as determined by the acid number. Although the reason for this upper limit addition of MA is not clear at this time, one possible explanation could be steric hindrance effects that impede further reaction of MA.

2.3.3 Characterization of Maleated Soy Oil

Maleation of soy oil is accompanied by a noticeable increase in the room temperature viscosity from 50 cPs of neat SO to 3500 cPs for the maleated SO (**Figure 2.10**).

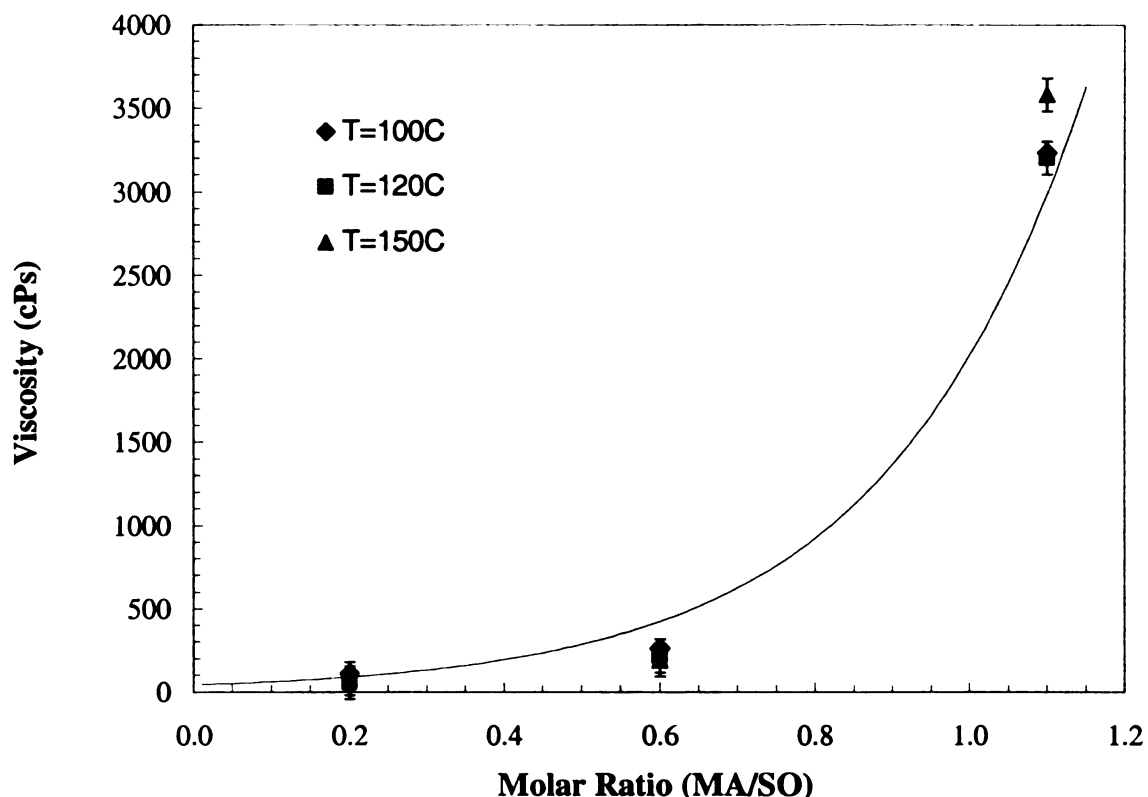


Figure 2.10: Change in Viscosity with Increases in MA Concentration

The increased viscosity is most likely due to an increase in hydrogen bonding as MA is grafted into the triglyceride structure. It is not due to opening of the anhydride ring and copolymerization through reaction of the carboxylic groups as has been suggested previously since esterification of the maleated SO with methanol yielded a product with an acid value of 0.1 and a viscosity of only 100 cPs.

There were no significant differences observed when the reaction temperature was adjusted to 100°C, 120°C, or 150°C. Under these conditions, MA was completely consumed within 30 minutes as shown in **Figure 2.11**. The degree of maleation was not affected by the reaction temperature and similar acid values were obtained when the initial temperature was set between 100°C to 150°C.

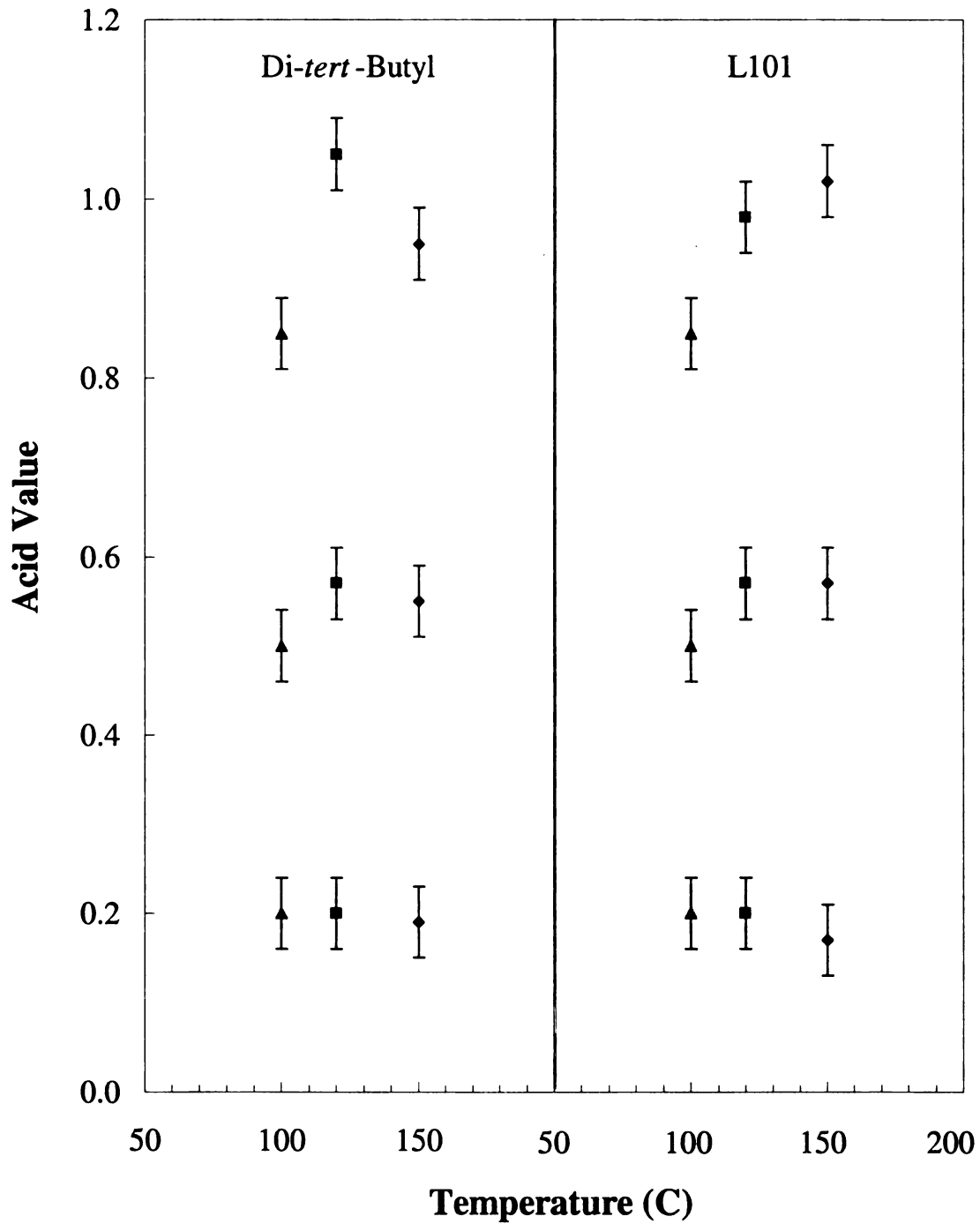
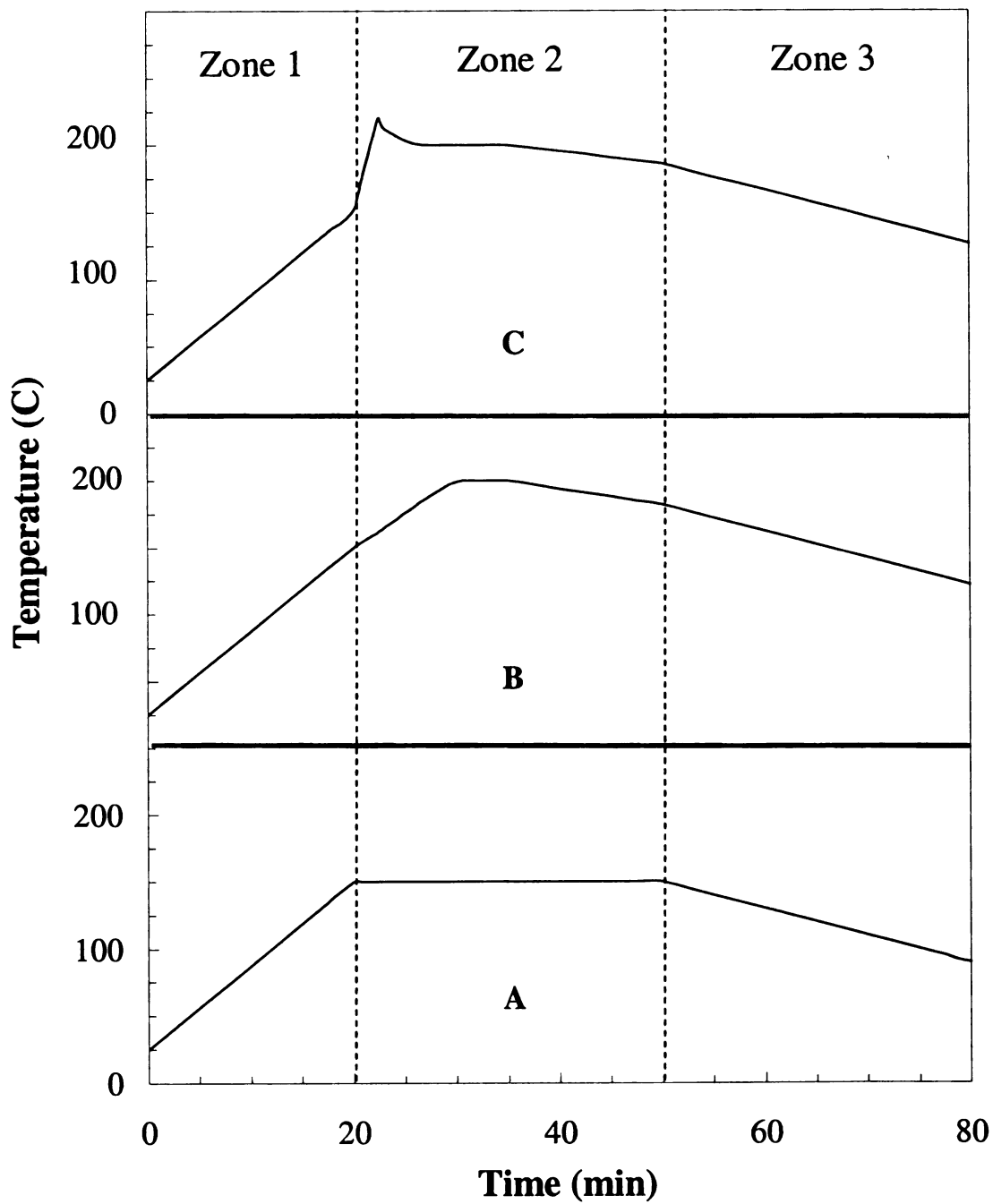


Figure 2.11: Effect of Reaction Temperature on Maleation of Soy Oil
 ▲ 100°C ■ 120°C ◆ 150°C

However, the temperature profile of the reaction was affected by the peroxide concentration as shown in **Figure 2.12**. Three distinct zones were clearly observed in the course of these reactions; Zone 1 represents the time it took to heat the reactor to the preset reaction temperature (e.g. **150°C in Figure 2.12**), Zone 2 is the time interval (usually, 30 minutes) the reaction was allowed to proceed after it reached the preset temperature and Zone 3 is the time period heating was stopped and vacuum was applied to remove any unreacted MA. The typical temperature profile of reactions with no initiator is shown in **Figure 2.12A** where the reaction proceeded to a set point of 150°C, which was sustained for 30 minutes until heating was terminated and vacuum was applied, resulting in slow cooling. Zone 1 is the same for all the different reactions and is determined by the applied heating. However, the temperature profile in Zone 2 is different when peroxide was included in the reaction mixture (**Figure 2.12B and 2.12C**). Here, the temperature continued to rise at the end of Zone 1 and although it was set to 150°C, it reached 200°C. This overheating beyond the preset temperature was particularly noticeable in the reactions with 0.01 wt% peroxide and was accompanied by an increase in the reactor pressure (25 psi). Although this exotherm may be partially attributed to the decomposition of the peroxide, we believe it is most likely due to the maleation reaction itself.



**Figure 2.12: Temperature Profile during Maleation
(A) 0 wt%, (B) 0.005 wt% and (C) 0.01 wt% L101**

The maleated soybean oil was further characterized by FTIR spectroscopy (Figure 2.13) and exhibits peaks at $\sim 1775\text{ cm}^{-1}$ and 1850 cm^{-1} not present in SO. These absorption peaks are related to the symmetric and asymmetric stretching of C=O in the MA (succinic anhydride derivative), respectively (11, 12). Furthermore, no absorption peaks related to -OH stretching due to the opening of the anhydride is observed, clearly indicating that the anhydride ring remained intact.

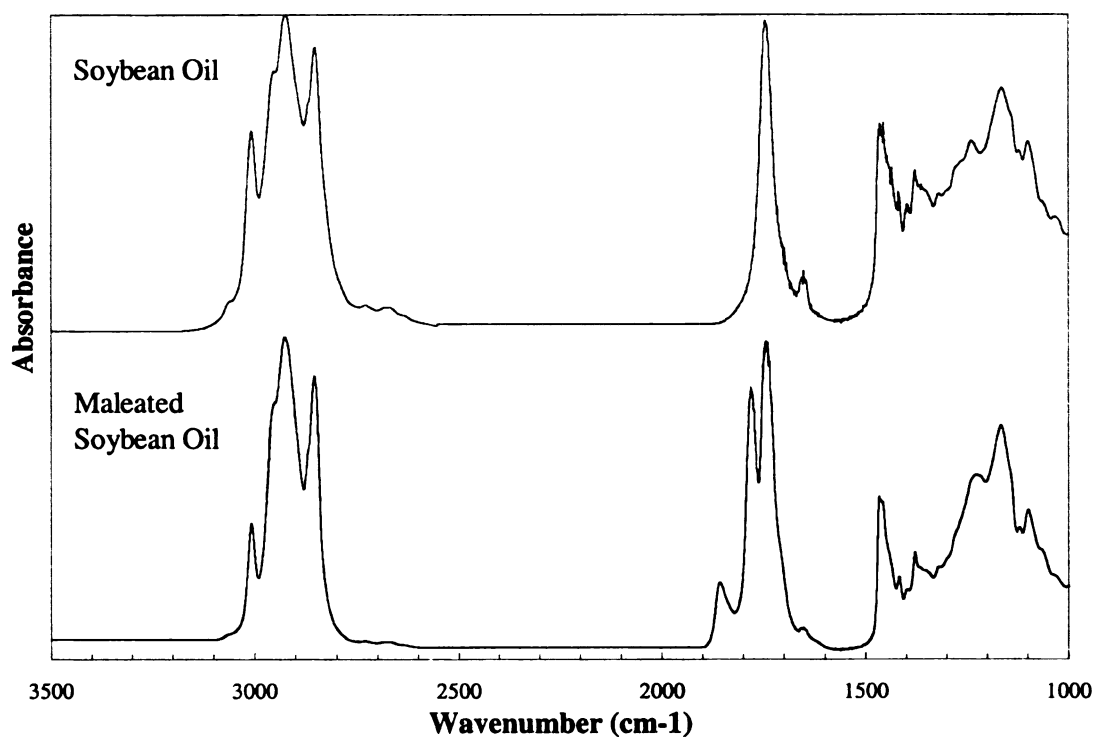


Figure 2.13: FTIR of Soybean Oil and Maleated Soybean Oil

2.4 CONCLUSIONS

Maleation of SO in a closed system at elevated temperatures and pressures is advantageous over open system processes. The maleated soy oil product we obtained is a pale yellow in color in contrast other studies where a red-orange liquid was obtained (13). Apparently, the use of high pressure in a close system is more advantageous and prevents premature decomposition and degradation of the soy oil. Furthermore, this closed system is also advantageous as it allows for a fast and simple one-step process. Unlike previous studies that required a reaction time of up to 7 hours for the maleation, with the MA being added to soy oil in aliquots (14), we have found that the reaction is completed within 30 minutes. Optimum process conditions for maleated SO in a closed system synthesis appear to be 30 minutes reaction time at 150°C in the presence of 0.005 wt % peroxide. The use of a pressurized closed system prevents loss of MA due to sublimation during the reaction. It was further found that the concentration of MA in the reaction mixture had the most pronounced effect on the extent of the reaction while the acid values were independent of the concentration and type of peroxide used. However, even when excess MA was present, the acid value did not increase above ~1.0 mole. The data appear to indicate that maleation reaction in the absence of a peroxide proceeds primarily through “ene chemistry” whereas a Diels Alder addition is favored when a peroxide is present. Thus, conjugation of the double bonds in the linoleic and linolenic fatty acid residues is expected to occur only in the presence of a catalyst and at high temperatures.

2.5 REFERENCES

1. Morrel R.S., and Samuels H., "Doubly conjugated system in alpha and beta-eleostearic acids", J. Chem. Soc. Abstracts 2251-2254 (1932)
2. Root F.B., Improvement of drying oils, U.S. Patent 2374381 (1945).
3. Clocker E.T., Condensation products for use in enamels, etc., U.S. Patent #2188882 (1940)
4. Bickford W.G., Fisher G.S., Kyame L., and Swift C.E., Autoxidation of fats. II. Preparation and oxidation of methyl oleate-maleic anhydride adduct, J. Amer. Oil Chem. Soc. 25, 254-257 (1948).
5. Teeter H.M., Geerts M.J., and Cowan J.C., Polymerization of drying oils. III. Some observations on reaction of maleic anhydride with methyl oleate and methyl linoleate, J. Amer. Oil Chem. Soc. 25, 158-162 (1948)
6. Kappelmeier C.P.A., Van Der Nuet J.H., Van Goor W.R., Maleic-treated oils, Paint Oil Chem. Rev. 113, 11-18 (1950)
7. Plimmer H. and Robinson E.B., Drying or semidrying oils and their derivatives, British Patent 565432 (1944)
8. Nagakura M. and Yoshitomi K., Reaction of maleic anhydride with unsaturated fatty acids in the presence of organic peroxides, Yukagaku 21, 83-91 (1972)
9. ASTM D1980, Standard Test Method for Acid Value of Fatty Acids and Polymerized Fatty Acids, Annual Book of ASTM Standards 06.03: 418-419 (2000)
10. ASTM D1959, Standard Test Method for Iodine Value of Drying Oils and Fatty Acids, Annual Book of ASTM Standards 06.03: 399-401 (2000)
11. Bellamy L.J., The Infra-Red Spectra of Complex Molecules, Wiley: New York, (1964).
12. Pouchert C.J., The Aldrich Library of Infra-Red Spectra, Aldrich Chemical Company; Milwaukee, WI, (1970).
13. Tarik E., Kuesefoglu S.H., Wool R., Polymerization of maleic anhydride-modified plant oils with polyols, J. Appl. Polymer Science 90, 197-202 (2003)
14. Warth H., Mulhaupt R., Hoffmann B., Lawrence S., Polyester network based upon epoxidized and maleinated natural oil, Angewandte 249, 79-92 (1997)

Chapter 3: Biocomposites from Modified Soy Oil and Biofibers

3.1 LITERATURE REVIEW

3.1.1 Research in Soy-based Polymers

Both thermoplastic and thermoset matrix biocomposites have been described in the literature; the resin matrix is generally a biopolymer or a synthetic biodegradable polymer and the reinforcing component is usually some biofibers (e.g. jute, flax, hemp, ramie, sisal, coir, cotton, etc). It should also be mentioned here that the use of natural fibers instead of traditional reinforcing materials such as glass fibers, talc, and mica provides further advantages in terms of lower cost, lower density, reduced tool wear, acceptable strength properties, energy recovery, and recyclability.

Currently, the most common chemical modification of soybean oil is the introduction of epoxy groups that replace some of the double bonds in the fatty esters. This epoxidation process was commercialized recently and the modified oil is being used primarily as a process aid in polyvinyl chloride to improve its stability, flexibility and processability. It is also being used in the preparation of adhesives for carpet backing, as a source of polyols for the preparation of rigid polyurethanes and as a reactive modifier or diluent of epoxy resin system (1). The reaction of maleic anhydride with soybean oil has also been reported in the literature and these chemically modified oils are used primarily in cosmetic applications as a component in shower gels, bar soaps, sunscreens, and skin treatment products (2).

Several researchers have investigated the use of chemically modified soybean oil in composites. However, it was found that the mechanical properties, primarily the tensile strength and stiffness, were too low, and thus limited their use in the market place. For

example, an early work with epoxidized soybean oil (ESO) produced flexible, semi-flexible, and rigid crosslinked polyesters (3, 4). Williams and Wool (5) prepared soy composites by free radical polymerization of acrylated and epoxidized soybean oil, which was then cured with styrene and divinylbenzene by resin transfer molding in the presence of hemp and flax. These composites were reported to have mechanical properties comparable to commercially available synthetic resins. However, the use of petroleum-based polymers was essential to enhance the mechanical properties. Lu et al. (6) reported the preparation of clay nanocomposites based on functionalized triglycerides such as acrylated epoxidized soybean oil, maleated acrylated epoxidized soybean oil, and soybean oil pentaerythritol maleates combined with styrene. Another type of composite was prepared by Taveerne-Valduizen et al. (7) from soybean oil by thermoplastic processing in the presence of a binding agent such as urea-formaldehyde copolymer or a protein that was added to the soybean oil. Can et al. (8, 9) focused on the preparation of copolymers from soy oil monoglycerides with styrene and soybean oil monoglyceride maleates with styrene. Zhu et al. (10) reported that epoxidized methyl soyate and epoxidized allyl soyate yielded resins that were highly reactive and provided a high degree of intermolecular crosslinking due to the addition of allyl soyate. These resins had higher modulus than similar resins obtained from unmodified ESO and thus, it was suggested that they could be suitable as composites for structural applications. Warth et al. (11) reported on the preparation of natural fibers reinforced soybean oil in polyester resin. Their work was based on networks of epoxidized and maleated soybean oil with hemp and flax fibers (10 wt %), where they were able to achieve tensile strengths of 6.0 and 6.2 MPa, respectively.

The goal of this work was to synthesize tough composites from natural biofibers and chemically modified soybean oil with no additional styrene, polyester or other petroleum-based polymers to supplement the soy matrix in order to enhance the mechanical properties. The soy-based composites were prepared by combining epoxidized soybean oil (ESO) with maleated soybean oil (MSO), or maleated methyl soyate (MMS), in the presence of selected biofibers. In contrast to previous studies, this work was focused on increasing the efficiency of the crosslink density, minimizing the sol fraction of the network in order to enhance the stiffness of the composites and eliminate possible “bleeding out” of the sol fraction from the gel network due to incomplete cure in order to avoid any adverse effects on the surface properties of the composites. It was thought that one common reason for a low gel fraction and incomplete cure in previous studies of epoxidized soy-based composites was related to incomplete cure between the epoxidized soy modified oil and the anhydride groups primarily due to the poor reactivity of the epoxy groups and steric hindrances. Thus, in this study, we explored the use of flexible spacer crosslinking amine catalysts (e.g. hexamethylene diamine (HMD) and 4-dimethylamino pyridine (4-DMAP)) that were expected to react with both epoxy and anhydride functional groups.

3.2 EXPERIMENTAL PROCEDURE

3.2.1 Reagents and Equipment

The soybean oil (Spectrum), 1/3 partially epoxidized soybean oil (Elf Atochem), and methyl soyate (Michigan Soybean Board) were used without further purification. Methylene chloride, maleic anhydride, isopropanol, hexamethylene diamine (HMD), 4-dimethylamino pyridine, and 2,5-bis(*tert*-butylperoxy)-2,5-dimethylhexane (L101) were purchased from Sigma-Aldrich. Biofibers were obtained from American Fillers & Abrasives, Inc. and (2-aminoethyl)-3-aminopropyl-trimethoxysilane was purchased from Gelest.

FTIR spectra were run on a Perkin-Elmer Model 1000 by evaporating a solution of a sample from the surface of a NaCl crystal. The composites were cured in Wabash Metal Products Model CM02871. Mechanical properties were run after aging the samples for 3 days at 23°C and 50% relative humidity on a tensile instrument made by United Testing Systems Model SFM-20.

3.2.2 Synthesis Methods

Maleation of Soy Oils

As reported in Chapter 2 (**Page 15**)

Cure Reactions of MSO (or MMS) with ESO

Approximately equimolar MSO (or MMS) and ESO were combined with a catalyst in a beaker and placed in a silicone oil bath heated at 5°C/min while stirring using a magnetic stirrer. The gels were then removed and extracted in a soxhlet apparatus for 3 days using methylene chloride as a solvent and the gel fraction was

determined. The results of the batch cure experiments are presented in **Table 3.1** and **3.2**.

MSO (mol)	MMS (mol)	ESO (mol)	4-DMAP (wt%)	T (°C)	Gel Time (s)	Gel Wt (%)
1	0	1	0	200	-	-
1	0	1	0.05	172	68	0.99
1	0	1	0.1	170	40	0.98
1	0	1	0.15	162	37	0.97
1	0	1	0.2	148	24	0.98
1	0	1	0.2	room	-	-
0	1	1	0	200	-	-
0	1	1	0.05	185	98 ^a	0.78
0	1	1	0.1	164	57	0.74
0	1	1	0.15	158	51	0.82
0	1	1	0.2	152	32	0.75
0	1	1	0.2	room	-	-

^a Gelation could have occurred over a long period of time or instantaneously

Table 3.1: Batch Curing Experiments in the Presence of a Base Catalyst

MSO (mol)	MMS (mol)	ESO (mol)	HMD (wt%)	T (°C)	Gel Time (s)	Gel Wt (%)
1	0	1	0	200	-	-
1	0	1	0.05	162	52	0.98
1	0	1	0.1	158	35	0.99
1	0	1	0.15	152	27	0.99
1	0	1	0.2	155	25	0.99
1	0	1	0.2	room	-	-
0	1	1	0	200	-	-
0	1	1	0.05	164	61	0.97
0	1	1	0.1	162	58	0.99
0	1	1	0.15	159	46	0.98
0	1	1	0.2	148	33	0.99
0	1	1	0.2	room	-	-

Table 3.2: Batch Curing Experiments in the Presence of a Diamine

From these results, further cure studies were done in an oven at 150°C. Each mixture was visually checked every few minutes. Initially, the color of the reaction mixture was light yellow and the catalyst was insoluble in the oil. However, after about 15 minutes at this temperature, a significant drop in the viscosity was noticed and all the catalyst appeared to have dissolved in the matrix. Thereafter, the viscosity of the reaction mixture continuously increased and the color of the mixture turned slightly darker. The reaction was allowed to continue for 3 hours and the gel was then removed from the oven,

extracted in a soxhlet apparatus for 3 days using methylene chloride as a solvent and the gel fraction was determined. Based on these experimental conditions, biocomposites containing various fibers were prepared as shown in **Table 3.3**.

Reactants	Resin Matrix Characteristics	Biofiber
ESO + MSO	Viscous Liquid	-
ESO + MSO + 4-DMAP	Soft and Sticky Solid	Kenaf, Kayocell, Protein Grits, & Solka-floc
ESO + HMD	Translucent Highly Viscous Liquid	-
MSO + HMD	Tranparent Highly Viscous Liquid	-
ESO + MSO + HMD	Semi-Rigid Solid	Kenaf, Kayocell, Protein Grits, & Solka-floc
ESO + MMS	Liquid	-
ESO + MMS + 4-DMAP	Soft Solid	Kenaf, Kayocell, Protein Grits, & Solka-floc
MMS + HMD	Tranparent Viscous Liquid	-
ESO + MMS + HMD	Semi-Rigid Solid	Kenaf, Kayocell, Protein Grits, & Solka-floc

Table 3.3: Soybased Biofiber Reinforced Natural Composite

Resin Transfer Molding

A measured weight of dried kenaf fiber mats sufficient to make 10 wt% composites was placed inside a rectangular mold. A flow media was placed over the top of the fiber mat, and a vacuum bag was placed over the entire system as shown in **Figure 3.1**. The reactants and catalyst were mixed at 60°C for 30 minutes, then, added to the fiber mat and vacuum was applied to ensure the fibers were completely saturated. The cure reaction was allowed to proceed for 3 hours in a vacuum oven at 150°C.

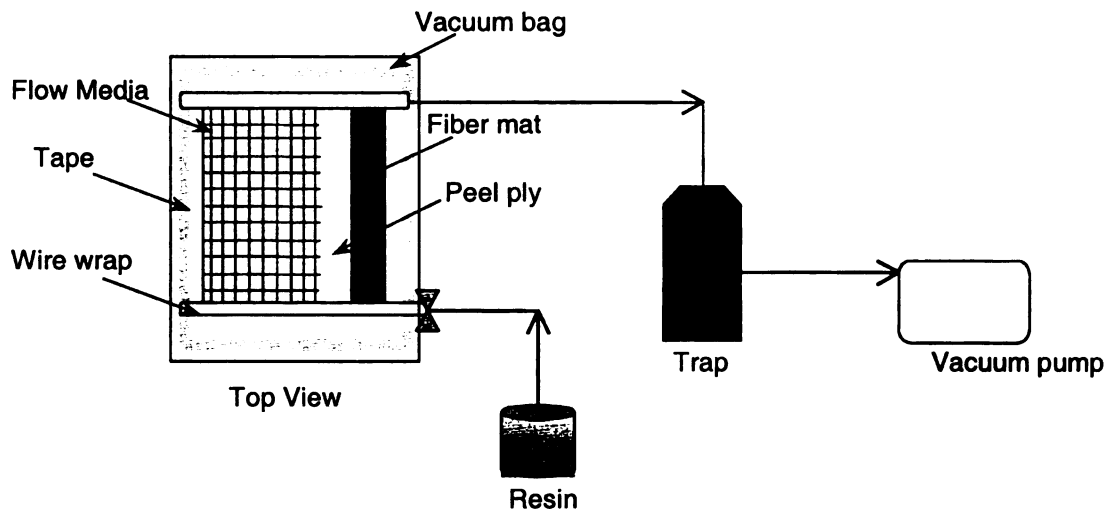


Figure 3.1: Preparation of Soy-based Composites by Resin Transfer Molding

Compression Molded Cures

The catalyst was combined with ESO and impregnated into the biofiber (10 wt %) and the mixture was heated with stirring until the catalyst was completely dissolved. Then, MSO was added, thoroughly mixed and the reaction mixture was poured into a rectangular mold and held at 150°C under 11 tons of pressure for 3 hours. Samples were removed from the press after it was cooled to RT by circulating cooling water through the platens.

Surface Treatment of Kenaf Fibers

Kenaf fibers were treated by dipping them briefly in a 2 wt% freshly prepared aqueous solution of (2-aminoethyl)-3-aminopropyl-trimethoxysilane. The fibers were then placed in a vacuum oven at 80°C and allowed to dry for 4 hours.

3.3 RESULTS AND DISCUSSION

3.3.1 Characterization of Soy-based Thermosets

The crosslinking reaction between epoxy functional polymers and anhydrides to yield a polyester resin is well known (12) and depends primarily on the reactivity of the anhydride, its molar ratio with respect to epoxy groups, the concentration and efficiency of the cure catalyst, and the reaction conditions. In our study, the resin network was obtained by reacting epoxy functional soy oil (ESO) and succinic anhydride functional soy oil (MSO or MMS) catalyzed by HMD or 4-DMAP. The cure was easily followed by the disappearance of the characteristic FTIR anhydride absorptions at 1780 and 1850 cm^{-1} (**Figure 3.2**). It was observed that the onset of gelation was directly proportional to the catalyst concentration and always appeared at lower temperatures when higher concentrations of the catalyst were used (**Table 3.1**). However, the nature of the gels was greatly affected by the choice of catalyst and the type of soy derivative that was used as shown in **Tables 3.1 and 3.2**. Thus, HMD catalyzed reaction between MMS and ESO produced a gel with very high gel fraction (low sol content), but the same reaction catalyzed with 4-DMAP produced a poor gel having unacceptable high sol content. Reactions between MSO and ESO for both catalyst systems yielded high gel fraction networks with essentially no weight loss after soxhlet extraction. In contrast, 4-DMAP catalyzed reaction between MMS and ESO yielded a poor network with high sol fraction.

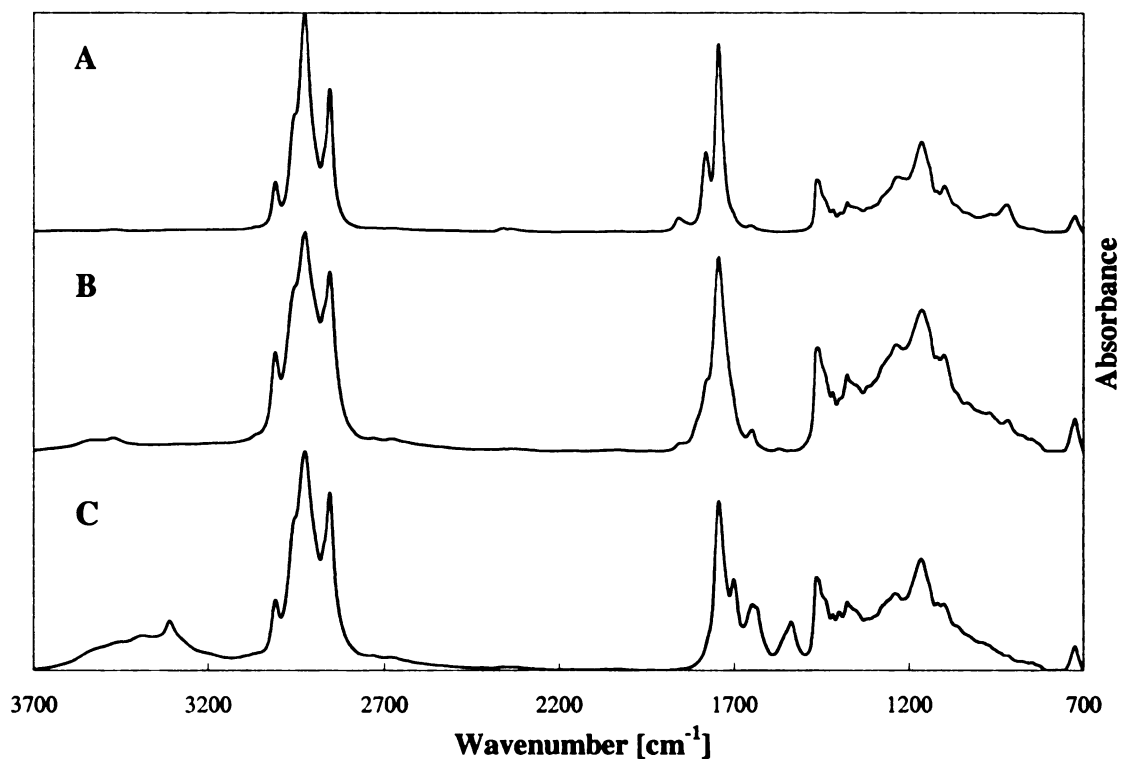


Figure 3.2: FTIR Spectra of MSO (A); MSO + ESO (B); and MSO + ESO + HMD (C)

These observations are in agreement with the curing mechanism of epoxy resins. It is generally agreed (13) that a non-catalyzed cure starts by the reaction of anhydride with hydroxyl (which is usually found in ESO) to yield a monoester and a carboxylic group. The carboxylic acid group then reacts with an epoxide to form a diester with a hydroxyl group, which subsequently reacts with another anhydride. However, in the presence of amine catalysts the cure reaction is initiated by complex formation of the amine with a proton donor and the active centers are the carboxylate and hydroxylate anions. The reaction mechanism in these cases depends to a great extent on the reactivity of the anhydride and, more important, on the type of amine catalyst. Apparently, in our case the cure catalysis with 4-DMAP was not as efficient compared with HMD catalysis.

The poor network with high sol fraction that was obtained in the case of ESO/MMS was most likely due to the presence of the non reactive saturated palmitic and stearic components in the methyl soyate oil. Since maleation occurs across the double bonds, these fatty acids, which are present in the soy oil at about 15 wt%, do not react with maleic anhydride and thus, are not incorporated into the network. Hence, they merely act as a plasticizer and are easily removed out of the resin by the soxhlet extraction. The fact that reactions between MMS and ESO in the presence of HMD also resulted in high gel fractions with nearly no weight loss after extraction is most likely due to rearrangement and formation of amide linkages with the carbonyl esters of the methyl soyate. Such ester saponification and amide formation allows for the saturated components that carry no anhydride groups to be incorporated into the gel matrix through amide linkages.

The cured soy-based resins, especially those cured with HMS, were very rigid and brittle unlike “flexible and rubber-like” resins prepared previously from ESO with succinic anhydride²⁵. Apparently, the use of the succinic anhydride functional soy oil in combination with a flexible amine catalyst led to a more efficient network formation compared with similar ESO matrices that were cured with low molecular weight cycloaliphatic anhydrides and catalyzed by benzyldimethylamine.

3.3.2 Mechanical Properties of Soy-based Composites

The mechanical properties were greatly enhanced when these soy-based resins were reinforced with biofibers. Generally, the tensile strengths of such composites cured with HMD as a catalyst had the best tensile strengths. The type of biofibers or the soy matrix (ESO with MSO or with MMS) had only secondary impact (**Figure 3.3**). In

contrast, composites cured using 4-DMAP as a catalyst had relatively poor mechanical properties as a result of lower resin crosslink density. In fact, it was observed that composites made from MMS-ESO and cured with 4-DMAP had a significant sol fraction that diffused out of the sample upon aging.

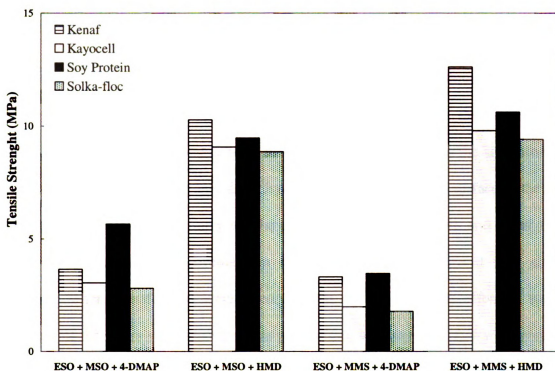


Figure 3.3: Tensile Strength of Composites Prepared by Compression Molding

Preparation of biocomposites by incorporation of kenaf fibers provided the best reinforcement due to good interactions between the soy matrix and these lignocellulosic fibers (Figure 3.3). Although the tensile strength of composites cured with 4-DMAP were generally lower than those cured with HMD, good tensile strength was observed in the samples that were reinforced with soy proteins. It is possible that in this particular case the presence of free amino groups in the protein grits contributed to the fiber/matrix adhesion and consequently led to higher than expected tensile strength

3.3.3 Silane Surface Treatment of Biofibers

Further enhancement in the mechanical properties was realized by surface treatment of the biofibers with (2-aminoethyl)-3-aminopropyl-trimethoxysilane coupling agent prior to incorporating them into the matrix (**Figure 3.4**). This coupling agent has been used extensively for surface treatment of various fibers (14). It is effective at low concentrations whereby the amine functional group enhances the solubility of the silane in water and at the same time provides multiple hydrogen bonding through interactions with hydroxyl groups on the surface of the fiber. After deposition, the amine groups further promotes hydrolysis and condensation of the alkoxy groups on the silane to yield insoluble oligomeric polysiloxanes and a hydrophobic network on the surface of the fiber (15). This surface treatment improved the adhesion between the resin and kenaf fibers and led to about 20% improvement in the tensile strength compared with similar composite where kenaf fibers were dried but was not treated. The effect of surface treatment of the fibers was somewhat less pronounced in composites that were prepared by resin transfer molding simply due to the difference in the wetting of the fibers in this process.

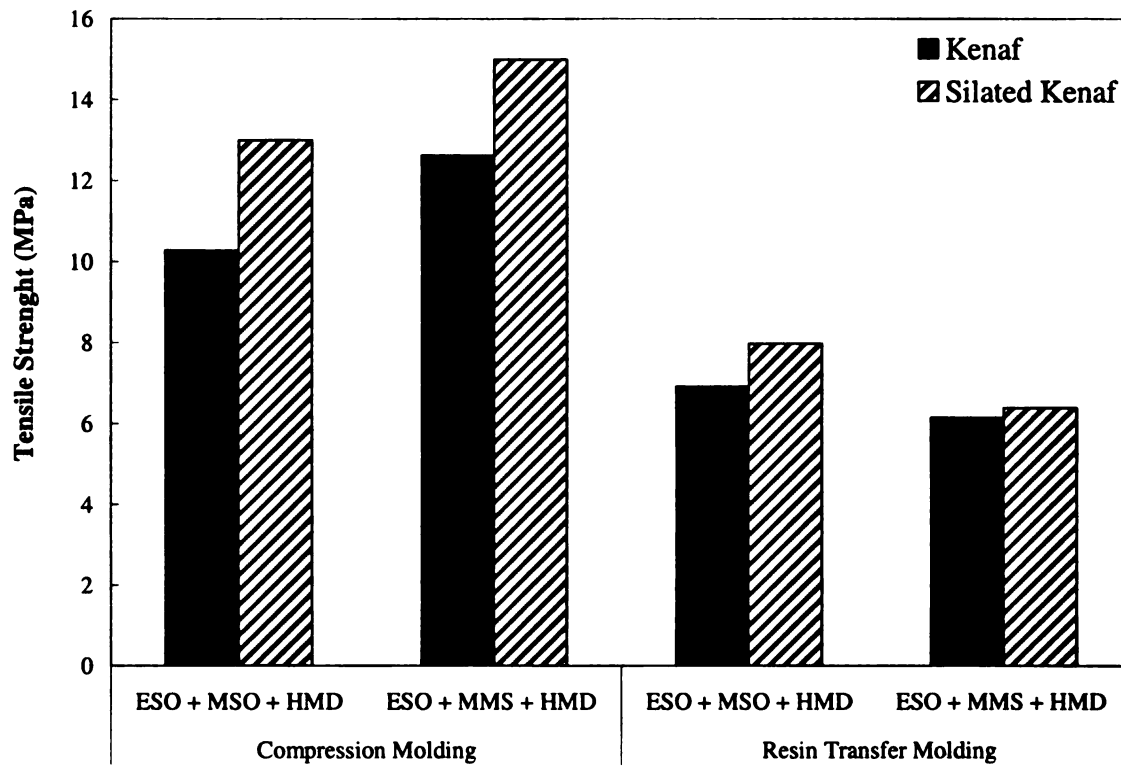


Figure 3.4: Tensile Strength of Soy Composites after a Silane Surface Treatment of Kenaf Fibers

3.4 CONCLUSIONS

Soybean oils and methyl soyate chemically modified with suitable functional groups (e.g. epoxy and anhydride) react in the presence of a flexible amine catalyst to create a three-dimensional crosslinked polyester matrix. The formation of these networks was followed by FTIR under different temperatures and reaction times. Biocomposites were prepared by curing these soy-based resins in the presence of various biofibers (e.g. flax, kayocell, protein grit, and solka-floc) using compression molding and resin transfer molding techniques. Rigid network resins with high gel fractions were obtained when ESO was reacted with MSO using HMD as a catalyst. Composites with high mechanical strength were achieved when kenaf fibers were first treated with (2-aminoethyl)-3-aminopropyl-trimethoxysilane in the reinforcement of these soy-based matrix resins.

3.5 REFERENCES

1. Karnani, R.; Krishnan, M.; Narayan, R. Polym Eng and Sci 1997, 37, 476
2. Mustata F. J Polym Eng 1997, 17, 491
3. Gripp, A.; Steinberg, D. In-Cosmetics Exhibition and Conference Proceedings, Barcelona, 1994, 293
4. Crivello, J.V.; Narayan, R. Chem Mat 1992, 4, 692
5. Crivello, J.V.; Narayan, R.; Sternstein, S.S. Chem Mat 1997, 64, 2073
6. Williams, G.; Wool, R.P. Appl Compos Mat 2000, 7, 421
7. Lu, J.; Hong, C.K.; Wool, R.P. J Polym Sci. Part B: Polym Phys 2004, 42, 1441
8. Taverne-Velduizen, W.; Simka, H.; Feil, H. Eur. Pat. Appl. 976790 (2000)
9. Can, E.; Kusefoglu, S.; Wool, R.P. J Appl Poly Sci 2001, 81, 69
10. Can, E.; Kusefoglu, S.; Wool, R.P. J Appl Poly Sci 2002, 83, 972
11. Zhu J.; Chandrashekhara, K.; Flanigan, V.; Kapila, S. J Appl Polym Sci 2004, 91, 3513
12. Warth, H.; Mulhaupt, R.; Hoffman, B.; Lawson, S. Ang Makomol Chem 1997, 249, 79
13. Root F.B. U.S. Patent 2374381 (1945)
14. Nagakura M.; Yoshitomi K. Yukagaku 1972, 21, 83
15. ASTM D1980, Standard Test Method for Acid Value of Fatty Acids and Polymerize Fatty Acids, Annual Book of ASTM Standards 2000, 6, 418
16. ASTM D1959, Standard Test Method for Iodine Value of Drying Oils and Fatty Acids, Annual Book of ASTM Standards 2000, 6, 399
17. Takahashi K.; Hitoshi F. Adv Polym Sci 1986, 80, 173
18. Trappe V.; Buchrd W.; Steinmann B. Macromolecules 1991, 24, 4738
19. Steinmann B. J Appl Polym Sci 1990, 39, 2005
20. Steinmann B. J Appl Polym Sci 1989, 37, 1753

21. Roesch J.; Muelhaupt R. Polym Bull 1993, 31, 679
22. Plueddemann E.P. In Silanes Surfaces and Interfaces, Leyden D.E., Ed.; Gordon and Breach Sci. Pub.: New York, 1986, Chap. 2.
23. Ishida H.; Naviroj S.; Tripathy S.K.; Fitzgerald J.J.; Koenig J.L. J Polym Sci. Part B: Polym Phys 1982, 20, 701

Chapter 4: Ozone Mediated Polyol Synthesis

4.1 INTRODUCTION

4.1.1 Properties of Ozone

Ozone is a natural component in the earth's atmosphere, where it is formed photochemically. It can be recognized by the clean, fresh odor of air after a thunderstorm, where lightning produces low levels of ozone (**Figure 4.1**).

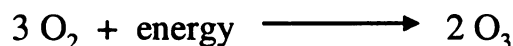


Figure 4.1: Generation of Ozone

The first odor of ozone was reported by Van Mauren in 1785, in the presence of an electrical discharge. The identity of the structure of the compound was confirmed in 1867 as triatomic oxygen. Ozone is an allotrope of oxygen (**Figure 4.2**).

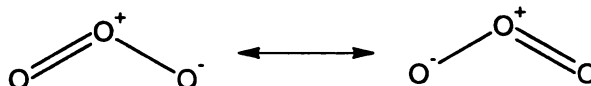


Figure 4.2: Resonance Structure of Ozone

Ozone (O₃) is formed by recombination of atomic (O) and molecular oxygen (O₂). It is the strongest oxidizing agent, able to be produced. A comparison of oxidation strengths of standard oxidants, ozone is 2.07 V as compared to chlorine (1.36 V) and chlorine dioxide (1.50 V). However, the molecules are unstable and cannot be stored for future use; thus, it must be generated near point of application and then immediately used. Ozone is relatively stable in air, with a half-life of several hours at low concentrations. It has a limited solubility; therefore the concentration of ozone in the gas stream becomes very important. Consequently, the solubility of ozone increases with an

increase in ozone concentration in the gas stream. Also, the ozone solubility decreases with an increase in temperature.

4.1.2 Ozone Generation

Ozone has been commercially used since 1893 when the first full scale drinking water treatment application was implemented. Today, it is used in thousands of water treatment applications, cooling towers, ultra pure water, marine aquaria, beverage industries, swimming pools, bottled water plants, agriculture, food processing, and chemical synthesis.

Ozone is generated by passing pure oxygen or dry air through an electric field, where a portion of the oxygen is converted into ozone. There are several other methods to produce ozone, such as corona discharge (CD), UV irradiation, and electrolysis. The CD generation is capable of producing high concentrations of ozone. An energy potential is used to split oxygen-oxygen double bonds, producing atomic oxygen. Collisions between atomic and diatomic oxygen forms ozone (Figure 4.3)

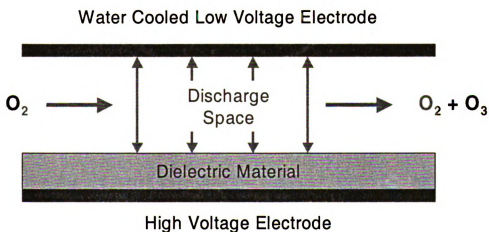


Figure 4.3: Ozone Generation by Corona Discharge

The quantity of ozone produced is dependent on several factors, such as voltage and frequency of the alternating current applied to the CD cell. When enough high energy electrons bombard gas molecules, ionization occurs emitting gaseous plasma, referred to as a corona. A typical CD ozone system consists of 4 fundamental components, an air preparation or oxygen production unit, a CD generator, an ozone diffuser/contacter, and an ozone off-gas destruction unit. Ozone generation by CD is an exothermic physico-chemical reaction, where most of the energy used for ozone generation is lost as heat, therefore cooling efficiency is an important factor. Recent advances in CD have achieved greater ozone production with less electrode surface area, reduced power consumption per kg of ozone produced, and the generator efficiency may be manipulated by varying frequency, wave form, voltage, etc.

Air preparation is very important to efficient and reliable operation of CD ozonators. Moisture and particulate matter have a detrimental effect on the generation cell electrodes and dielectric material. Moist air in the ozone generator will form nitric acid decreasing ozone production, and corroding components. Also, the presence of wet air will cause arcing and sparks within the generator. Although, oxygen feed results in higher ozone concentrations and reduced power consumption, for economic reasons most applications use air as the feed gas.

4.1.3 Ozone Chemistry

Ozone was discovered more than 150 years ago, but the first ozonolysis reaction to cleave carbon-carbon double bonds was only carried out in 1903 by Harris. Ozone is a very powerful oxidant, which leaves only oxygen as a side product after oxidation. It can be generated on-site without “chemistry”. No other oxidizing agent is capable of

cleaving double bonds in such a fast, clean, and selective way to yield carbonyl compounds. While studying the resonance structure it became clear to Criegee that ozone can act as a dipole adding to double bonds such that the first step in the reaction is a 1,3-dipolar cycloaddition, forming a primary ozonides (**Figure 4.4**).

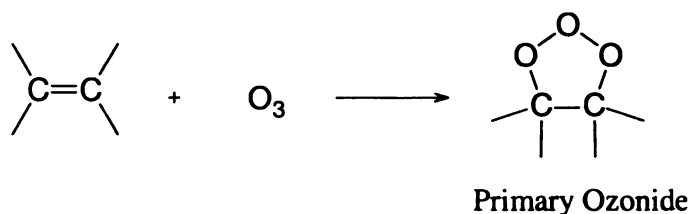


Figure 4.4: Formation of Primary Ozonide

However, the primary ozonide is a very unstable 5 member ring, 1,2,3-trioxolane. Practical ozonolyses are run at $-78 - 25^{\circ}\text{C}$, and under these conditions the primary ozonide decomposes immediately by selective cleavage of the carbon-carbon bond and one oxygen-oxygen bond leading to a carbonyl compound and the Criegee “Zwitterion”, a peroxidic carbonyl oxide, as a second fragment (**Figure 4.5**).

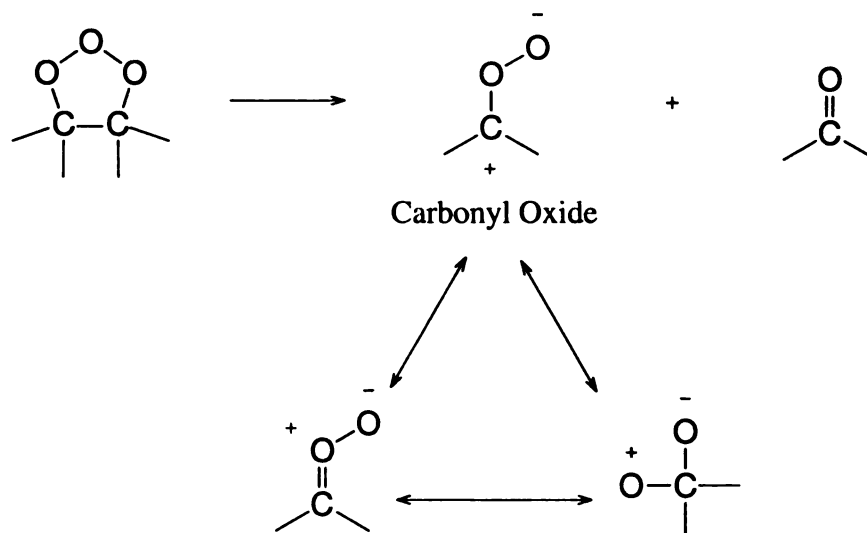


Figure 4.5: Ozonolysis Reaction Mechanism

Due to the large oxygen content of these molecules, the carbonyl oxide is very unstable and tends to decompose. Polymeric peroxides are of particular concern because of their low solubility and tendency to precipitate. Therefore for safety consideration maintaining low concentrations of these species is important. This can be achieved by using a continuous process or working in dilute solutions.

It was proposed by Marshall and Garafalo that under basic conditions, the ozonolysis of alkenes in methanolic NaOH could redirect the decomposition to form methyl esters (Figure 4.6). Their work included an ozonolysis of methyl oleate in methanolic NaOH, which yielded dimethyl azelate and methyl nonanoate at 77 and 78 wt%, respectively.

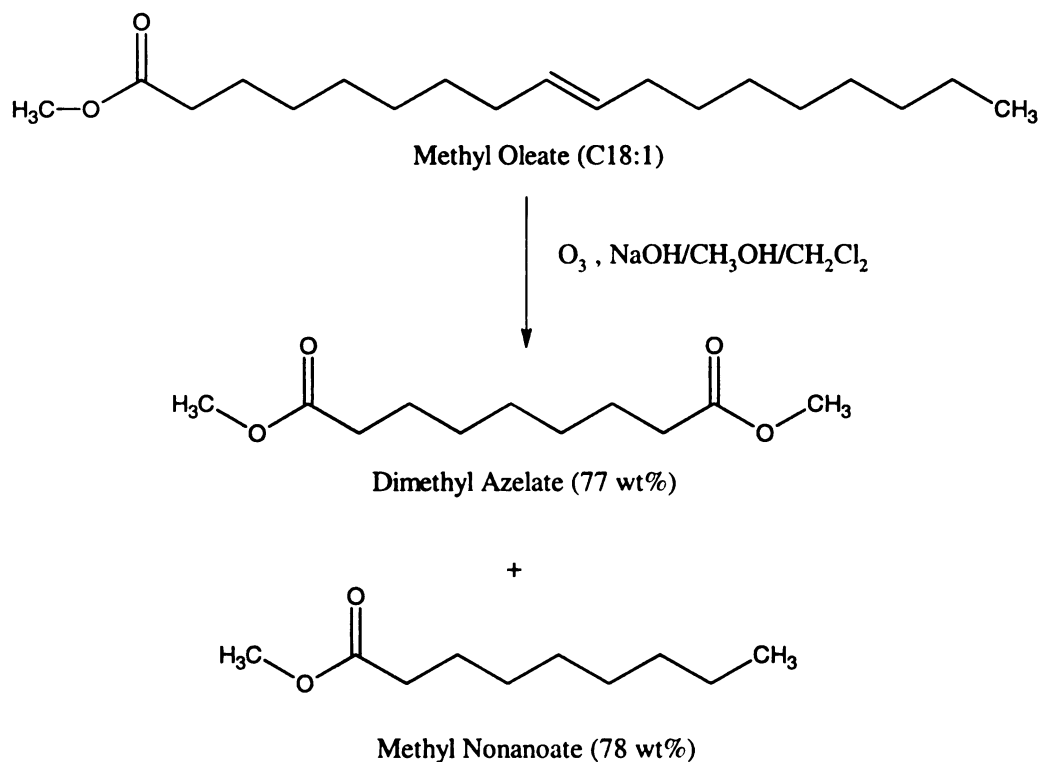


Figure 4.6: Ozonolysis Products of Methyl Oleate in Methanolic NaOH

Nominally, the ozonolysis of methyl oleate would lead to a mixture of aldehydes and carboxylic acids. A new synthesis was developed to prepare soy polyols by reacting soy oil with a diol in an alkaline medium using ozone.

4.2 LITERATURE REVIEW

4.2.1 Methods of Polyol Preparation of Vegetable Oils

One of the early methods to prepare polyols from various vegetable oils is based on transesterification of the fatty acids in the triglycerides with a polyol such as glycerol, glycerin, pentaerythritol, α -methylglucoside or sucrose (1, 2). Unfortunately, premature degradation occurs by this process due to high temperatures and a relatively long period of time in this reaction. Another method is based on reacting vegetable oils with peroxy acid to yield epoxidized fatty acids. The epoxide rings are then opened (3, 4) or hydroxylated (5) with polyfunctional alcohols to yield secondary alcohols. Epoxidized soy oil is available commercially but the reactivity of this oil is low due to the nature of the secondary alcohols. Furthermore, several hydroxyl groups per fatty acid residue are obtained (at least these fatty acids that contain more than one double bond). Consequently, multiple numbers of hydroxyl groups having varying reactivity are present, which tend to complicate subsequent reactions that could lead to premature gelation. Hydroformylation offers another method to prepare polyols whereby an aldehyde functional vegetable oil is first obtained, which is then hydrogenated to alcohols (6, 7). Polyurethanes prepared from these polyols had different mechanical properties depending on the hydroformylation catalyst that was used. Thus, rigid materials at room temperature were obtained with a rhodium catalyst while cobalt catalyzed hydroformylation led to rubbery materials (8). An alternative method to prepare primary

polyols is based on oxidizing an olefin having a carbonyl group with molecular oxygen followed by hydrolysis and reduction of the acetal (or ketal) to an alcohol (9). Although this method appears somewhat complicated and must be run at high pressure, good yields were reported. A somewhat less complicated method, also based on an oxidation process to yield polyols, is based on catalytic oxidation using an organic hydroperoxide in the presence of OsO_4 and a NaBr cocatalyst (10). An alternative process is to use ozone to cleave and oxidize the double bonds in the vegetable oil and then reduce the decomposing ozonides to alcohols using NaBH_4 or similar reducing agents.

It is apparent that there is a need to improve the chemistry as well as the process and devise a more efficient method to prepare vegetable oils containing primary alcohols. Reported is a new method to synthesize such soy-based primary polyols in a single-step ozonolysis procedure. Our method takes advantage of the ease and efficiency of the oxidation methods mentioned earlier but it is relatively simple, fast and gives high yields in a single step.

4.3 EXPERIMENTAL PROCEDURES

4.3.1 *Materials and Methods*

Degummed soybean oil was purchased from Spectrum Chemicals in a 20L container and was used without further purification. Linoleic acid (purity>99%) was purchased from Eastman Chemical. Ethylene glycol, sodium hydroxide, pyridine, 4-dimethylamino-pyridine (4-DMAP) and CaCO₃ were purchased from Sigma-Aldrich. Ozone was produced by passing dry oxygen (0.25 ft³/min) through a Praxair Trailigaz generator (Cincinnati, OH), model number OZC-1001. The exit port of the ozone generator was connected to the bottom of the reaction bottle and allowed the ozone (about 6 wt% in oxygen) to bubble through a fritted disc as fine gas bubbles in the reaction mixture. The very small gas bubbles allowed good dispersion of ozone within the reaction medium. Excess gas and unreacted ozone was vented through the top of the reaction bottle through aqueous KI solution to destroy any unreacted ozone. Unless noted all the ozonolysis reactions were run at 0°C and maintained at this temperature with ice/water bath.

4.3.2 *Catalytic Ozonolysis*

Reactions with a Model Compound

Linoleic acid was used as a model compound for evaluation of the ozone attack on the double bonds. Linoleic acid and ethylene glycol were placed in the 500 ml reaction bottle and cooled with ice/water to 0°C. Ozone was allowed to bubble through while samples were removed periodically and analyzed to determine the extent of double bond disappearance by iodine test.

Ozonolysis of Soybean Oil

Soybean oil, ethylene glycol and various amounts of catalysts (NaOH, pyridine, 4-DMAP or CaCO₃) were placed in a 500 ml gas wash bottle and cooled to 0°C in an ice water bath and then ozone was bubbled through the reaction mixture. The product was then washed with distilled water 5 times (twice with 0.2M HCl to neutralize the base) in order to remove any excess ethylene glycol and catalyst (when CaCO₃ was used as a catalyst, it was filtered out through a fine filter paper). The product was then dried over molecular sieves for 48 hours prior to testing.

4.3.3 Characterization Procedures

The number of double bonds was determined by measuring the iodine value according to ASTM test method D1959. The iodine value is defined as centigrams of I₂ per gram of sample. The hydroxyl value was determined by ASTM test method D1957. Hydroxyl value is defined according to this test as the number of milligrams KOH equivalent to hydroxyl content of 1 g of sample.

Functional groups were identified using Perkin-Elmer FTIR model 1000 using at least 64 scans. The spectra were obtained after polyol samples were dissolved in chloroform and a drop of the solution was placed on a sodium chloride plate. The solvent was allowed to evaporate leaving a thin film on the surface of the crystal. The sample cell was constantly purged with dry nitrogen while the signal was acquired.

NMR spectra were obtained on a 500 MHz model INOVA 500 instrument. Samples were dissolved in deuterated chloroform, and the ¹³C NMR spectra were obtained at room temperature.

4.4 RESULTS AND DISCUSSION

4.4.1 Reactions with Ozone

Ozone is a very powerful oxidation agent and is well known to attack and cleave double bonds in alkenes. Aside from its high oxidation potential, ozone oxidation is convenient since unreacted ozone simply decomposes back to oxygen and no special neutralization or separation are required at the end of the reaction. Furthermore, since ozone is being produced “on site” it does not require complex logistics in transport, storage and disposal as many other oxidation agents. The oxidation of linoleic acid under our reaction conditions was used as a model compound for the ozonolysis reaction by following the disappearance of carbon-carbon double bonds (**Figure 4.7**).

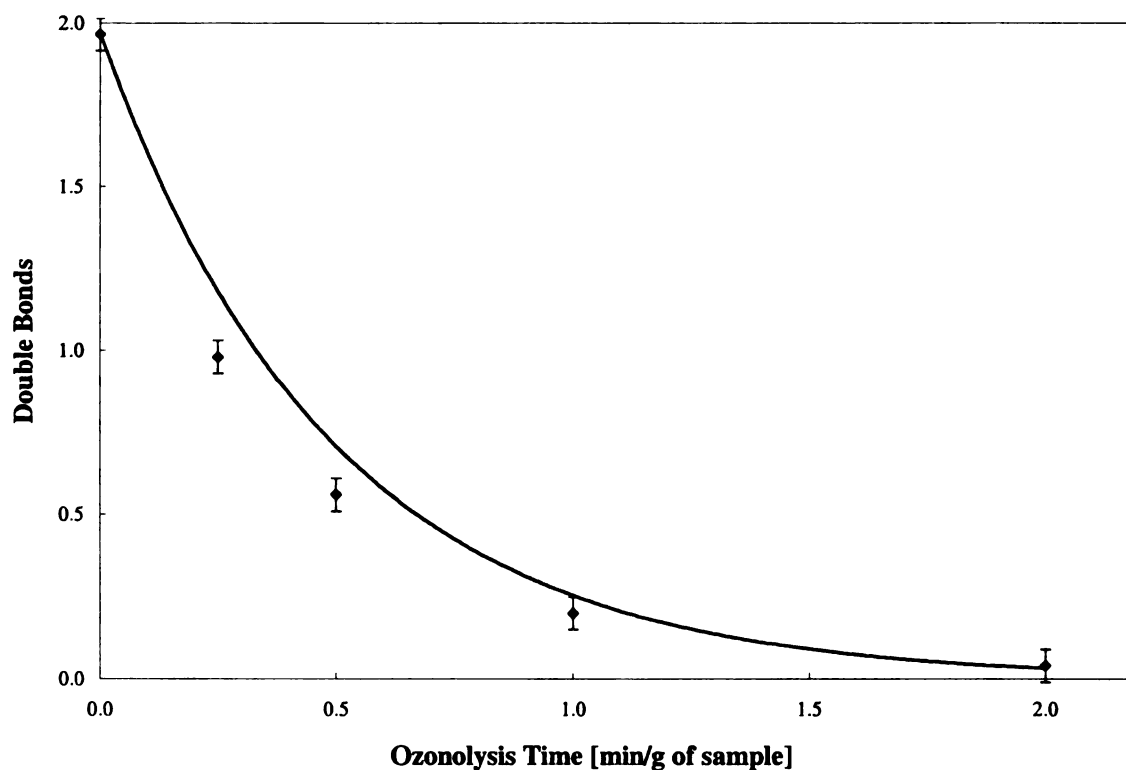


Figure 4.7: Ozonolysis Reaction with a Model Compound

It is observed that under these conditions all the double bonds were cleaved within 2 minutes (g of soy oil basis). It is well known that in the absence of participating solvents, unstable 1, 2, 4-trioxolane and peroxide oligomers are formed by the Criegee mechanism and these species eventually decomposed to a mixture of aldehydes and carboxylic acids. Some products containing hydroxyl groups were also noted when ethylene glycol was present, even after excessive washing and separation to remove any traces of this alcohol from the oil. This is not surprising since alcohols (and protic solvents in general) are known to impact the rate of the reaction and react with the ozonide intermediate (11). However, the course of the reaction is changed in the presence of an alkaline catalyst, which leads to an ester linkage between the decomposing ozonide intermediate and the alcohol (12).

Fraction	Composition	Symbol	Frequency	-OH
I	Nonanoate, Nonanoate, Nonanoate	NNN	0.23520	3
	Nonanoate, Nonanoate, Palmitate	NNP	0.09240	2
	Nonanoate, Nonanoate, Stearate	NNS	0.04200	2
	Nonanoate, Palmitate, Stearate	NPS	0.01100	1
	Palmitate, Palmitate, Nonanoate	PPN	0.01210	1
	Palmitate, Palmitate, Palmitate,	PPP	0.00053	0
	Palmitate, Palmitate, Stearate	PPS	0.00072	0
	Stearate, Stearate, Nonanoate	SSN	0.00250	1
	Stearate, Stearate, Palmitate	SSP	0.00033	0
	Stearate, Stearate, Stearate	SSS	0.00005	0
	Bis(2-hydroxyethyl) malonate	EE	0.26984	2
II	(2-hydroxyethyl) nonanoate	E1	0.09524	1
	(2-hydroxyethyl) hexanoate	E2	0.20635	1
	(2-hydroxyethyl) propionate	E3	0.03175	1

Table 4.1: Statistical Distribution of Soy Polyol

Nominally, the ozonolysis reaction of alkene with excess ethylene glycol and an alkaline catalyst (e.g. NaOH) is expected to yield a mixture of polyols as shown in

Figure 2.8:

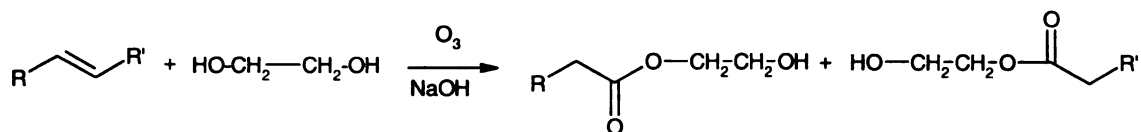


Figure 4.8: Catalytic Ozonolysis of Alkene with Ethylene Glycol

4.4.2 Composition of Ozone Treated Soy Oil

Similarly, when soy oil was exposed to ozone in the presence of ethylene glycol and NaOH the cleavage of the carbon-carbon double bonds and the reaction of hydroxyl groups with the ozonide intermediate yielded a mixture of polyols as shown in **Figure 4.9**. This product mixture was clear, and had a lower viscosity than the starting soy oil. A closer examination into the composition of this polyol mixture indicates two distinct fractions of about equal weights (**Table 4.1**); a relatively high molecular weight triglyceride fraction and a low molecular weight fraction. The high molecular weight fraction consists of the triglycerides that were cleaved at the 9th position of the unsaturated fatty acid residues and reacted with ethylene glycol. Thus, NNN denotes a triglyceride composed of only 2-hydroxyethyl nonanoate esters. This triglyceride was obtained from any triglycerides that contained only unsaturated fatty esters (e.g. oleic, linoleic, or linolenic). Since the first double bond is always found at the 9th position, cleavage occurs there and this active center reacts with ethylene glycol as indicated in scheme 1. Similarly, NNS denotes a triglyceride composed of two 2-hydroxyethyl nonanoate esters and one stearic ester. Since stearic acid does not contain double bonds, it

is not affected by the ozonolysis reaction and remains unchanged. However, the other two fatty acids in the original triglyceride contained double bonds and, thus, produced 2-hydroxyethyl nonanoate esters. The low molecular weight fraction is composed of the fragments that were cleaved beyond the double bonds of the unsaturated fatty acid.

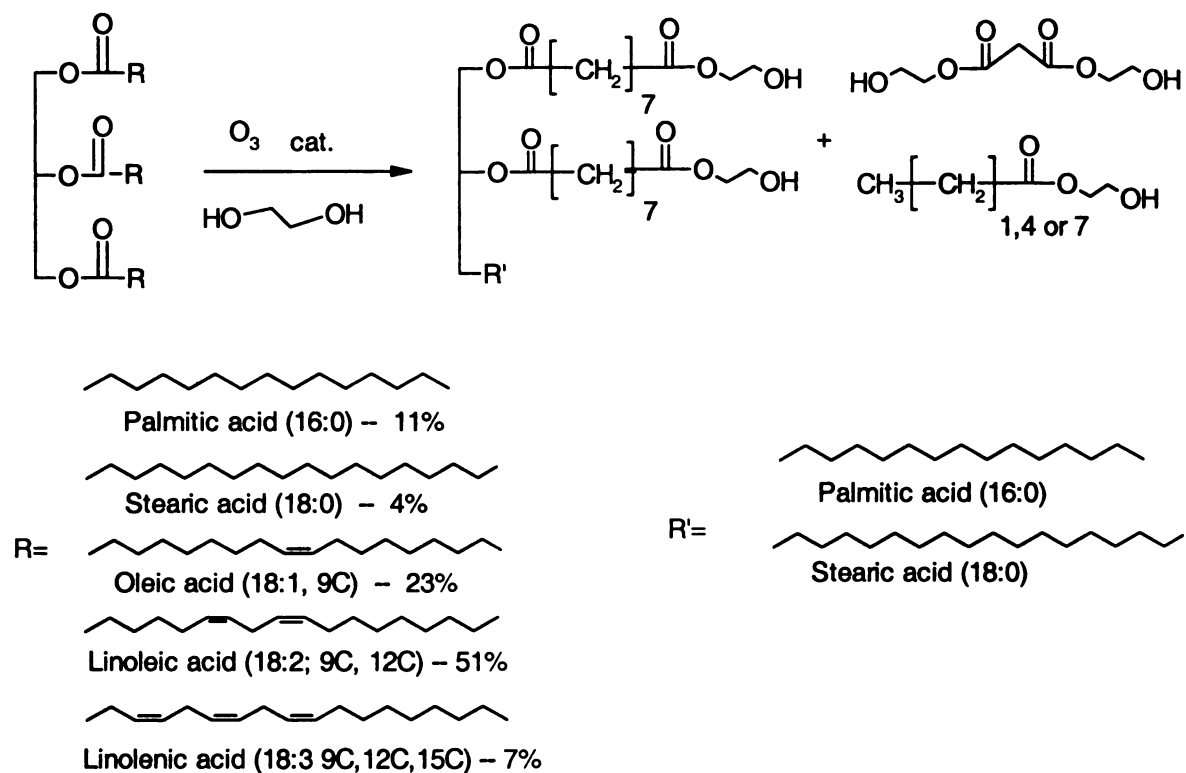


Figure 4.9: Catalytic Ozonolysis Products of Soy Oil with Ethylene Glycol

It should be noted that about 45% of these fractions are composed of the diol bis(2-hydroxyethyl) malonate and the rest is a mixture of mono functional alcohols (**Figure 4.10**). Fraction 1 contains about 24 wt% triols (NNN), 13 wt% diols (NNP and NNS), less than 3 wt% mono functional alcohols (NPS, PPN and SSN) and a very small fraction (less than 0.2 wt %) of unreactive triglycerides having no hydroxyl groups.

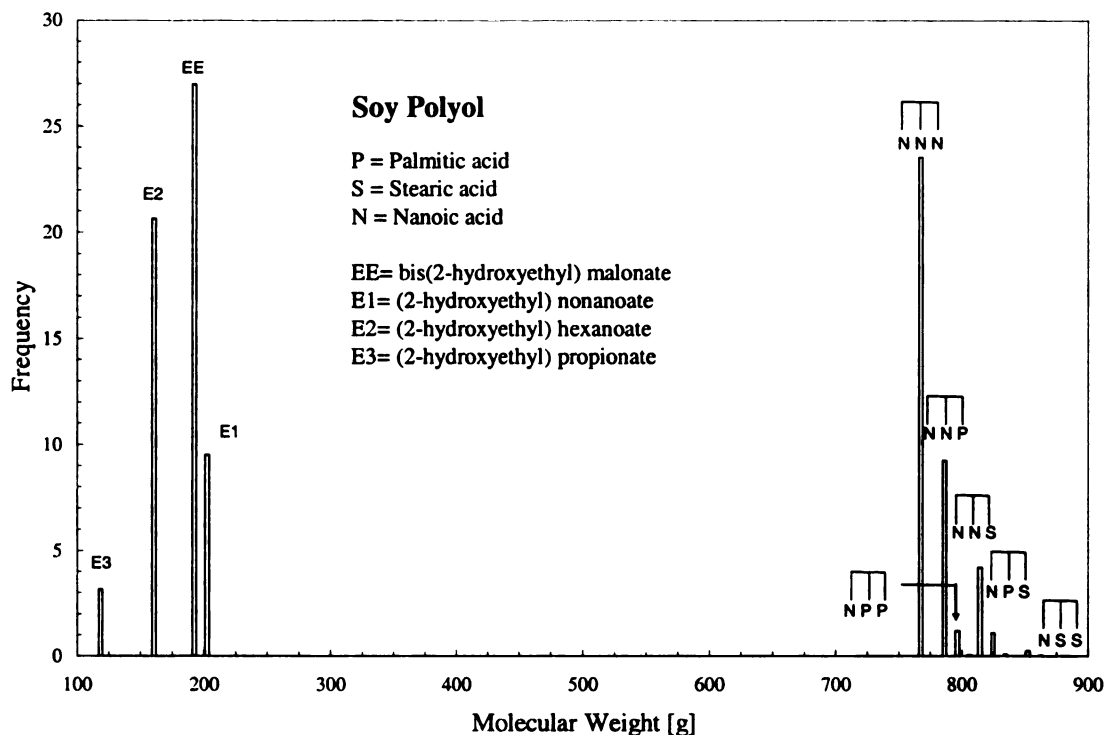


Figure 4.10: Statistical Distribution of Soy Polyols

The average functionality of the soy polyol can be calculated based on these statistical data using:

$$f_{av} = \frac{\sum n_i f_i}{\sum n_i}$$

Figure 4.11: Average Functionality

Where, n_i , is the number of moles of species containing functionality f_i . Accordingly, the maximum hydroxyl functionality is 1.9 per mole of soybean oil (**Figure 4.11**).

In practice, the hydroxyl functionality may be higher if the ozonolysis reaction is not terminated after all the double bonds are consumed and hydrocarbon chains are cleaved. Similarly, a hydroxyl functionality lower than 1.9 is expected if the ozonolysis reaction is terminated before all the double bonds are consumed. Additionally, our

calculation did not take into account complications such as the reaction of both hydroxyl groups of ethylene glycol. In this case a high molecular weight product is expected if ethylene glycol reacts with two triglycerides. On the other hand, intramolecular reactions, where ethylene glycol reacts with two fatty acids in the same triglyceride, will lead to cyclization and loss of hydroxyl functionality. Similar complications could arise when any of the hydroxyl terminated fragments in fraction II reacts with another triglyceride instead of ethylene glycol. Most of this complication could be avoided, or at least greatly minimized, by using a large excess ethylene glycol in the reaction mixture.

The process conditions can further be adjusted to control the molecular weight and the hydroxyl number of the product by using triols or other common low molecular weight polyols instead of ethylene glycol. Alternatively, the catalyzed ozonolysis reaction with polyethylene glycols of different molecular weights, instead of ethylene glycol, yields products containing different polyether chain lengths. Subsequent reaction of these polyols with isocyanates gives flexible polyurethane foams with various degrees of flexibility, depending on the molecular weight of the polyethers used in the ozonolysis reaction.

As expected, the soy polyol mixture is characterized by a broad hydroxyl stretching peak around 3500 cm^{-1} , the complete disappearance of the $=\text{C}-\text{H}$ band at 3005 cm^{-1} and the $\text{C}=\text{C}$ stretch at 1650 cm^{-1} (**Figure 4.12**). This set of FTIR spectra further indicates that at the end of the ozonolysis reaction the carbonyl stretch at 1743 cm^{-1} became broader suggesting the formation of new carbonyl compounds. A significant increase in the 1105 cm^{-1} band was also observed and that was assigned to $\text{C}-\text{O}$

stretching. It is important to note here that no absorptions were noted around 2900–2700 cm^{-1} indicating the absence of aldehydic C---H stretch.

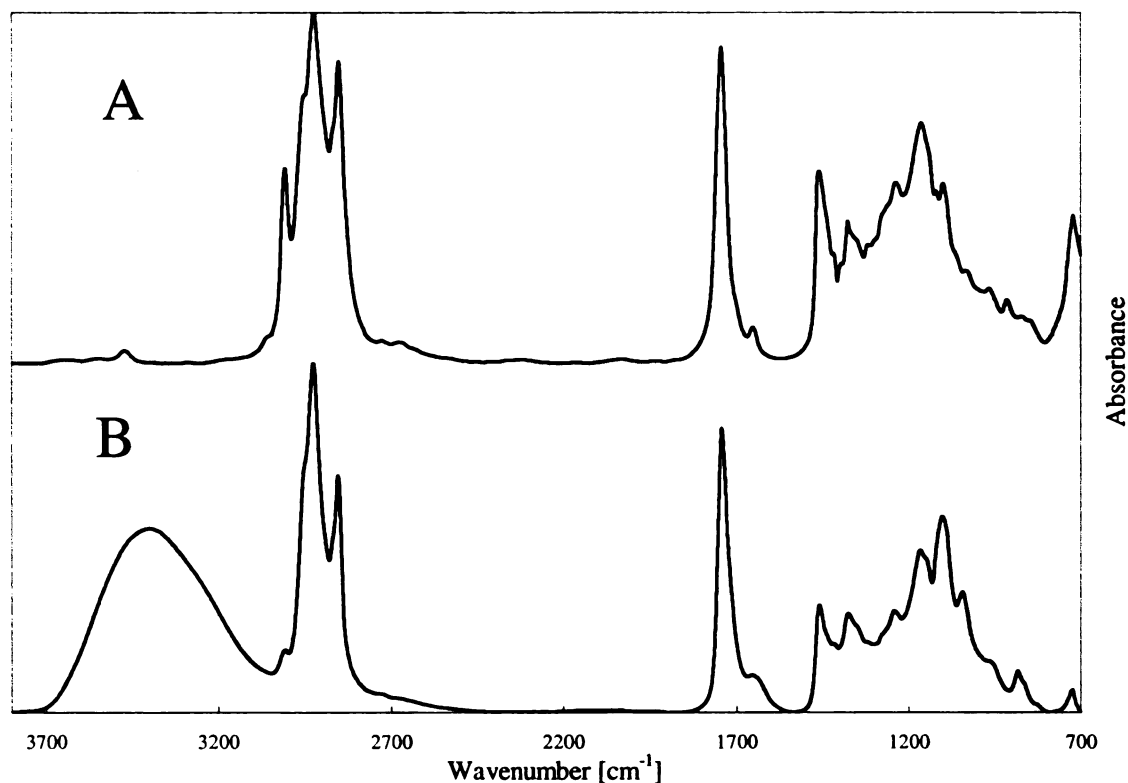


Figure 4.12: FTIR of Soy Oil (A) and Soy Polyol (B)

It was also observed that while keeping the reaction time constant, the hydroxyl number was directly proportional to the concentration of the NaOH and increased to 1.96 when 0.4 M NaOH was used. However, further attempts to use higher NaOH concentrations caused saponification of the triglyceride ester linkages and the formation of free glycerol.

Possible saponification and the difficulty associated with removing traces of NaOH from the reaction mixture even after neutralization and repeated washing led us to examine alternative base catalysts. One class of potential catalysts we examined was various amines (e.g. 4-dimethylamino pyridine (4-DMAP), pyridine, triethylamine, tributylamine, dimethylamine and hexamethylene diamine). It was observed that similar

soy polyol products were obtained when any of these amines were used (**Appendix A**). As was the case with NaOH, the number of double bonds continuously decreased as a function of ozonation time and the hydroxyl number simultaneously increased (**Figure 4.13**).

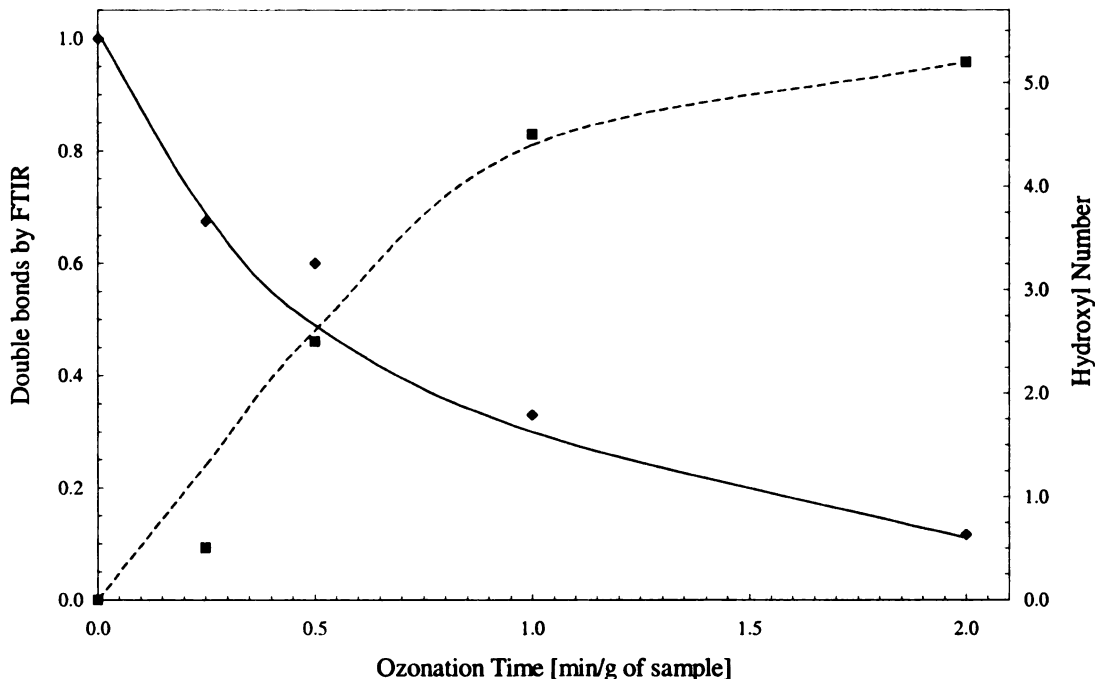


Figure 4.13: Hydroxyl Number (---) and Double Bonds (—) as a Function of Ozonolysis Time

It is important to note that unlike previous methods in the literature describing preparation of soy polyols, our one step ozonolysis process appears to yield high hydroxyl numbers and primary alcohols in a simple, fast reaction. The rate of cleavage of the double bonds was independent of the amine catalyst and was directly proportional to the amount of ozone and the dispersion of the ozone bubbles in the reaction medium. Hydroxyl numbers were directly related to the type of amine used and its concentration. Although the reaction proceeded as anticipated it was noted that the polyol product was

dark-yellow to brown depending on the type of amine that was used due to its oxidation in the course of the reaction (13). It was further noted that strong bases like 4-DMAP led to saponification of the fatty esters in the soy oil as observed with NaOH.

4.4.3 Reactions with Heterogeneous Catalysis

Another class of potential catalysts that appeared most useful was inorganic alkaline oxides and carbonates (such as MgO and CaCO₃). These heterogeneous catalysts are effective and can simply be filtered out and removed from the reaction mixture with no need for neutralization. These heterogeneous catalysts can further be recycled and reused without any special treatment. To the best of our knowledge, only zeolites (14) were claimed to be heterogeneous catalysts in ozonolysis reactions although these catalysts were used without additional hydroxyl compounds to in the production of dicarboxylic acid from alkenes by ozonolysis. The progress of the reaction whereby double bonds were cleaved and hydroxyl groups were incorporated is clearly seen by FTIR (**Figure 4.14**). In addition to convenient removing and recycling this heterogeneous catalyst, the soy polyol product is light-yellow, low viscosity oil suitable for further use in the production of polyurethanes and polyesters without further purification.

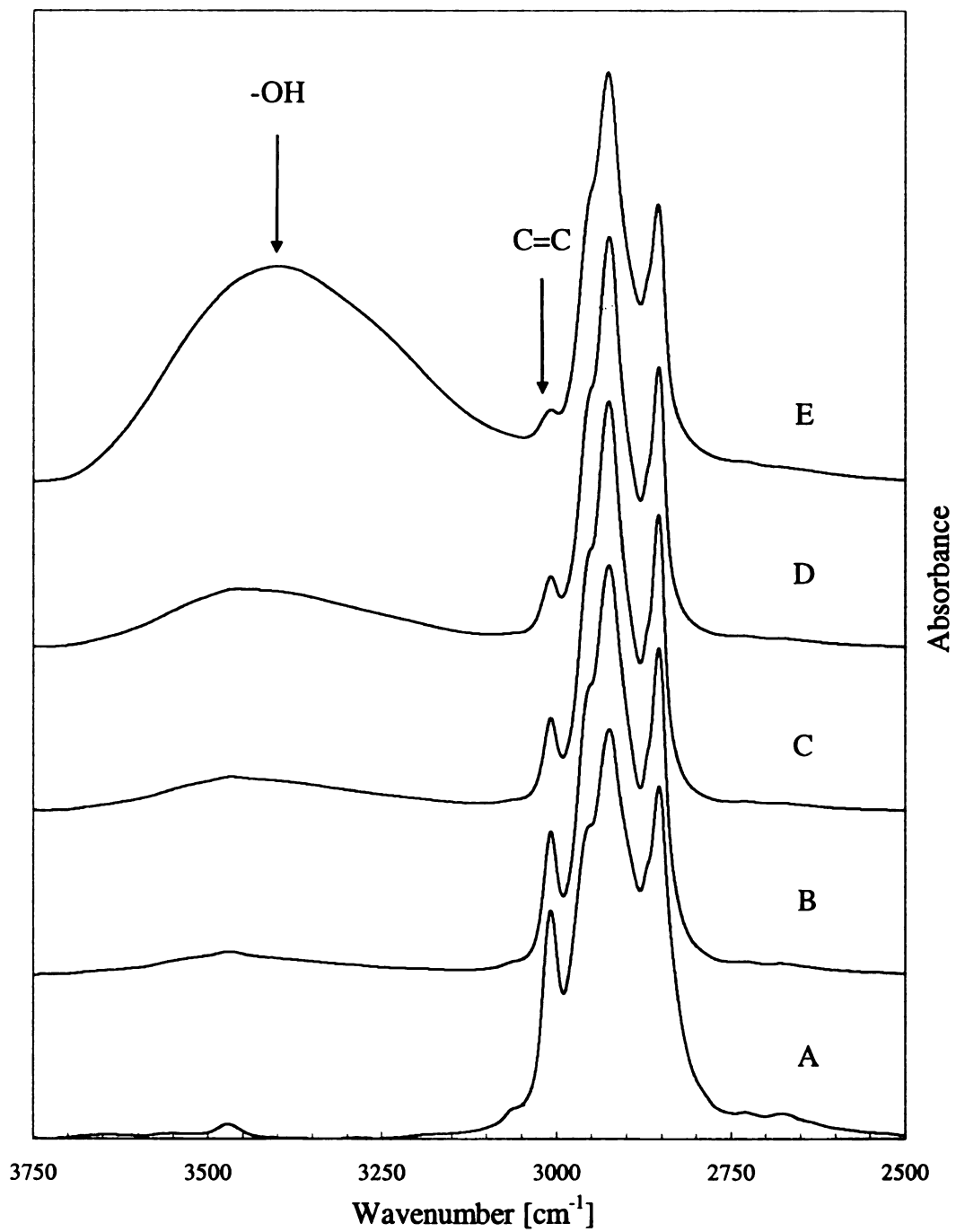


Figure 4.14: Hydroxylation of Soy Oil using CaCO_3 at Different Ozonolysis Times: (A) $t=0$; (B) $t=0.25$; (C) $t=0.5$; (D) $t=1.0$; and (E) $t=2.0$ min/g of soy oil

Further confirmation of the soy polyol structure was obtained from ^{13}C NMR spectra (Figure 4.15 and 4.16). The characteristic double bonds peaks at 130 ppm, related to the unsaturated fatty acid in the soy oil, are missing in the soy polyol spectrum indicating complete cleavage of the double bonds. The carbonyl ester peaks (177 ppm) and the various methylene peaks (between 25 and 36 ppm) remained unchanged as were the glycerol carbons (64 and 69 ppm). Additionally, new resonance peaks appear at 66 ppm related to ethylene oxide carbons as well as peaks at 60 ppm related to the new C-OH functional groups. It is apparent from the NMR data that the hydroxylation of soybean oil progressed as expected to yield the desired polyols.

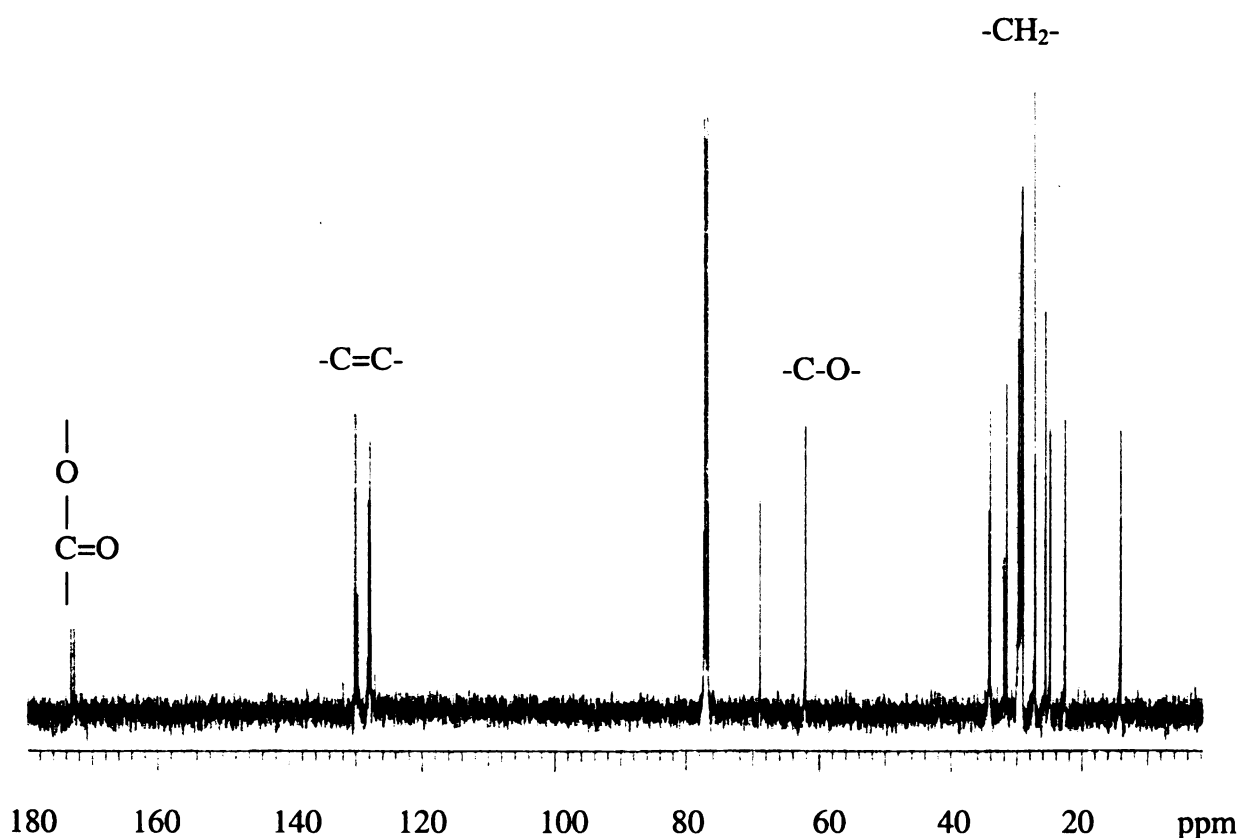


Figure 4.15: ^{13}C -NMR of Soy Oil

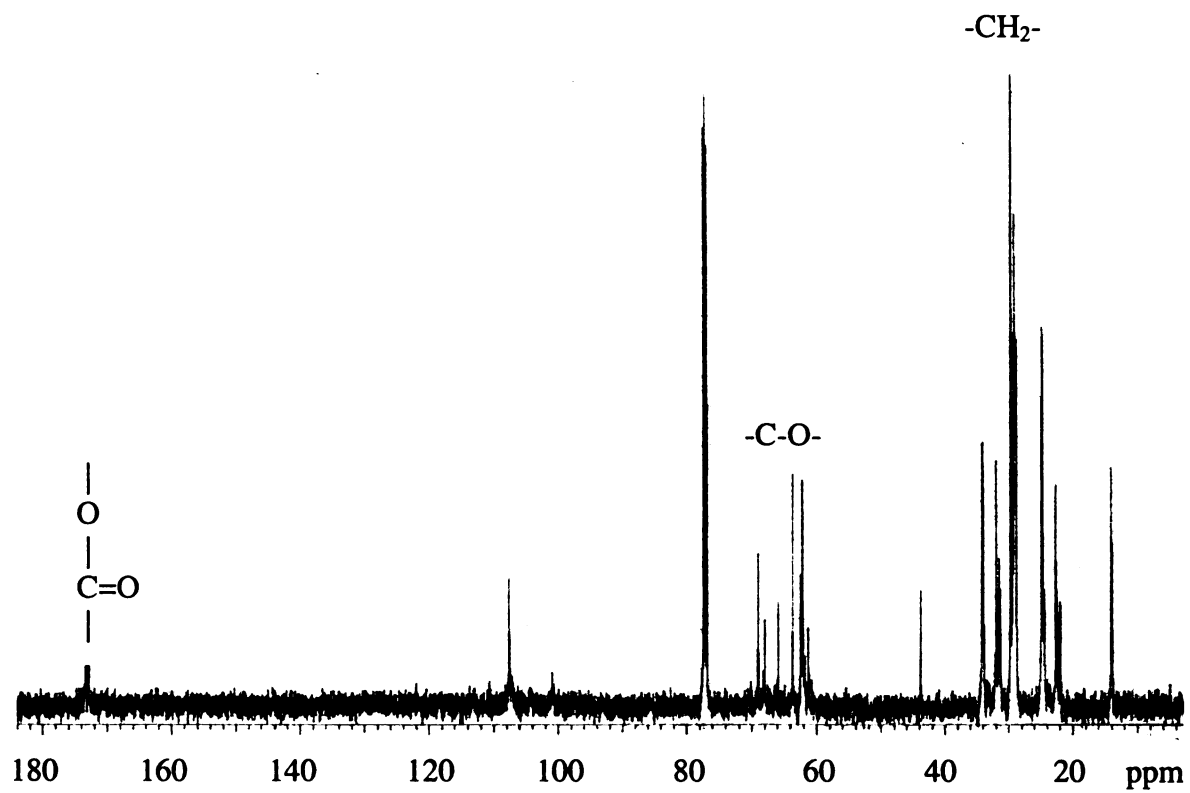


Figure 4.16: ^{13}C -NMR of Soy Polyol

4.5 CONCLUSIONS

A new class of soy-based polyols was prepared using a simple single step synthesis. This novel synthesis involves an ozone mediated reaction between soy oil with a multi-functional hydroxy compound in an alkaline medium. The reaction proceeded rapidly at room temperature, without an additional solvent. The alkaline medium facilitated the redirection of the decomposition of the ozonides to form ester linkages between the soy oil molecules and a hydroxy compound. The reaction proceeded with both strong bases (NaOH) and mild bases (pyridine). Sodium hydroxide was not a desirable catalyst because of its limited solubility and side reactions such as saponification. Pyridine was used because it had good solubility, however, its negative health effects make it an unlikely candidate for potential large scale commercial applications. Thus, triethylamine was used as an alternative. The resulting polyols were a dark yellow to brown color due to oxidation of the amine. Tributylamine, was evaluated because it has better oxidative stability, however, these polyols also changed color over time. Using an alkaline heterogeneous catalyst, such as CaCO_3 , solved previously mentioned difficulties. CaCO_3 did not cause saponification of the triglyceride; however, it was sufficient to promote the formation of the ester linkages. Furthermore, the CaCO_3 could easily be removed and recycled by filtering. Using CaCO_3 a series of soy polyols with varying hydroxyl functionalities was prepared varying the hydroxyl compound (eg – ethylene glycol, 1,4-butanediol, glycerol, PEG, PVOH, starch). Additionally, soy-based amino compounds were prepared by using ethanolamine. Using ozone chemistry as a platform, a portfolio of biobased building blocks were prepared as an alternative to traditional petroleum feedstocks.

4.6 REFERENCES

1. Stanton, J.M., Isocyanate-Modified Drying Oils, J. Am. Oil Chem. Soc. 36: 503-507
2. Wells, E.R., and J.C. Hixenbaugh, Am. Paint J. 46: 88 (1962).
3. Sherringham, J.A., A.J. Clark, and B.R.T. Keene, New Chemical Feedstocks from Unsaturated Oils, Lipid Technology 12: 129-132 (2000).
4. Gruber, B., R. Hoefler, H. Kluth, and A. Meffert, Polyols on the Basis of Oleochemical Raw Materials, Fett Wissenschaft Technologie 89: 147-151 (1987).
5. Heidbreder, A., R. Gruetzmacher, U. Nagorny, and A. Westfechtel, Use of Fatty Ester-based Polyols for Polyurethane Casting Resins and Coating Materials
6. Frankel, E.N., and E.H. Pryde, Catalytic Hydroformylation and Hydrocarboxylation of Unsaturated Fatty Compounds, J. Am. Oil Chem. Soc. 54: 873-881 (1977).
7. Khoe, T.H., F.H. Otey, and E.N. Frankel, Rigid Urethane Foams from Hydroxymethylated Linseed Oil and Polyol Esters, J. Am. Oil Chem. Soc. 49: 615-618 (1972).
8. Guo, A., D. Demydov, W. Zhang, and Z.S. Petrovic, Polyols and Polyurethanes from Hydroformylation of Soybean Oil, Polym. and the Environ. 10: 49-52 (2002).
9. Takahara, J., and T. Setoyama, Process for Preparation of Polyhydric Alcohols by Oxidation of Olefins having a Carbonyl Group and Catalytic Hydrogenation, WO Application Patent 2002049999 (2002).
10. Michaelson, R.G., and R.C. Austin, Hydroxylation of olefins, US Patent 4314088 (1982).
11. Ledea, O., J. Molerio, M. Diaz, D. Jardines, A. Rosado, and T. Correa, Revista CENIC, Ciencias Quimicas 29: 75-78 (1998).
12. Marshall, J.A., and A.W. Garofalo, Oxidative Cleavage of Mono-, Di-, and Trisubstituted Olefines to Methyl Esters through Ozonolysis of NaOH, J. Org. Chem. 58: 3675-3680 (1993).
13. Bailey, P.S., J.E. Keller, D.A. Mitchard, and H.M. White, Ozonation of Amines, Advances in Chemistry Series 77: 58-64 (1968).
14. Rebrovic, L., Catalyzed Process for Oxidation of Ozonides of Unsaturation to Carboxylic Acids, US Patent 5,399,749 (1995).

Chapter 5: Continuous Process for the Catalytic Ozonolysis of Soy Oil

5.1 INTRODUCTION

5.1.1 Soy Polyol Production

Present day commercial applications of continuous ozonolysis are primarily for water treatment applications and odor removal on farms. Recently, Cognis has commercialized the preparation of nonanoic and azelaic acid by the ozonolysis of oleic acid in water. Common to all the processes is the low organic concentration within the aqueous mixture. Among the novelties of the proposed catalytic ozonolysis is the absence of a solvent. In the proposed process a high fatty acid mass composition is possible because the alkaline medium facilitates the decomposition of the ozonides, to prevent the formation of polymeric peroxides (**Chapter 4**). The ozone mediated synthesis of soy polyols involves a series of competitive reactions as seen in **Figure 5.1**. Competitive reactions of ozone are:

- 1) Decomposition back to O_2
- 2) Reaction with H_2O to form H_2O_2
- 3) Reaction with double bonds to form a molozonide

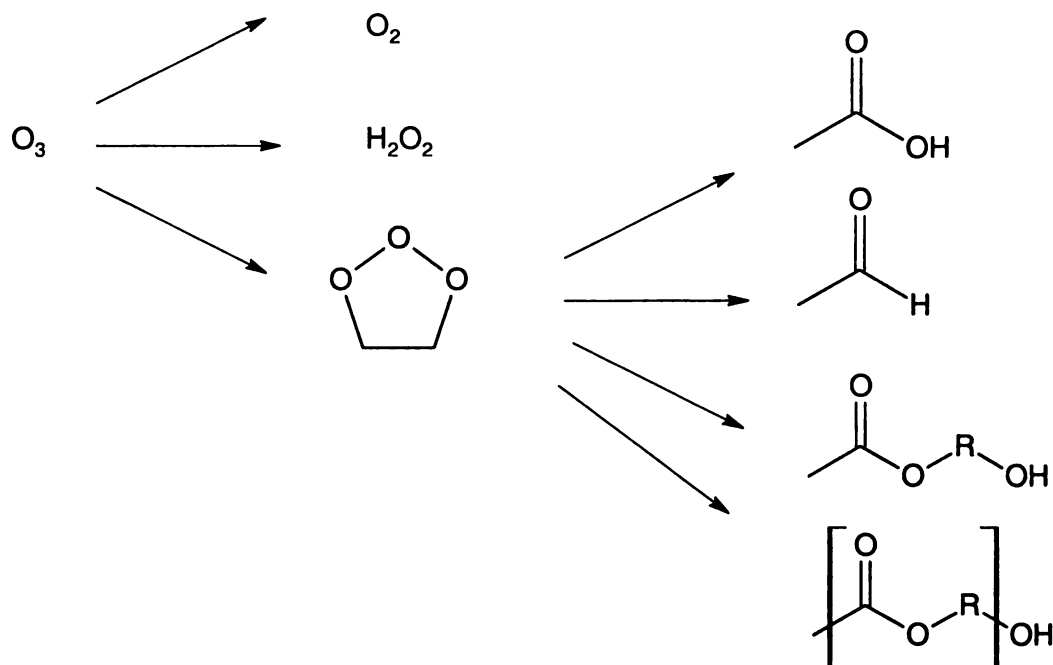


Figure 5.1: Competing Reactions of Ozone

Of these competing reactions the selectivity of ozone favors the reaction with double bonds. The molozonide being an unstable 5 member ring, further undergoes decomposition resulting in the formation of aldehydes and carboxylic acids. However, in the presence of an alkaline medium it is further observed that the decomposition of the ozonides can be redirected to form ester linkages with hydroxyl groups. Furthermore if reactions are carried out in the presence of multifunctional compounds, such as ethylene glycol, soy-based polyols can be prepared. The soy polyols can further undergo oligomerization reactions with decomposing ozonides. To increase the yield of the soy polyols and/or oligomers of the soy polyol various process parameters were studied and optimized, and a proof-of-concept was established for the continuous production of soy polyols using ozone chemistry.

5.2 REACTOR DESIGN THEORY

5.2.1 Batch and Continuous Reactors

In – Out + Generation = Accumulation

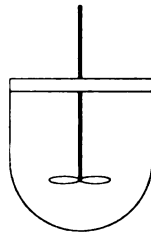
$$F_{in} - F_{out} + \int_V r_i dV = \frac{dN_i}{dt} \quad \text{“Figure 5.2: General Mole Balance”}$$

Batch Reactor:

- There is no flow in or out of the system.
- Perfect mixing so there is no spatial variation in the reaction rate.
- In this case the mole balance simplifies.

$$\frac{dN_i}{dt} = r_i V \quad \text{“Figure 5.3: Batch Reactor Mole Balance”}$$

There are 2 primary types of batch reactors: Constant Volume and Constant Pressure



$$\frac{dC_i}{dt} = r_i \quad \text{“Constant Volume”}$$

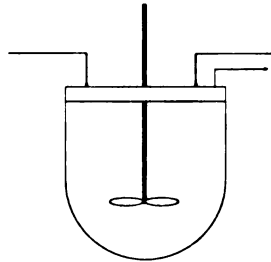
$$\frac{dC_i}{dt} + \frac{C_i d \ln V}{dt} = r_i \quad \text{“Constant Pressure”}$$

Figure 5.4: Batch Reactor Design Equation

Batch reactors are not favorable for large-scale ozone application. Due to the large oxygen content the reaction intermediates are unstable. Thus, the ozonide concentration should be minimized. Gaseous ozone becomes explosive when concentrations reach 240 g/m³. Most ozonation systems are in the range of 50-200 g/m³. So, for safety concerns large-scale batch applications would require the use of solvents. Alternatively, the ozonide concentration can be minimized using a continuous flow reactor. There are 2 general types of flow reactors.

Continuous Stirred Tank Reactor (CSTR):

- Good mixing resulting in no spatial variations in concentration, temperature, or reaction rate throughout the reactor
- Easy maintenance and good temperature control
- However, CSTR has the lowest conversion per reactor volume for flow reactors
- For a CSTR the mole balance simplifies to:



$$V = \frac{F_{in} - F_{out}}{-r_i}$$

Figure 5.5: Continuous Stirred Tank Reactor Design Equation

Plug Flow Reactor (PFR)

- The concentration does not vary in the radial direction
- Reactants are consumed as the flow through the length of the reactor (Reaction rate varies as the concentration changes axially)
- The extent of reaction depends on the reactor volume, and not shape
- The mole balance for a PFR simplifies to:

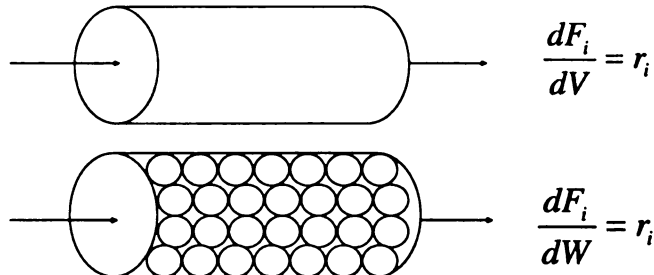


Figure 5.6: Plug Flow Reactor Design Equation

- For heterogeneous reactions, the reaction rate is based on the mass of the solid catalyst

5.3 REACTOR DESIGN METHODOLOGY

5.3.1 Comparison of Reactors

A CSTR offers the advantage of no spatial variations in temperature, concentration, or reaction rate. We will also consider non-ideal mixing which can result from the increased viscosity of the polyol. If mixing is determined to be highly non-ideal, alternative techniques such as residence time distribution (RTD) will be used. The major drawback of CSTR is they have the lowest conversion per reactor volume. A CSTR operates under the condition of lowest reactant concentration (eg – exit concentration), and thus the lowest value of the reaction rate.

A PBR has increased conversion per reactor volume. The main parameters when using a PBR are the temperature control, pressure drop, and reduced reactant concentration. Although, there is expected to be a pressure drop across the PBR, however, since the reaction is liquid phase; we are going to ignore the pressure drop because the concentration of reactants is insignificantly effected by changes in pressure (incompressible flow). So, the pressure drop is ignored for the liquid-phase kinetics. Alternatively, the decrease in concentration of ethylene glycol is expected to hinder the reaction because of oligomerization effects, or ozonides decomposition to a carboxylic acid (presence of H₂O) or the aldehyde.

Stoichiometry:

For our proposed process, if we consider each reaction between ozone and the double bonds present in soybean oil. The general reaction stoichiometry is:

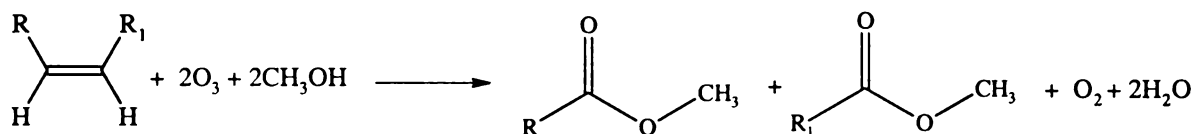


Figure 5.7: Ozonolysis Mole Balance

From the stoichiometry the relative reaction rates are: -1:-2:-2:1:1:1:2, respectively.

Nominally, the rate of reactant disappearance becomes:

$$-\frac{d[\text{DB}]}{dt} = -2\frac{d[\text{O}_3]}{dt} = -2\frac{d[\text{EG}]}{dt} \quad \text{“Figure 5.8: Rate of Reactant Disappearance”}$$

Where DB = Double Bonds

EG = Ethylene Glycol

While the rate of product formation equals:

$$2\frac{d[\text{Polyol}]}{dt} = 2\frac{d[\text{H}_2\text{O}]}{dt} = \frac{d[\text{O}_2]}{dt} \quad \text{“Figure 5.9: Rate of Product Formation”}$$

For every double bond 1 mole of ozone will react to form a primary ozonide which readily decomposes to form an aldehyde and carbonyl oxide (**Figure 4.3**). It is proposed that in an alkaline median the decomposition can be redirected to for ester linkages with hydroxyl groups (**Appendix A**). Furthermore, if a diol such as ethylene glycol is used, ester linkages with terminal hydroxyl groups will form. The reaction products are 2 moles of polyol, 2 moles of water and 1 mole of oxygen. Absent any side reactions 1 mole of soy oil (~4.6 double bonds per mole) could theoretically yield ~9 moles of polyol.

5.4 RESULTS AND DISCUSSIONS

5.4.1 Processing Parameters Consideration

Preliminary studies were done to further investigate the formation of the soy polyols using a heterogeneous catalyst. Variables such as reaction time, temperature, catalyst concentration, and catalyst particle size were studied. Based on the batch synthesis inside the gas wash bottle, it was observed that after 2 minutes of reaction time per gram of soy oil, 30% of the double bonds remained. Considering the reaction stoichiometry, a mass balance of the system shows only 30% of the ozone charged into the reacted with the soy oil. Although, some of the ozone could have reacted with moisture in the system, it is believed that most of the ozone simply exits the system into the destruction unit. A change of the frit location to face downward (initially ~130 degree angle), nearly doubled the reaction rate of the soy oil as seen in **Figure 5.10**

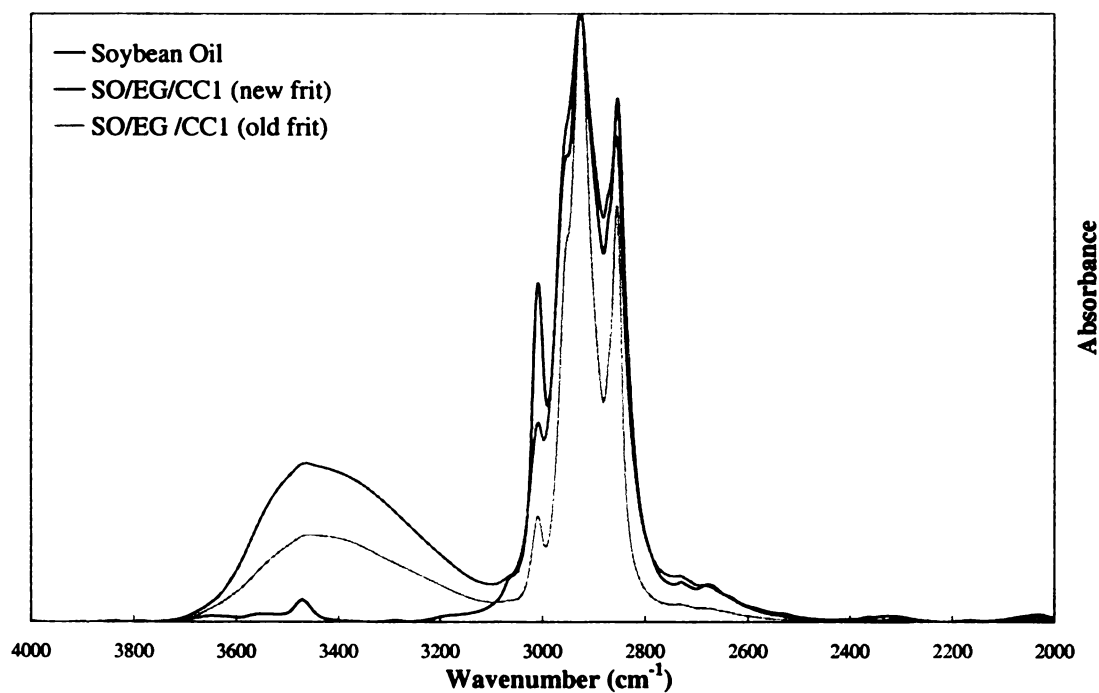


Figure 5.10: FTIR of Soy Polyol using Different Frit Locations

From these data it appeared that changing the frit location increased the hydroxyl content by increasing the mass transfer of ozone within the reaction mixture and thus improving the reaction yield. Positioning the frit at the bottom of the reactor increased the ozone dispersion within the reaction mixture. Under this condition the double bonds consumed within 1 minute were comparable to the 2 minute reaction time as noted previously.

Alternatively, for the reaction temperatures considered (0-25°C) the reaction rate was generally unaffected. In general terms the reaction rate tends double for 10°C increases in the reaction temperature. However, in the case of ozone reaction with double bonds, the activation energy is very small (ozone has a very high oxidation potential), so the reaction temperature does not significantly impact the reaction rate constant (which is related through the Arrhenius equation). Alternatively, increasing the temperature adversely effects the reaction rate since the activation energy is low, the reactions occur instantaneously, whereas the solubility of ozone is inversely related to the temperature. Consequently, these reactions appear to be mass transfer limited and not reaction limited

Furthermore, the catalyst concentration was found to be directly proportional to the hydroxyl content of the product. It was found that increasing the catalyst loading from 1 wt% to 10 wt% increased the rate of hydroxyl formation as seen by the intensity of the stretching at 3500 cm^{-1} as seen in **Figure 5.11**.

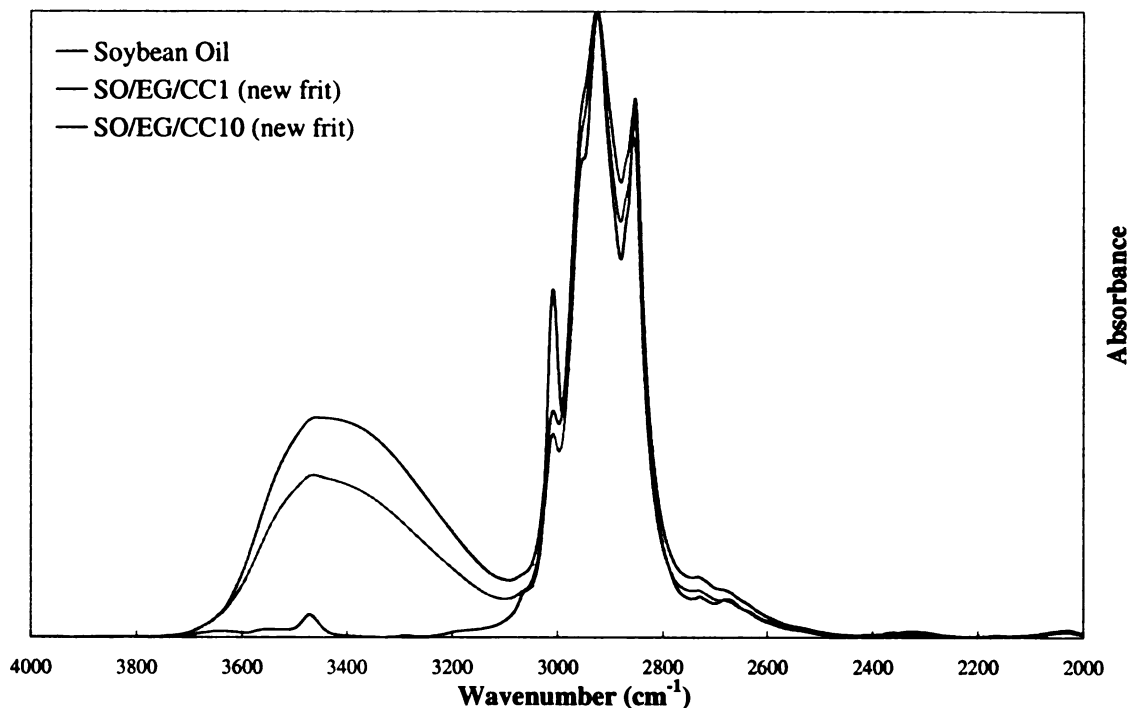


Figure 5.11: FTIR of Soy Polyol for Catalyst Loadings of 1 wt% & 10 wt%

Further increase in the catalyst loading may further increase the hydroxyl formation but operation above 10 wt% becomes difficult due to the resulting slurry of soy oil, ethylene glycol, and CaCO₃).

FTIR data indicate that the conversion was better when 10 mm CaCO₃ particles were used compared with smaller particle size CaCO₃ (micron) were used (**Figure 5.12**). Since, for equal catalyst loading (~10 wt %), the larger CaCO₃ particle will have less surface area than the smaller particle CaCO₃. These experiments suggest that the reaction is diffusion limited and not surface limited.

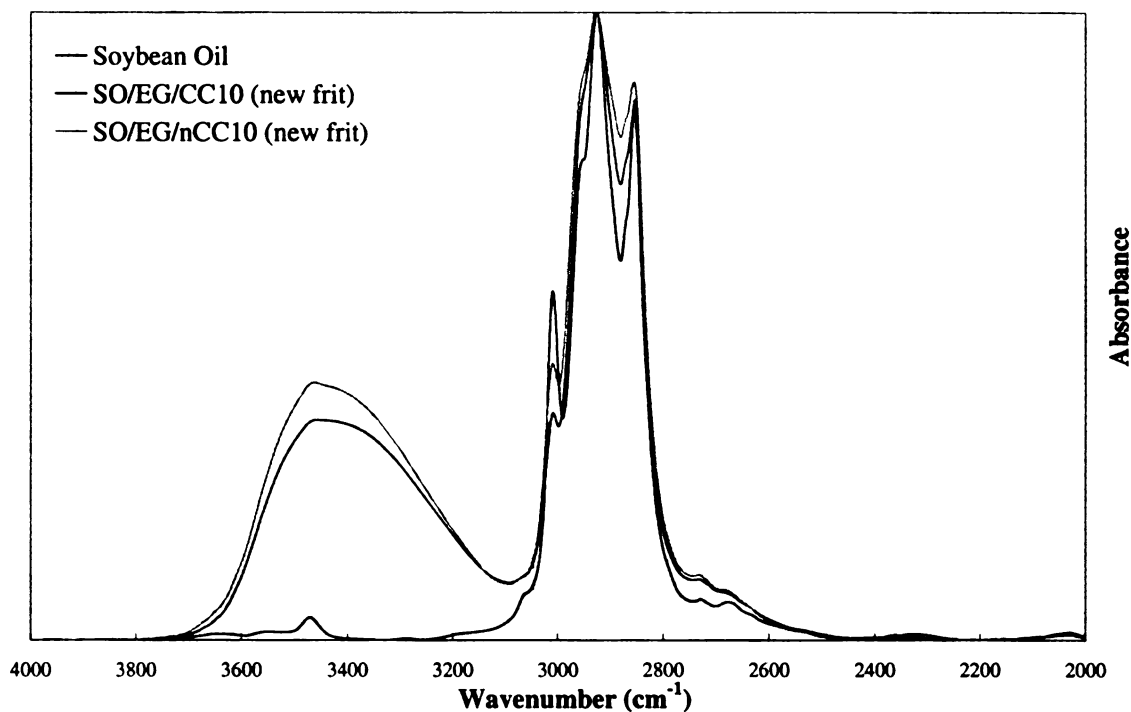


Figure 5.12: FTIR of Soy Polyols using Different Particle Sizes of CaCO₃

To verify this observation hydroxyl value and acid value were determined by titration.

CaCO ₃	Hydroxyl	Acid
10 mm	50	82
50 μm	128	10
10 μm	172	8

Table 5.1: Hydroxyl and Acid Value of Soy Polyols

The results of the titration suggest the larger absorption around 3500 cm⁻¹ in the FTIR using large particle size CaCO₃ is derived from the combination of -OH and -COOH functional groups. Alternatively, when smaller particles of CaCO₃ were used, the -COOH formation was considerably less. It should be noted that when no catalyst was used the hydroxyl number was very low (< 8 mgs of KOH/g of sample) indicating very

little polyol formation. Also, the moisture content was ~8 wt% (determined by TGA). The titrations suggest the hydroxyl is affected by the catalyst surface area. To rule out the hydroxyl number was not due to ethylene glycol remaining in the polyol, a repeat of the earlier experiment was done using methanol instead of ethylene glycol (residual methanol was stripped off) as seen in **Figure 5.13**.

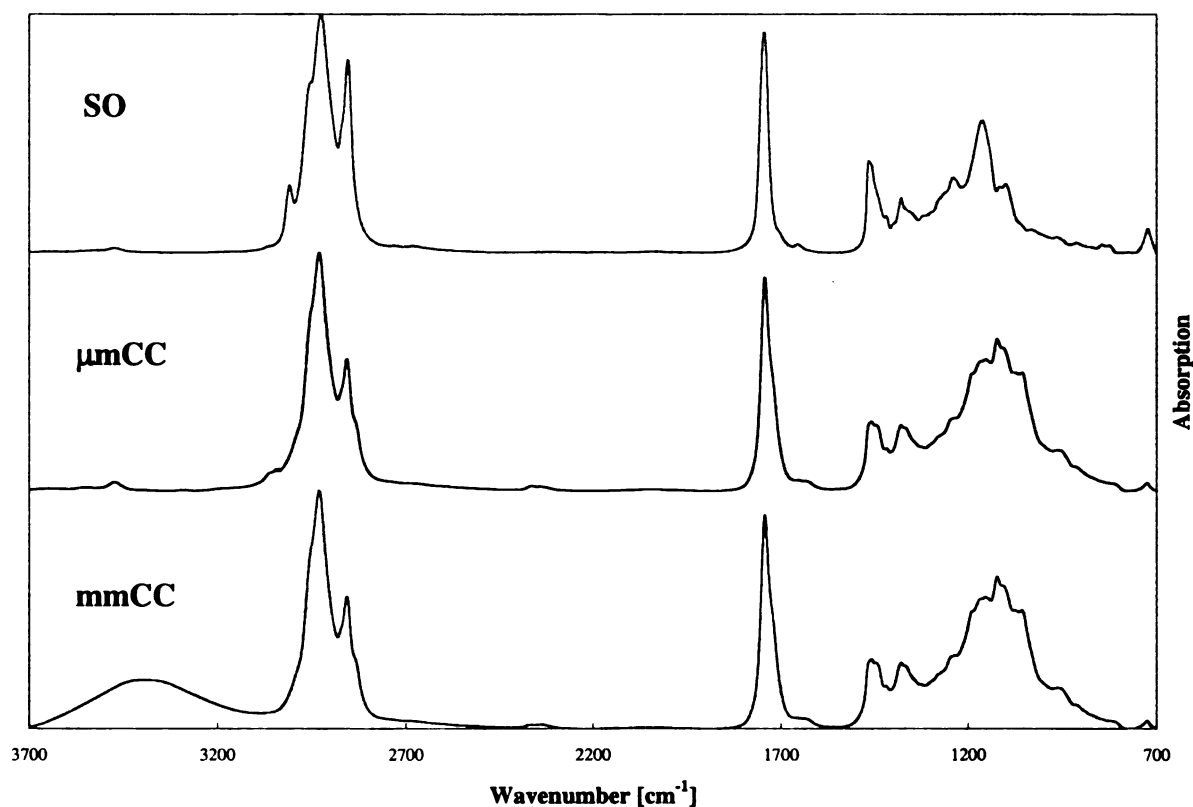


Figure 5.13: Variation of Catalyst Particle Size using a Model Compound

FTIR from the reaction using methanol indicates using larger particle size CaCO_3 had a substantially absorbance at 3500 cm^{-1} whereas there is only a slight absorbance when smaller particle CaCO_3 is used. It should be further noted, that even finer CaCO_3 particle size lead to an increase in the hydroxyl content and decrease in the carboxyl content, however, removing the CaCO_3 became very difficult. Commercially, the extent of

increased hydroxyl formation has to be weighed against the difficulty in removing the catalyst.

Heterogeneous catalyst offers the advantages of recyclability and ease of removal. Preliminary studies suggest the optimal reaction conditions to be 10 wt% loading of 50 μm particle size CaCO_3 . Due to the reactivity of ozone towards double bonds (low activation energy), the optimal temperature is room temperature (with cooling water available for safety). The greatest impact to the reaction rate is the mass transfer of ozone, and specifically the residence time of ozone within the system as seen by the changing of the frit location. Additionally, an economic evaluation of the current polyol production cost is most sensitive to production cost of ozone (**Figure 5.14**).

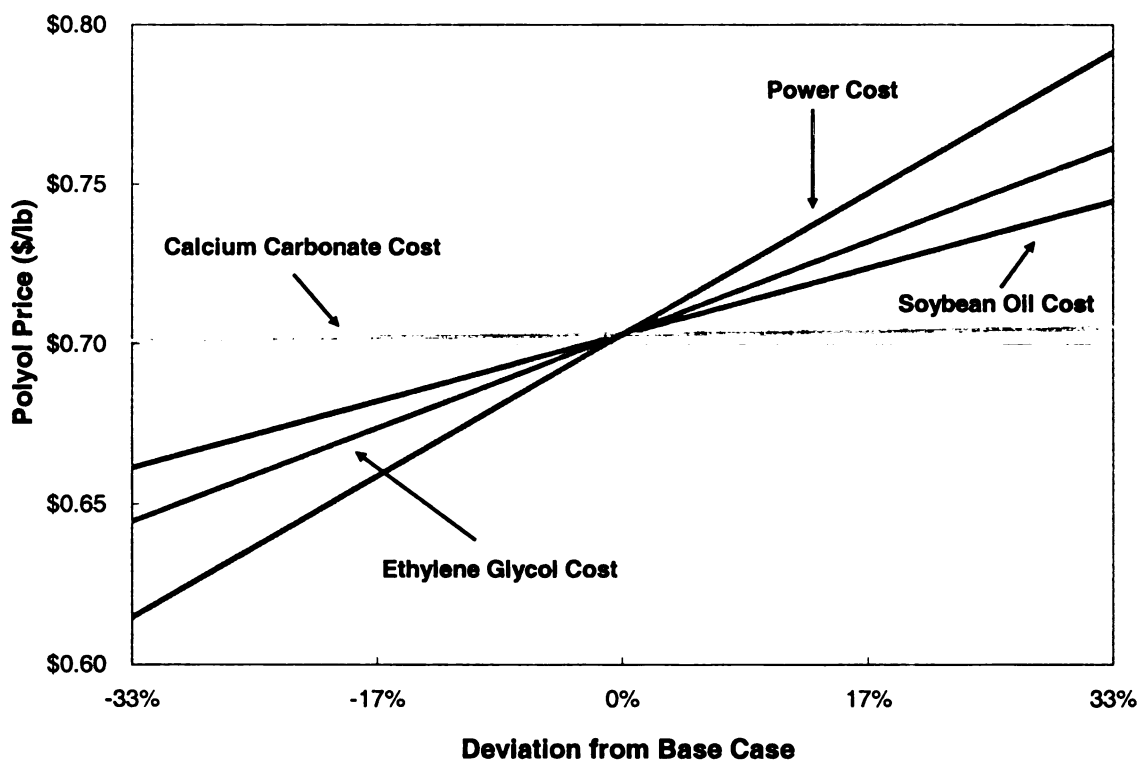


Figure 5.14: Sensitivity Analysis of Soy Polyol Cost

5.5 CONTINUOUS REACTOR DESIGN

5.5.1 Reactor Selection and Sizing

There are several difficulties associated with continuously producing polyol such as maintaining uniform contact between the gas and liquid, different residence times for the gas and liquid, and obtaining the residence times as long as those in a batch reactor.

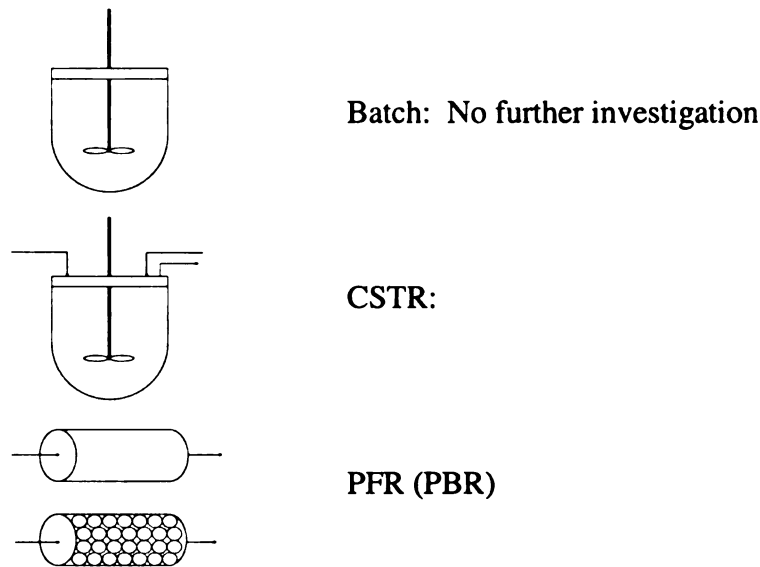


Figure 5.15: Reactor Design Selection

A PBR would further offer the advantage of removing an additional unit operation for catalyst recovery. However, due to the constraint of ozone production (equipment specification) the maximum volumetric flow rate is not sufficient to generate turbulent flow for enhanced mass transfer of the gas and liquid. Thus the reactor decided upon for the continuous production of soy polyol was CSTR. The 3 impellers are used to enhance mass transfer by creating turbulent flow. The ozone enters into the reactor through a sparging ring located at the bottom of the reactor. Directly above the gas inlet is flat blade turbine used to further shear the gas bubbles, followed by 2 pitch blade turbines

used to direct the flow downward to further increase residence times. Additionally, 4 baffles are used to create turbulent flow.

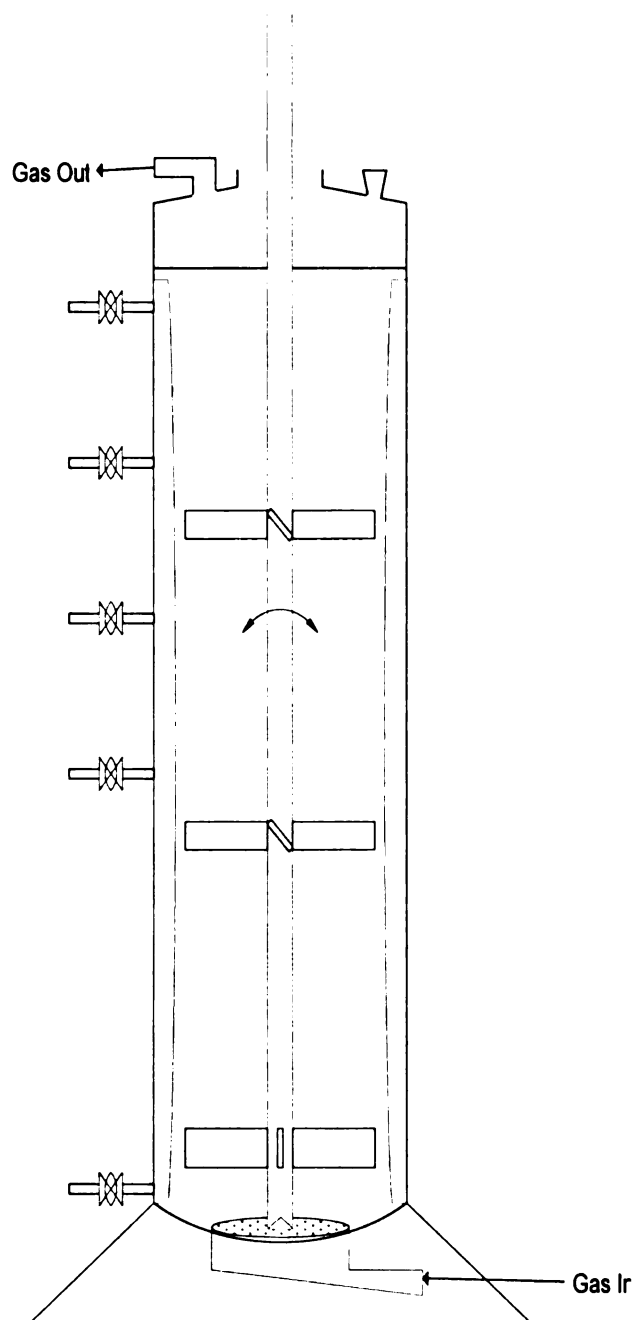


Figure 5.16: Continuous Production of Soy Polyol

The reactor was sized according to the apparent residence time:

Based on the available ozone flow rate (~0.013 moles/min) a maximum volumetric flow rate of 4.03 ml/min can be used.

$$\text{apparent residence time} = \frac{\text{reactor volume}}{\text{volumetric flow rate}}$$

Height		Volume (3" diameter)		Residence Time	
inches	cm	cm ³	L	min	hr
6	15.24	695	0.69	173	2.9
8	20.32	927	0.93	231	3.8
10	25.4	1158	1.16	288	4.8
12	30.48	1390	1.39	346	5.8

Table 5.2: Apparent Residence Time

The residence times were selected to allow for sufficient reaction time.

5.5.2 Process Scale-up

The current continuous soy polyol process uses a CSTR as seen in **Figure 5.17**.

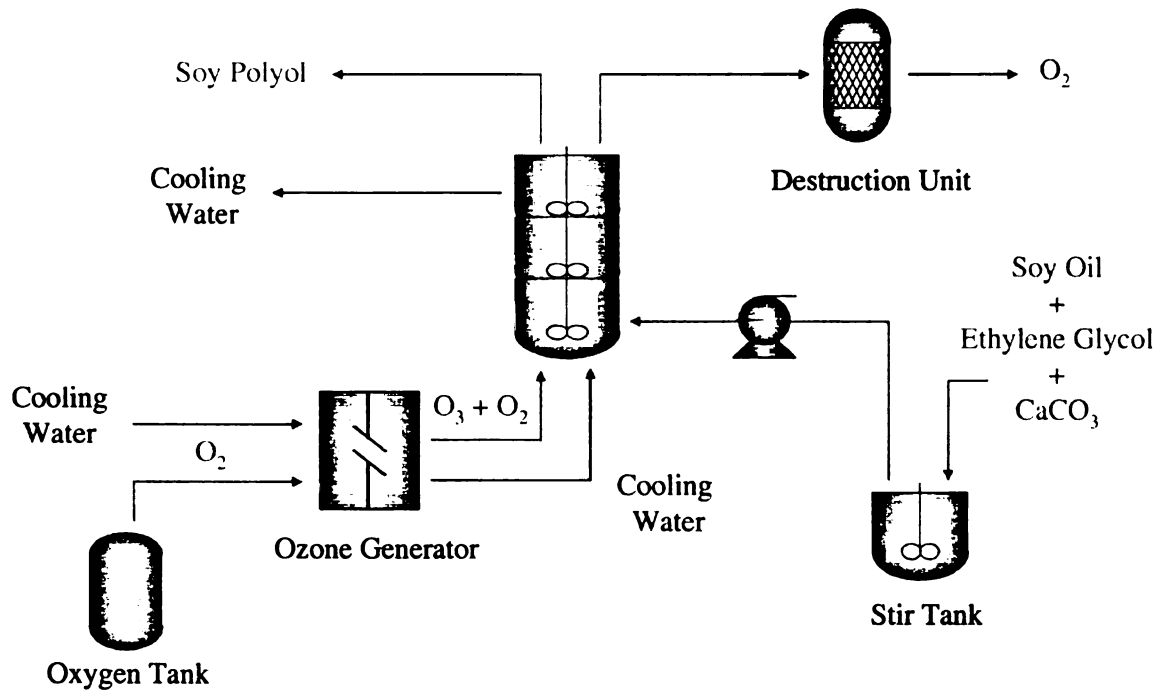


Figure 5.17: Process Flow Diagram for Continuous Polyol Production

For reduced production cost, the polyol synthesis should be down stream from soy oil extraction (Figure 5.18).

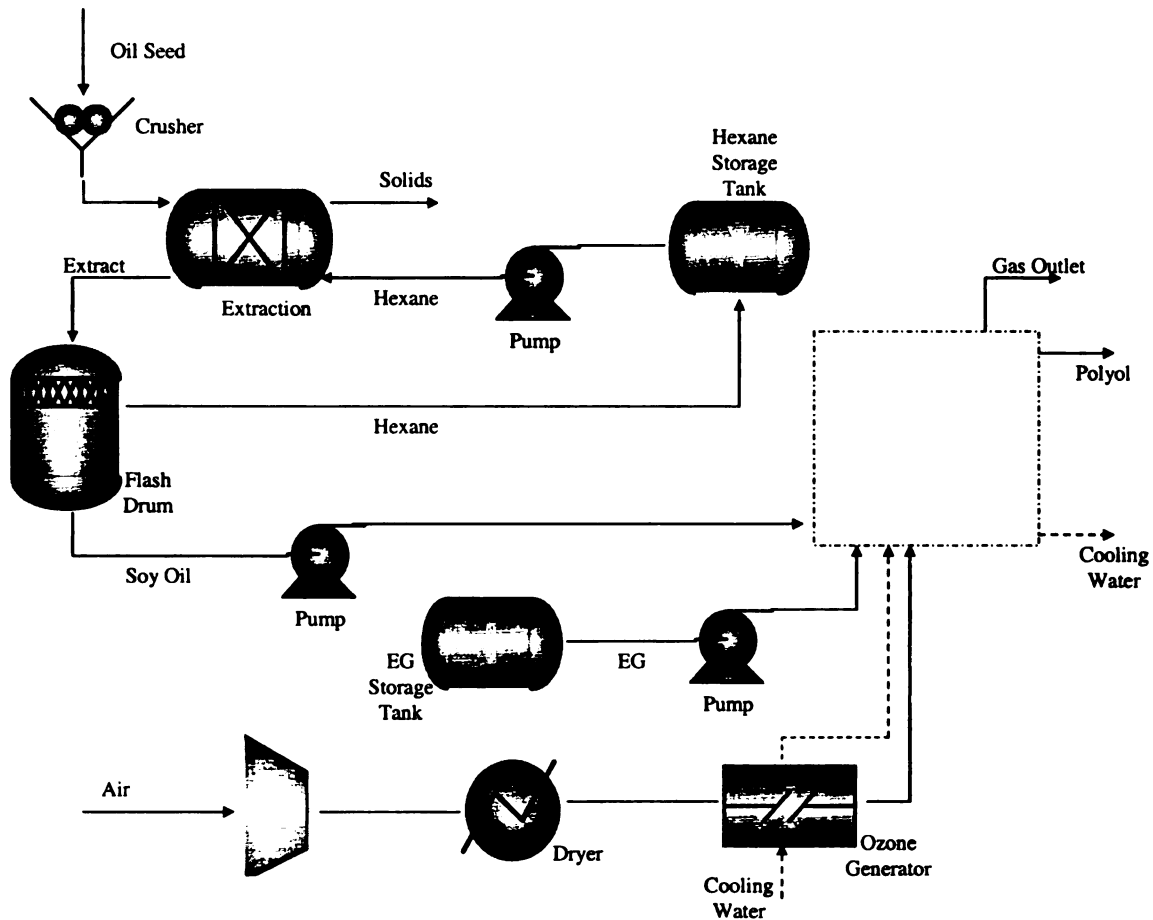


Figure 5.18: Polyol Production Downstream from Soy Oil Extraction

For “large” scale productions where flow rates are sufficient for turbulent flow a PBR could offer further cost reduction. Unit operations can be removed for making a slurry of the catalyst and reactants before entering the reactor and another for removal/recycling of the catalyst. With the larger flow rates, alternative methods for ozone delivery can further enhance ozone mass transfer. Three methods for ozone delivery are proposed.

Figure 5.19 uses a venturi injector to deliver ozone to a mixture of soy oil and ethylene glycol.

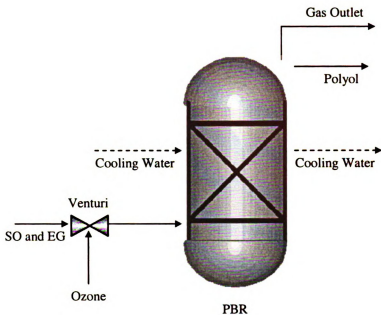


Figure 5.19: Ozone Injected to a Mixture of Soy Oil and Ethylene Glycol

Experimentally it was found that in the absence of a catalyst the reaction would proceed to form aldehydes and carboxylic acids. A possible solution is to inject the ozone into the ethylene glycol stream, and charge the reactor with soy oil (**Figure 5.20**).

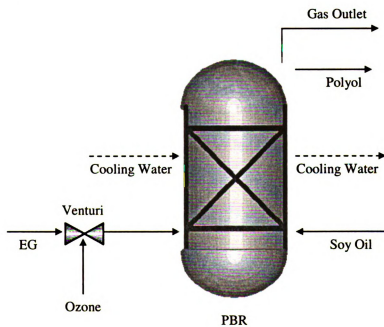


Figure 5.20: Ozone Injected into Ethylene Glycol

The third option is deliver ozone by gas sparging through a diffuser as seen in **Figure 5.21**.

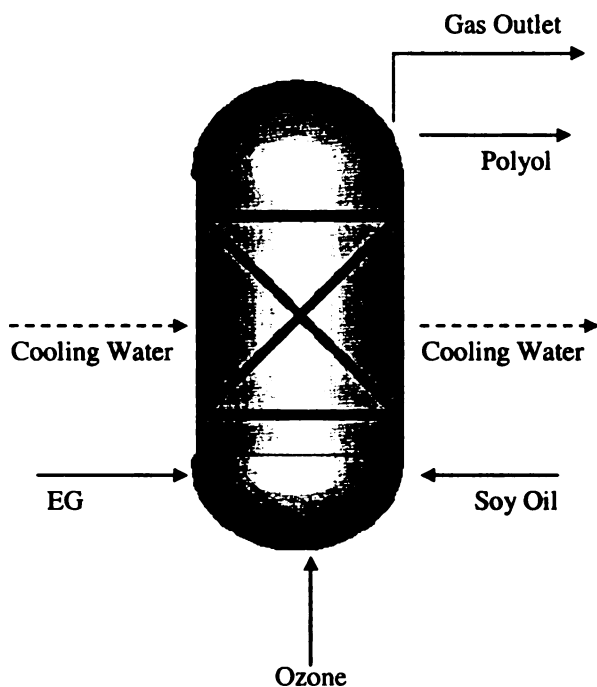


Figure 5.21: Ozone Injected by Gas Sparging

5.5.3 Process Economics

Based on an annual polyol production rate of 500 lbs/hr the production cost is \$0.51 per pound. A capital investment of \$1.2 million dollars was assumed with a 5 year debt write-off. The ozone reaction efficiency was taken to be 80%, and the plant would operate 70% of the year. The calculations are detailed in **Appendix C**.

Chapter 6: Thermal-Oxidatively Stable Biobased Lubricants

6.1 LITERATURE REVIEW

6.1.1 Soy oil based lubricants

Soybean oil lubricants are preferred to petroleum oils because they are cheap, renewable and have performance advantages (1). Soybean oil has low volatility due to the high molecular weight. In addition the presence of polar ester groups results in good boundary lubrication due to adhesion with metal surfaces. Alternatively, one of the major challenges to using SO as a lubricant is poor oxidative stability (2). The poor oxidative stability can be attributed to the reactivity of the double bonds present within SO. On average SO contains 4.3-4.6 double bonds per mole depending on the origin of the seed. The presence of unsaturation can undergo reactions such as free radical oxidation, fragmentation, rearrangement, disproportionation and polymerization, which reduces oxidative stability. Various methods such as chemical modification and genetic modification have been used to improve the oxidative stability. Although, additives technologies can be used to improve the overall oxidative stability of the lubricant, it has only an indirect effect on the oxidative stability of SO.

Several researches have investigated the use of chemical modification as a means of enhancing oxidative stability (3). Adhvaryu and coworkers (4, 5) reported on the use of epoxidized soybean oil and alkoxyated triacylglycerols as lubricants. Other chemical modifications were done by sulfurization and phosphate modification (6, 7). However, these schemes did not account for the complexity of SO. Soybean oil is a complex mixture of primarily five fatty acids (palmitic, stearic, oleic, linoleic, and linolenic acids) with very different melting points, oxidative stability, and chemical functionalities. Thus,

there is expected to be variability in performance resulting from the varying selectivity of the chemical modification. In other studies the chemically modified SO were just evaluated in less severe applications, such as emulsions in water for a cutting fluid (8). Other studies have used genetic modification to improve the oxidative stability of SO. Researchers at Dupont increased the oleic acid content of SO to ~80% (9). Conventional SO contains oleic acid levels of ~25% and polyunsaturated fatty acid levels of over 60%. The presence of bis allylic protons is highly susceptible to radical attack and subsequently undergoes oxidative degradation. More recently, Buhr et al. (10) achieved SO with greater than 85% oleic acid content and relatively low polyunsaturated fatty acid content (3-5%). While improving the oxidative stability of SO is possible through genetic modification; these approaches are generally longer routes which are not necessarily welcomed due to concerns regarding genetically modified crops.

High oxidative stability is a critical property for lubricants. The purpose of this study is to use novel chemical modifications to improve the oxidative stability of SO and to evaluate their lubricant base oil properties. Two different chemical modifications were investigated. The first scheme used a free radical initiated addition of maleic anhydride to SO, followed by an esterification with an alcohol. The second scheme involved passing ozone through a solution of soybean oil and a mono-functional alcohol in the presence of an alkaline catalyst.

6.2 EXPERIMENTAL PROCEDURES

6.2.1 *Materials and Methods*

Degummed soybean oil was purchased from Spectrum Chemicals in a 20L container and was used without further purification. Maleic anhydride (MA), 2,5-Bis(tert-butylperoxy)-2,5-dimethylhexane (L101), Methanol, butanol, methoxy-polyethylene glycol (Mw = 350), sodium hydroxide, pyridine, potassium iodide, 4-dimethylamino-pyridine (4-DMAP), CaCO₃ and all other reagents were purchased from Sigma-Aldrich (Milwaukee, WI). Ozone was produced by passing dry oxygen (0.25 ft³/min) through Praxair Trailigaz generator (Cincinnati, OH), model number OZC-1001. The exit port of the ozone generator was connected to the bottom of the reaction bottle and allowed the ozone (about 6 wt% in oxygen) to bubble through a fritted disc as fine gas bubbles in the reaction mixture. The very small gas bubbles allowed good dispersion of ozone within the reaction medium. Excess gas and unreacted ozone was vented through the top of the reaction bottle through aqueous KI solution to destroy any unreacted ozone. Unless noted all the ozonolysis reactions were run at 0°C and maintained at this temperature with ice/water bath.

6.2.2 *Synthesis Techniques*

Maleation of Soybean Oil

Reactions were carried out by charging a 2L Parr Reactor equipped with a motorized stirrer, thermocouple, and heating element with MA, SO, and the initiator. The reactor was purged with N₂ for 5 minutes, sealed and heated. The initial reaction time was taken at the time the reactor temperature reached 150°C, where it was maintained for 30 minutes. At the end of each reaction, the reactor was connected to a

vacuum pump for 30 minutes and any volatile products were collected in a solvent trap immersed in isopropanol dry ice bath (Figure 6.1).

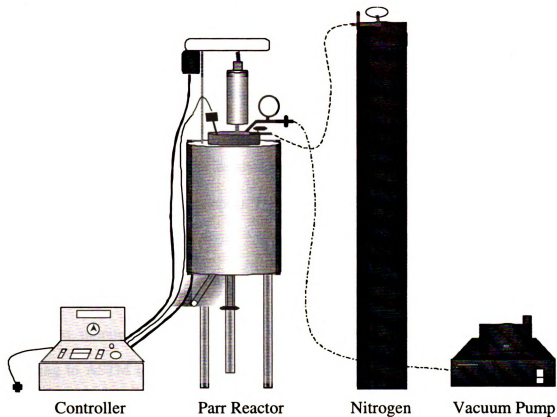


Figure 6.1: Soy Oil Maleation and Esterification Apparatus

Esterification of Maleated Soybean Oil

Maleated SO and a large excess of alcohol (10:1 molar ratio alcohol to SO) was added to a 2L Parr Reactor equipped with a motorized stirrer, thermocouple, and heating element. The reactor was purge with N_2 for 5 minutes, sealed and heated. The initial reaction time was taken at the time the reactor temperature reached 200°C , where it was maintained for 30 minutes. At the end of each reaction, the reactor was connected to a vacuum pump for 30 minutes and any volatile products were collected in a solvent trap immersed in isopropanol dry ice bath.

Ozonolysis of Soybean Oil

Soybean oil, an alcohol (methanol, butanol, octanol, dodecanol, or methoxy-PEG350) and various amounts of catalysts (NaOH, pyridine, 4-DMAP or CaCO₃) were placed in a 500 ml gas wash bottle and cooled to 0°C in an ice water bath and then ozone was bubbled through the reaction mixture. Unless otherwise noted, all reactions were run for 2 hours and the product was then washed with distilled water 5 times in order to remove any excess alcohol and catalyst (when CaCO₃ was used as a catalyst, it was filtered out through a fine filter paper). The product was then dried over molecular sieves for 48 hours prior to testing.

6.2.3 Characterization Procedures

The number of double bonds was determined using iodine value testing, according to ASTM test method D1959. The iodine number in this test is defined as centigrams of I₂ per gram of sample.

The acid value was determined according to ASTM test method D1980. The acid number in this test is defined as milligrams of KOH per gram of sample.

Functional groups were identified using Perkin-Elmer FTIR model 1000 using at least 64 scans. Prior to recording a spectrum, the sample holder was flushed with nitrogen to remove moisture and CO₂ and the background was recorded. The spectra were obtained after polyol samples were dissolved in chloroform and a drop of the solution was placed on sodium chloride crystals. The solvent was allowed to evaporate leaving a thin film on the surface of the crystal. The sample cell was constantly purged with dry nitrogen while the signal was acquired.

Thermo-gravimetric analysis (TGA) was carried out with a TA Instruments (New Castle, DE) Model TGA 2950 thermobalance. The instrument was operated in the dynamic mode with a heating rate of 5°C/min, where 40°C and 350°C were the initial and final temperatures, respectively. On average, 4 mg was the initial mass of each sample analyzed. Air was used instead of inert atmosphere, to study the effect the thermal oxidation.

NMR spectra were obtained on a 500 MHz model INOVA 500 instrument. Samples were dissolved in deuterated chloroform, and the ¹H NMR and ¹³C NMR spectra were obtained at room temperature.

Thermo-oxidation Engine Oil Simulation Test (TEOS) was used to simulate oxidation in a moderately high temperature deposit conditions in the piston ring zone of modern smaller, more highly, stressed engines. Due to the known poor oxidation stability of soy oil in this test, a sample was run for only 10 hours at 285°C rather than the normal 24 hours. Accordingly, 8.5 g of oil was recirculated continuously over the special steel rod heated to 285°C. Air is circulated continuously over the rod to increase exposure to oxygen. In addition, any volatile material is caught by the walls of a surrounding mantle and collected separately, thus increasing the stress on the remaining oil. The weight of the rod before and after the test was then determined as the main criterion of the extent of oxidation.

Scanning Brookfield Technique (SBT) was used to determine the low temperature profile of the lubricant by continuously measuring the viscosity as the temperature is slowly (1°C/hr) decreased from 0°C to the maximum viscosity of the viscometer head. Any structures that were built-up in the sample caused an increase in viscosity above the

exponential relationship expected from a Newtonian fluid, which by definition, is free of gel-forming tendencies. The presence of such structures was found by taking the first derivative of a linearized treatment of the viscosity-temperature curve. In the case of these studies, the temperature range chosen was from 0°C to the lowest temperature possible of the viscometer head.

Friction and Wear were measured by a modified Falex pin and Vblock. In this test, Two V-blocks press against a rotating pin from opposite sides, 'pinching' the pin between them with a force that is progressively increased in steps by the test operator. The contact between the V-blocks and the pin are four straight lines and permit evaluation of the lubricant tested in the so-called quasihydrodynamic region of lubrication. This region can produce wear and ultimate seizure of the contiguous contacting surfaces. The test was conducted with increasing 50 lb steps of force with five minutes residence time at each step. Wear, friction and pin temperature were measured at each step.

6.3 RESULTS AND DISCUSSION

The presence of double bonds in vegetable oils is largely responsible to the poor oxidative and thermal stability of these oils, two chemical routes were explored to remove the double bonds and introduce ester functionality. The first route involves insertion of maleic anhydride across the double bond followed by esterification with an alcohol. The second route consisted of catalytic ozonation of the double bonds in the presence of an alcohol to cleave the double bonds and attach the alcohol to the new terminal carbon via ester linkages.

6.3.1 Transformation of Double Bonds via Maleation

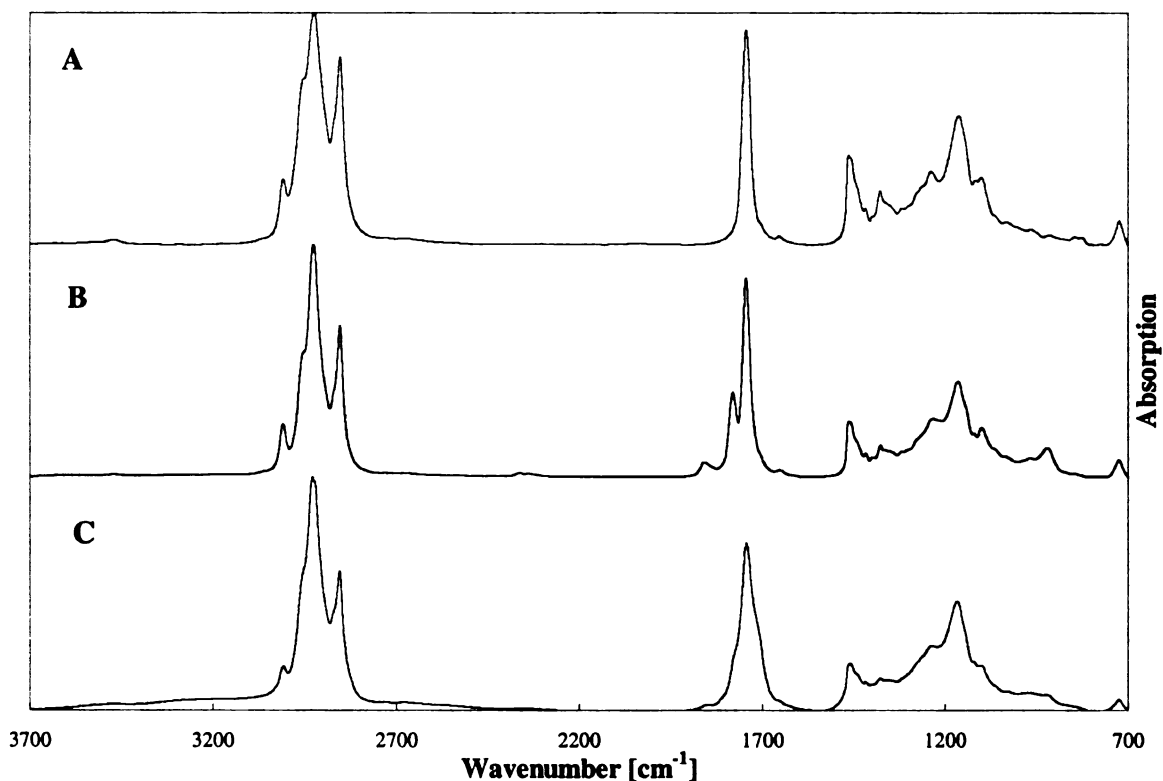


Figure 6.2: FTIR of Soybean Oil (A); Maleated Soybean Oil (B); and Esterified Maleated Soybean Oil (C)

The first modification was done by introducing an anhydride functionality to SO, followed by an esterification using an alcohol. Soybean oil was functionalized using single-step free radical initiated chemistry. The anhydride functionality was confirmed by FTIR spectroscopy (**Figure 6.2**). The spectra shows the maleated soybean oil exhibits peaks at $\sim 1775\text{ cm}^{-1}$ and 1850 cm^{-1} not present in SO. These absorption peaks are related to the symmetric and asymmetric stretching of C=O in the MA, respectively. Furthermore, no absorption peaks related to -OH stretching due to the opening of the anhydride is observed, clearly indicating that the anhydride ring remained intact. Additionally, the alcohol esterified maleated SO also shows no absorption peaks $\sim 3500\text{ cm}^{-1}$, suggesting complete esterification and half ester formation. Nominally, the esterification proceeds as presented in **Figure 6.3**.

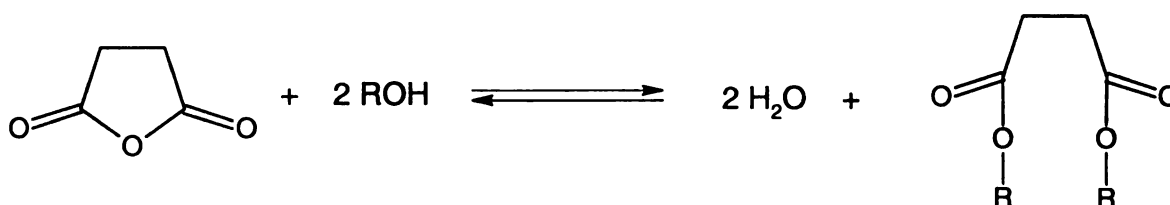


Figure 6.3: Esterification of Maleated Soybean Oil with an Alcohol

To favor the formation of the ester over the acid, the esterification was done at elevated temperature (200°C) and pressure with excess alcohol. A series of aliphatic alcohols with increasing molecular weight were considered (methanol, ethanol, butanol, octanol and methoxy-PEG). Experimentally, it was observed that the oxidative stability increased with the molecular weight of the alcohol. However, when alcohols with molecular weight greater than butanol were used, the oxidative stability was found to decrease.

Additionally, the use of linear aliphatic alcohols was preferred over branched alcohols such as t-butyl alcohol as it offered greater thermo oxidative stability.

The structural modification with the best thermo oxidative stability is carried out in 2 stages:

- 1) Free radical maleation of soybean oil in a closed system
- 2) High temperature and pressure esterification of maleated soybean oil using excess butanol.

6.3.2 Transformation of Double Bonds via Catalytic Ozonolysis

Somewhat similarly the same series of aliphatic alcohols with increasing molecular weight were (methanol, hexanol, octanol and methoxy-PEG350) used in a catalytic ozonolysis to transform the bonds to more thermal-oxidatively stable ester linkages (**Figure 6.4**).

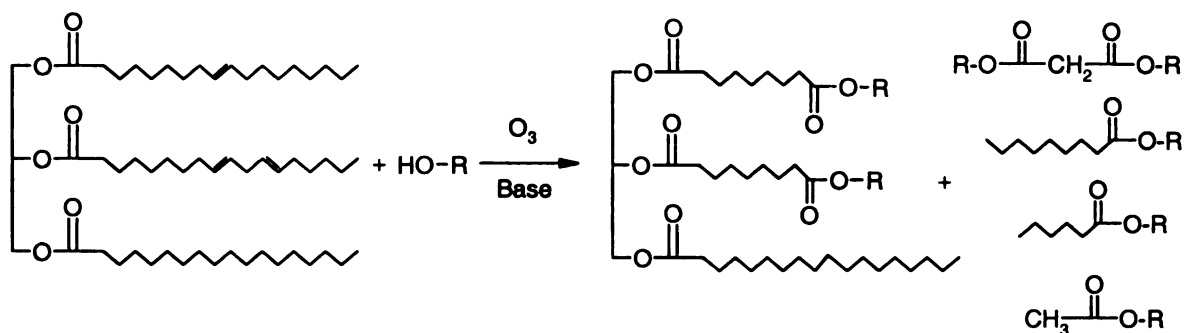


Figure 6.4: Catalytic Ozonolysis of Soy Oil in the Presence of an Alcohol

The lower molecular fragment derived from cleavage of the double bonds must be removed because of their volatility. These low molecular weight fragments are expected to have low boiling points, reducing the thermal stability. However, these fragments compose almost ~40 wt% of the mixture. It can also be seen the fragments have a significant effect on the molecular weight distribution (**Table 6.1**).

Alcohol	Whole Distribution		Fragments Removed	
	Mn	Mw	Mn	Mw
Methanol	350	553.3	676.3	679.6
Hexanol	480.1	669.6	850.2	850.3
Octanol	532.2	721.2	919.8	920.6
MEG350	736.9	921	-	-
Soy Oil	871.7	871.8	-	-

$$Mn = \frac{\sum n_i M_i}{\sum n_i}$$

$$Mw = \frac{\sum n_i M_i^2}{\sum n_i M_i}$$

Where: n_i = mole fraction of species i
 M_i = molecular weight of species i

Table 6.1: Calculated Molecular Weight Distribution

Where Mn and Mw are the number average molecular weight and the weight average molecular weight, respectively. The molecular weights were calculated as:

The mole fractions were calculated based on the fatty acid distribution as seen in **Figure 1.4**. A sample calculation for reactions with methanol is summarized in **Table 6.2**.

Triglyceride	Frequency	MW	Fragments	Frequency	MW
NNN	0.2352	644	RO	0.0952	172
NNP	0.1008	698	RL	0.2698	132
NNS	0.0336	727	RL1	0.2063	130
PPP	0.0007	807	RL2	0.0317	88
PPN	0.0007	753	<p style="text-align: center;">Complete Mixture Mn = 350 Mw = 553 Fragments Removed Mn = 676 Mw = 680</p>		
PPS	0.0144	835			
SSS	0	891			
SSN	0.0016	809			
SSP	0.0002	863			
NPS	0.0096	781			

Table 6.2: Molecular Weight Distribution for Reactions with Methanol

To reduce the volatility of the lower molecular weight fragments, higher molecular weight alcohols were used as opposed to removal of low boilers. Experimentally, it was observed that methoxy-PEG350 had the best thermal stability because of the volatility of the lower molecular weight species resulting from the cleavage of the double bonds (Figure 6.5).

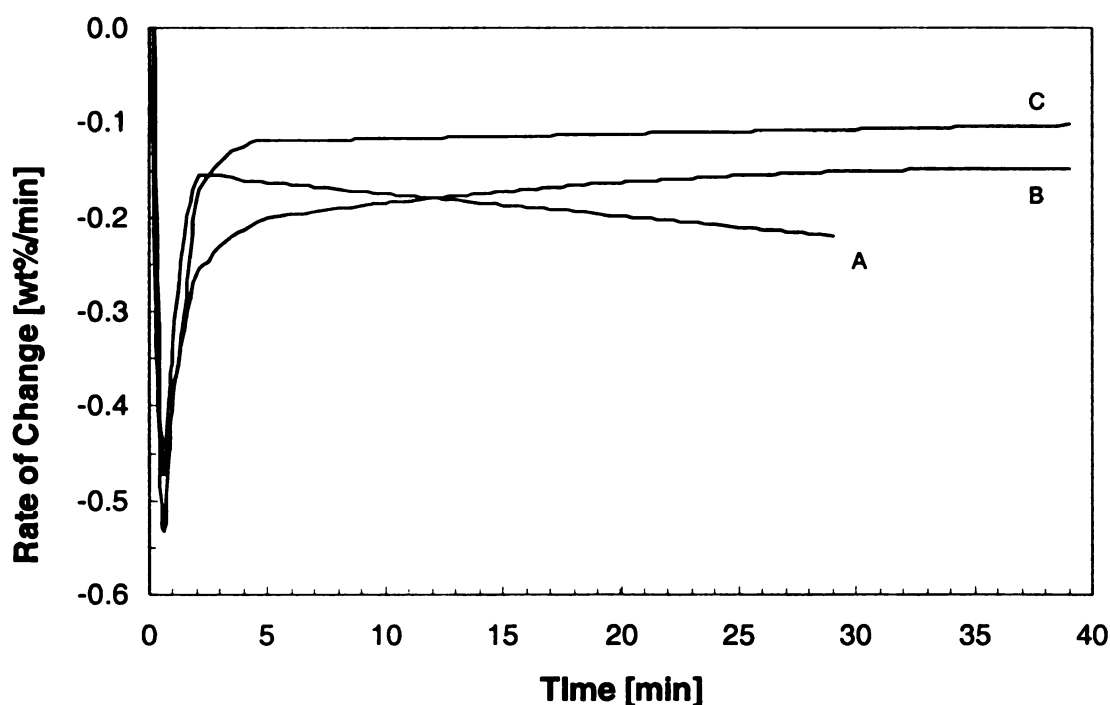


**Figure 6.5: Rate of Decomposition of Ozone Treated MEG350 and Soy Oil
0 min reaction (A); 10 min reaction (B); and 30 min reaction (C)**

As the reaction time increases, the rate of decomposition decreases. Both ozone treated samples, rate of decomposition levels off after an initial drop in weight. This initial weight loss is probably due to residual moisture, and lower weight fragments. However, in the case of plain soy oil, the decompositions progresses further. This is most likely due to further oxidation resulting in a breakdown of soy oil. The corresponding weight loss in an oxidizing atmosphere is presented in Figure 6.6.

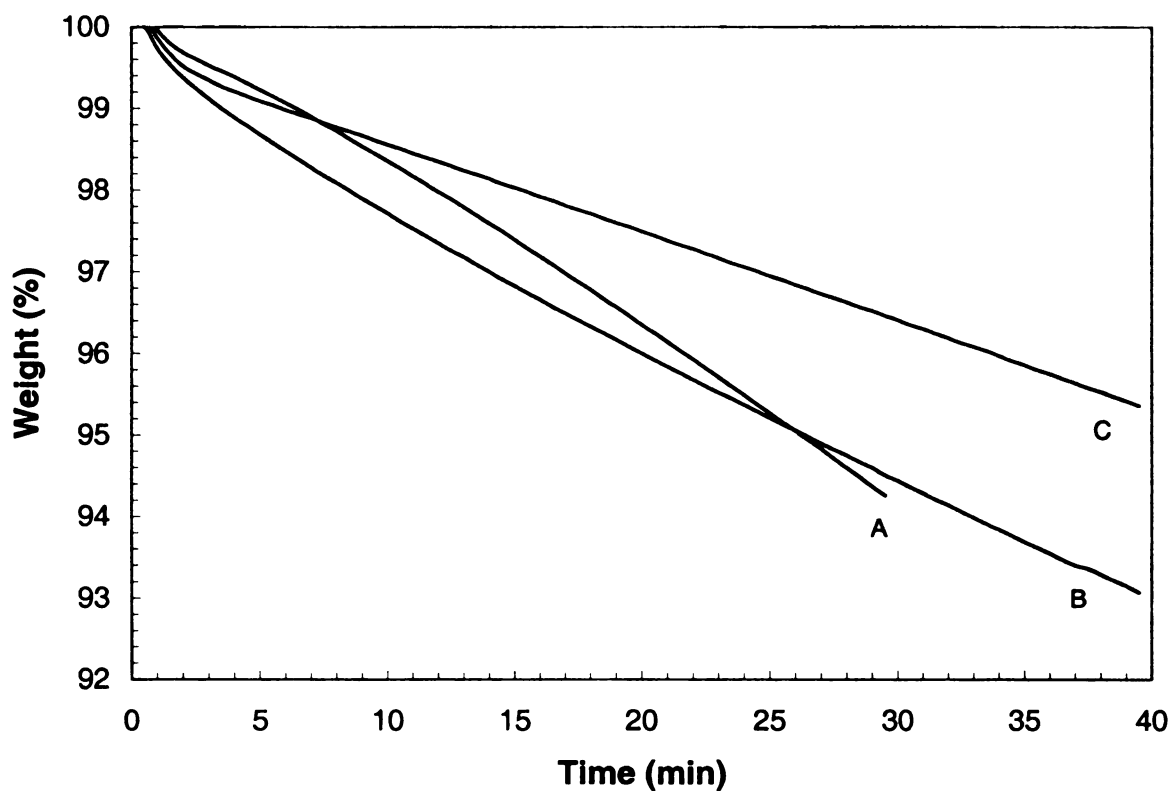


**Figure 6.6: Weight Loss of Ozone Treated MEG350 and Soy Oil
0 min reaction (A); 10 min reaction (B); and 30 min reaction (C)**

The FTIR of the ozonized soy oil shows near complete removal of the double bonds in soy oil (Figure 6.5). The stretching at 3005 cm^{-1} from the C=CH is significantly less in the ozone treated sample than from soy oil. It can also be seen that there is negligible acid formation ($\sim 3500\text{ cm}^{-1}$).

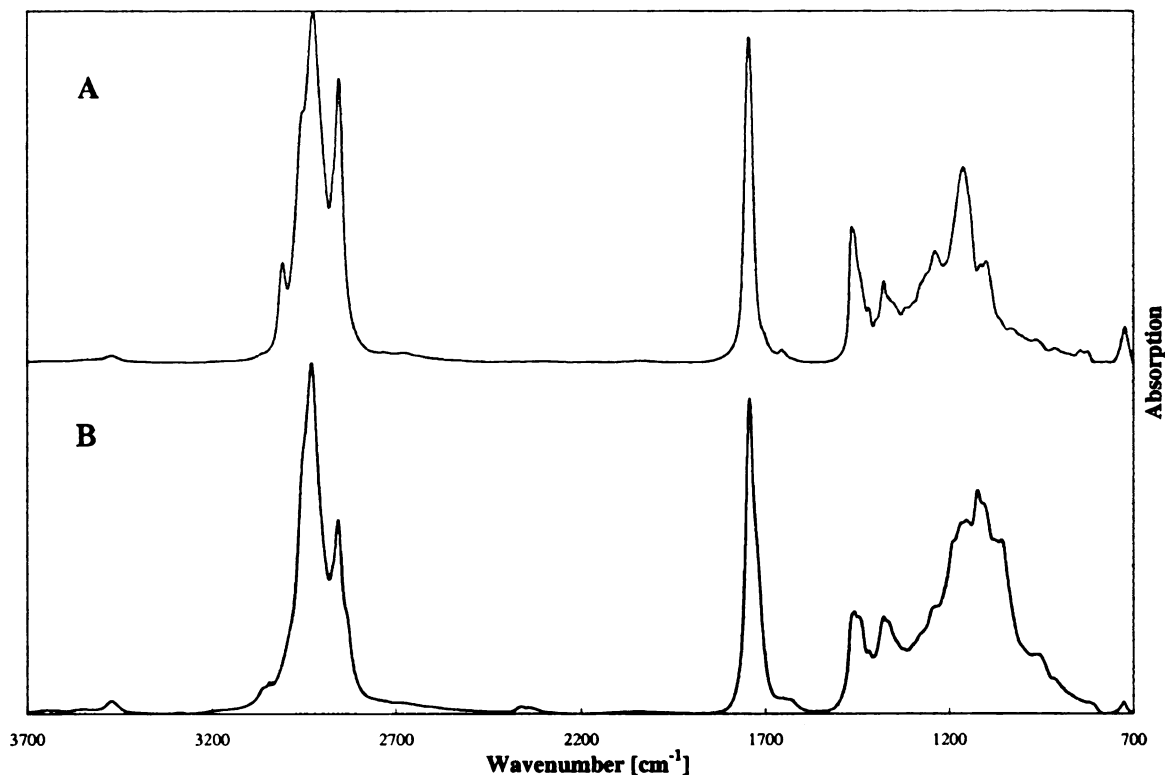


Figure 6.7: FTIR of Soy Oil (A) and Ozonized Soy Oil with Methoxy-PEG350 (B)

6.3.3 Evaluation as a Biobased Lubricant

Based on improved oxidative stability, the butanol esterified maleated soy oil and methoxy-PEG350 ozonized samples lubricating properties were evaluated. Both modified soy oils showed reduced tendency to form deposits as compared to soy oil (**Figure 6.8**). This is most likely due to the reduced number of double bonds present. This is further supported by the ozone modified soy oil having the best performance with the least number of double bonds among the samples. In the case of the maleated sample, there is a net reduction of 1 double bond, whereas near complete removal of double bonds in the ozone modified soy oil.

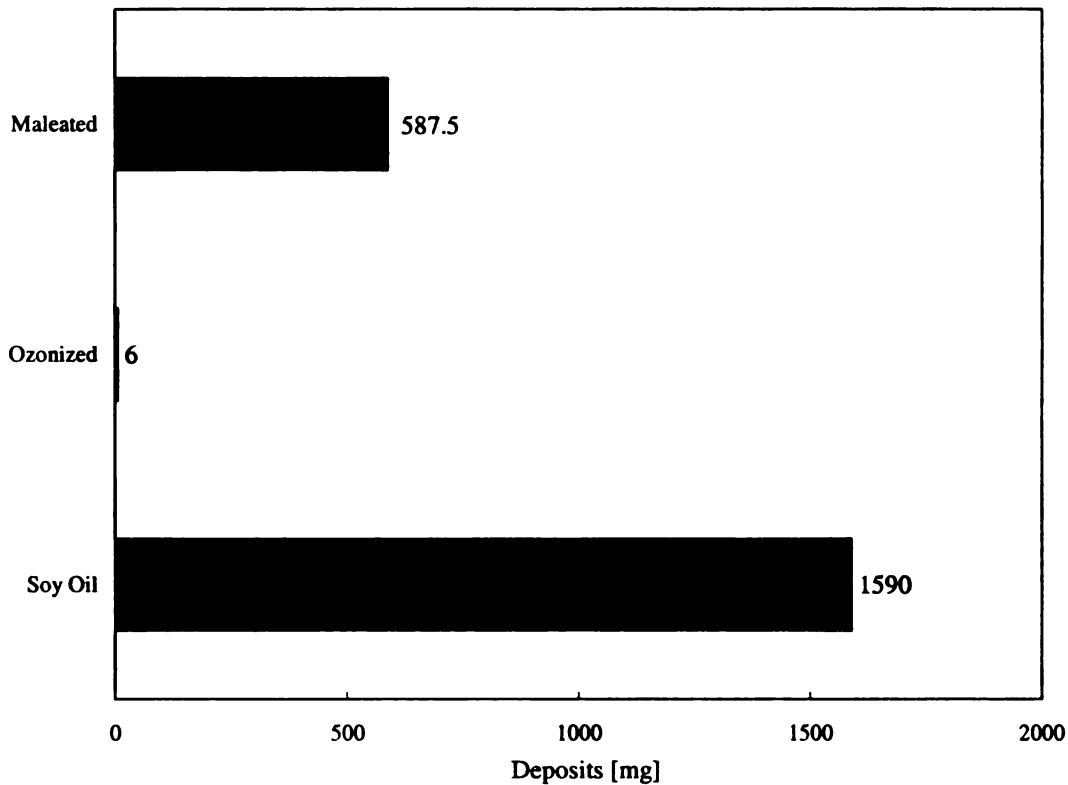


Figure 6.8: Deposits Formation of Lubricant Sample

Similarly, the ozone modified soy oil also had the best the cold flow property performance as seen in **Figure 6.9**. The cleavage from the ozone treatment results in a series of fragments improving the cold flow properties of standard soy oil. Alternatively, the esterified-maleated soy oil structure still resembles that of soy oil, thus their cold flow properties remain relatively unchanged.

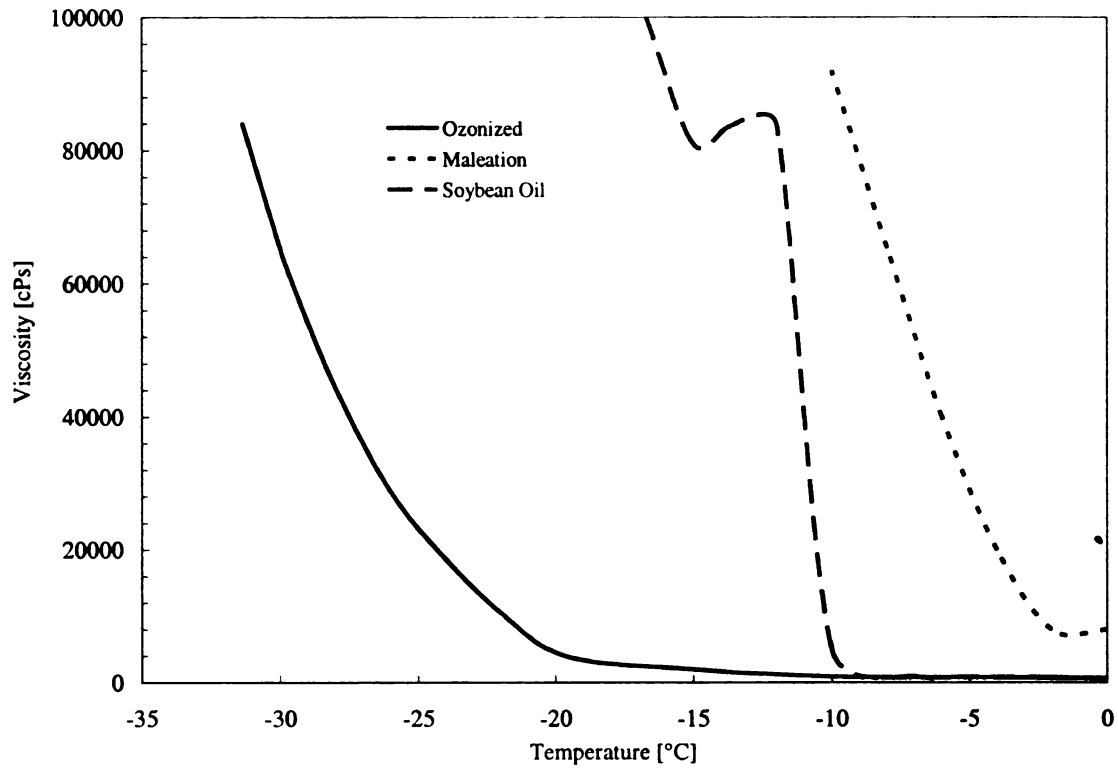


Figure 6.9: Cold Flow Properties of Lubricants

Both modified soy oil could greater loads before failure than untreated soy oil (**Figure 6.10**). Additionally, it can also be seen that durability the ozone modified soy oil is better than the esterified-maleated soy oil. The wear plots for the two modified soy oils can be seen in **Figures 6.11 and 6.12**, the ozone modified oil shows less wear with increasing load than the esterified-maleated soy oil.

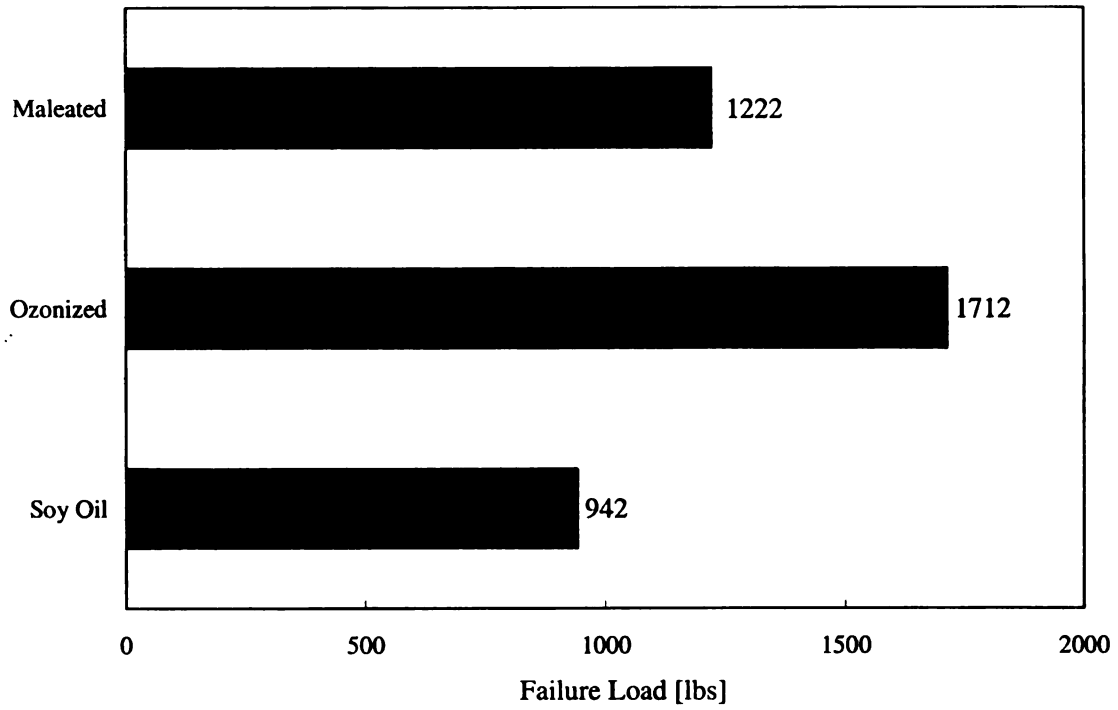


Figure 6.10: Failure Load for Soy-based Lubricants

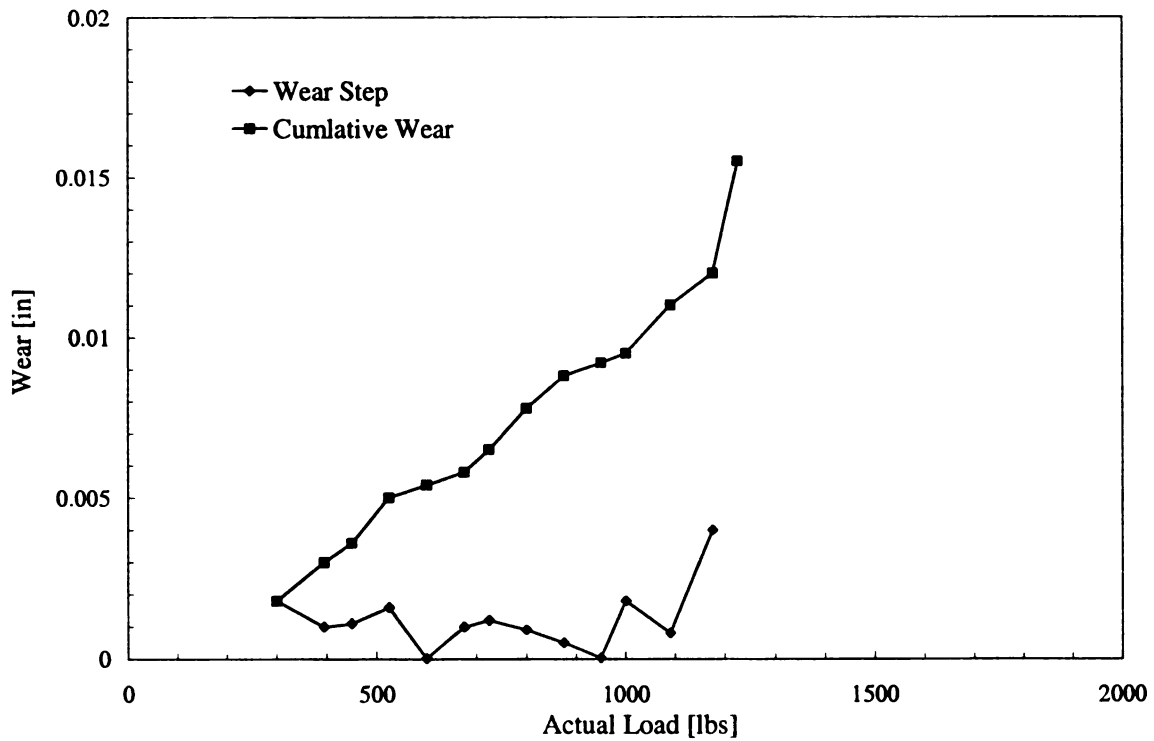


Figure 6.11: Wear Plot of Esterified-Maleated Soy Oil

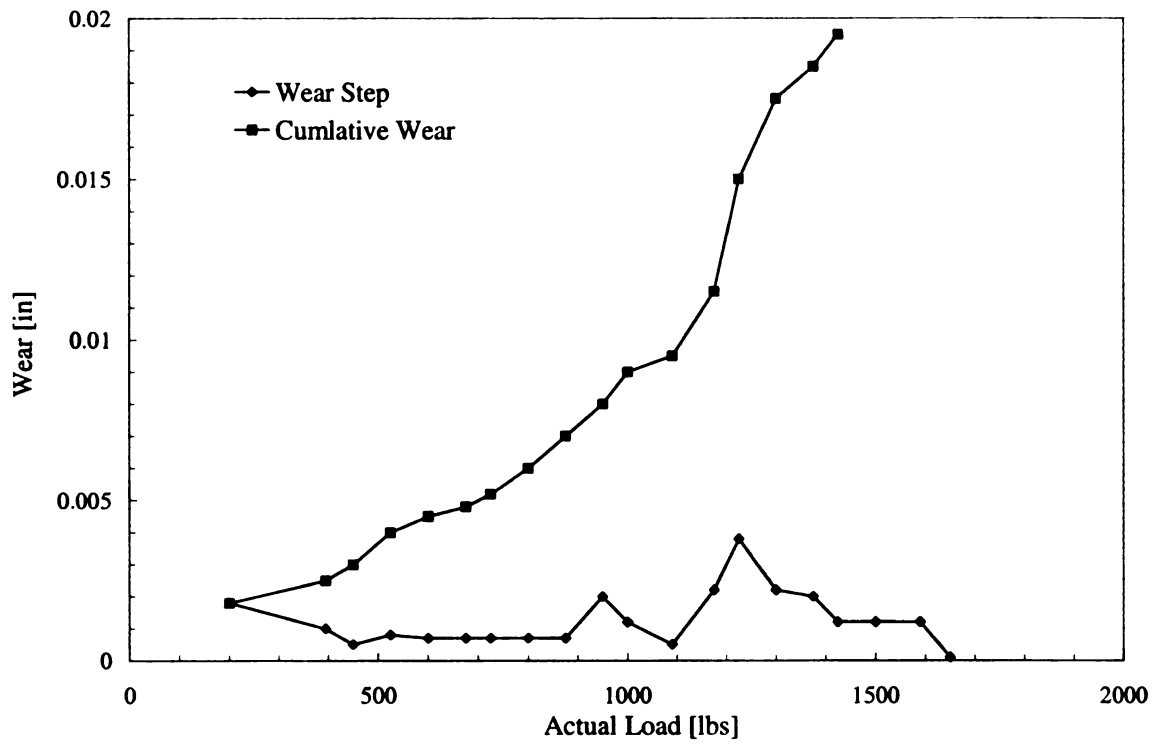


Figure 6.12: Wear Plot of Ozone Modified Soy Oil

6.4 CONCLUSIONS

The oxidative degradation of soybean oil was greatly reduced by transforming the double bonds into more oxidatively stable esters were done using to two chemical modifications.

- Maleation followed by an esterification using an butanol
- Catalytic ozonolysis in the presence of an methoxy-PEG350

The present study shows that both processes were found to significantly reduce soy oil tendency to form deposits (insoluble matter) by removing oxidation-susceptible sites from the soy molecules. However, from the viewpoint of effects on low-temperature properties – dependent on the physical configuration of the soy molecules and their tendency to associate into larger, more flow-resisting structures at low-temperature – the processes have little effect. Additionally, both modifications were found to significantly improve lubrication performance in comparison to the untreated soy oil.

6.5 REFERENCES

1. Erhan S.Z. and Asadauskas S., Lubricant basestocks from vegetable oils, Ind. Crops Prod. 11, 277-282 (2000)
2. Asadauskas S., Perez J.M., and Duda J.L., Oxidative stability and anti-wear properties of high oleic vegetable oils, Lubr. Eng. 52, 877-882 (1996)
3. D'Sousa V., DeMan L., and DeMan J.M., Polymeric behavior of high melting glycerides from hydrogenated canola oil, J. Am. Oil Chem. Soc. 68, 907-911 (1991)
4. Adhvaryu A. and Erhan S.Z., Epoxidized soybean oil as a potential source of high-temperature lubricants, Ind. Crops Prod. 15, 247-254 (2002)
5. Adhvaryu A., Liu Z., and Erhan S.Z., Synthesis of novel alkoxyated triacylglycerols and their lubricant base oil properties, Ind. Crops Prod. 21, 113-119 (2005)
6. Schwab A.W. and Gast L.E., Free radical unsaturated oils addition of hydrogen sulfide to conjugated and nonconjugated methyl esters of vegetable oils, J. Am. Oil Chem. Soc. 47, 371-373 (1970)
7. Schwab A.W., Gast L.E., and Rohwedder W.K., Nucleophilic addition of hydrogen sulfide to methyl oleate, methyl linoleate, and soybean oil, J. Am. Oil Chem. Soc. 52, 236-239 (1975)
8. Jacob J., Bhattacharaya M., and Raynor P., Emulsions containing vegetable oils for cutting fluids application, Colloids and Surf. 237: 141-150 (2004)
9. Adhvaryu A. and Erhan S.Z., Epoxidized soybean oil as a potential source of high-temperature lubricants, Ind. Crops Prod. 15, 247-254 (2002)
10. Warth H., Mulhaupt R., Hoffmann B., Lawrence S., Polyester network based upon epoxidized and maleinated natural oil, Angewandte 249, 79-92 (1997)
11. Bellamy L.J., The Infra-Red Spectra of Complex Molecules, Wiley: New York, (1964).
12. Pouchert C.J., The Aldrich Library of Infra-Red Spectra, Aldrich Chemical Company; Milwaukee, WI, (1970).

Chapter 7: Silane Functionalized Soybean oil

7.1 LITERATURE REVIEW

7.1.1 *Silane Addition to Soy Oil*

Several strategies have been used in the past to enhance the reactivity of vegetable oils by manipulation of the double bonds such that they can be crosslinked at room temperature which were then used as coating, adhesives, or sealants. Preparation of these silane-modified vegetable oils involved methods that initially yielded polyols derivatives of the vegetable oil, either by transesterification, epoxidation, or oxidation. Typically, these polyols were then reacted with excess diisocyanate and end-capped with different amino functional silane coupling agents (1). It was noted that coatings based on this epoxidized 10-undecenoic acid triglyceride had excellent UV stability. Alternatively, a solution of soybean oil and Cl_3SiH could be irradiated with Hg lamps to hydrosilylate the oil and incorporate the trichlorosilane onto a double bond (2). In this case too, exposure to moisture will hydrolyze the chlorosilane to silanols, which will then condense to form the siloxane crosslinking bridges. The added advantage of silicone species covalently bonded to the oil is their reactivity with inorganic silicates surfaces. Thus, it was claimed that silane modified soy oil has good adhesion to concrete and could be used as a water repellent surface coatings for masonry structures.

Here reports the results of our studies where vinyltrimethoxy silane is reacted with soy oils under anhydrous conditions and allowed then, to cure upon exposing to ambient atmosphere.

7.2 EXPERIMENTAL PROCEDURES

7.2.1 *Materials and Methods*

Unhydrogenated soybean oil (SO) was purchased from Spectrum Chemicals (Gardena, CA). Linoleic Acid (LA), Oleic Acid (OA), Dibutyltin dilaurate, Tyzor 131, 2,5-Bis(tert-butylperoxy)-2,5-dimethylhexane (L101), BF₃-methanol complex and all other reagents were purchased from Sigma-Aldrich (Milwaukee, WI). Vinyltrimethoxysilane (VTMS) was obtained from GE Silcones (Friendly, WV).

7.2.2 *Synthesis Techniques*

Silane Functionalization of Soy Oil (or Fatty Acids Derivatives)

Silylation reactions were carried out by charging a 2L Parr Reactor equipped with a motorized stirrer, thermocouple, and heating element with the VTMS, SO, and the initiator (**Figure 6.1**). The initial reaction time was taken at the time the reactor temperature reached a preset temperature. The effects of reaction time, temperature, catalyst type and concentration were investigated. At the end of each reaction, the reactor was connected to a vacuum pump for 30 minute and any volatile products were collected in a solvent trap immersed in isopropanol dry ice bath.

Room Temperature Cure Studies

Room temperature curing reactions were done by adding the 50 grams of silane functionalized soy oil (or fatty acid derivative) to a glass petri dish and left in controlled environment at 25°C and 50% relative humidity. The effects of cure time and catalyst concentration were investigated. The cure was allowed to continue and the gel was then removed and extracted in a soxhlet apparatus for 3 days using methylene chloride as a solvent and the gel fraction was determined.

7.2.3 Characterization Methods

Infra red spectra were recorded using a Perkin-Elmer model 1000 with a NaCl window and 64 scans. Prior to recording a spectrum, the sample holder was flushed with nitrogen to remove moisture and CO₂ and the background was recorded. The sample cell was constantly purged with dry nitrogen while the signal was acquired.

NMR spectra were obtained on a Varian 500 MHz model INOVA instrument. Samples were dissolved in deuterated chloroform, and ¹H-NMR and ¹³C-NMR spectra were obtained at room temperature.

TGA was performed using TA Instruments Q-2950 high resolution TGA equipment. The samples were raised to a temperature of 600⁰C at 20⁰C/min in an atmosphere of air and then held isothermal for 20 minutes.

The degree of swelling was determined by immersing the cured sample for 24 hours in a series of solvents with varying CED (cohesive energy density). The cured samples were removed and the swollen weight was determined. The samples were then placed in a vacuum oven and dried to constant weight (polymer dry weight).

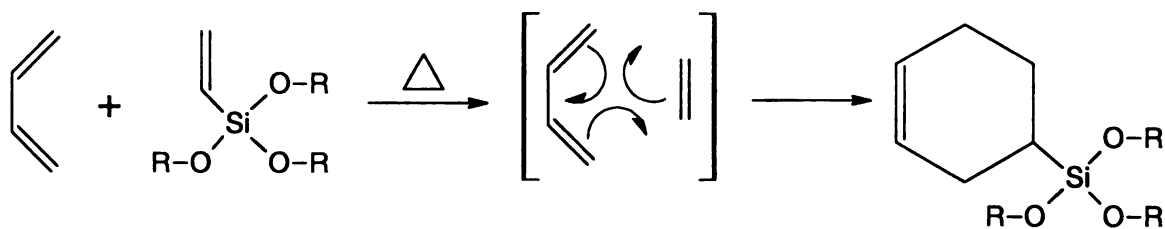
7.3 RESULTS AND DISCUSSIONS

Soybean oil is an abundant biorenewable resource composed of a mixture of triglycerides consisting of glycerin and saturated and unsaturated long chain fatty acid. Some typically natural oil fatty acid compositions are presented in **Table 1.1**. Depending on the origin of the oil seed, the number of double bonds can vary from 4.3-4.6 per mole. Although the fatty acid composition may vary, common among all samples of SO are the internal position of the double bonds and the cis configuration (**Table 1.2**).

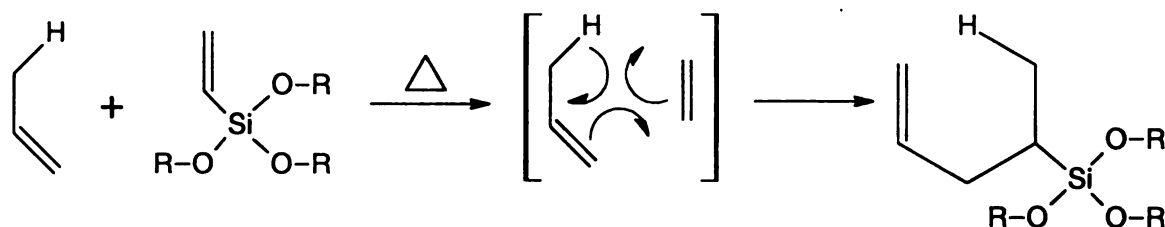
7.3.1 Evaluation of Processing Parameters

The effects of reaction time, initiator concentration, and MA concentration were studied in details using two different initiators, L101 and BF₃-methanol. The degree of VTMS addition was determined gravimetrically, and the products were further characterized using FTIR spectroscopy, ¹H-NMR, ¹³C-NMR and iodine value. The VTMS functionality is calculated as the moles of VTMS per mole of SO. Similarly, the number of double bonds is calculated from the iodine value (cgs of I₂/g of sample).

In previous work we found that maleic anhydride (MA) could react with the double bonds within SO by an “ene” addition or Diels-Alder adduct depending on the reaction conditions. It was found that reactions between MA and SO in the presence of a peroxide facilitated conjugation of the double bonds resulting in a Diels-Alder type adduct, whereas when no peroxide was used the “ene” addition product was formed. Nominally, the addition of VTMS to SO is expected to yield products as shown in **Figure 7.1**.



Scheme 1: Diels-Alder Addition



Scheme 2: Ene Addition

Figure 7.1: Diels-Alder and Ene Addition Product

The addition of VTMS to SO in a closed system under high temperatures and pressures proceeded relatively fast with and without an initiator. Three systems were considered; reactions with no catalyst, a peroxide initiated reaction, and a Lewis acid catalysis. Since soy oil contains internal non-conjugated double bonds the “ene” addition type is expected, which could be further promoted using Lewis acid (e.g. – BF₃-methanol). Similarly, a peroxide (e.g. L101) was used to promote conjugation of the double bonds within the polyunsaturated fatty acids. In all cases the reaction proceeded to completion within ~120 minutes as shown in **Figure 7.2**. Gravimetric determination of the reaction product between SO and VTMS after pulling a ½ hour vacuum at 150°C correlated to the addition 3 moles of VTMS per mole of SO. It is further interesting to note that the type of catalyst had little effect on the progress of the reaction and essentially the same reaction rates were observed for both L101 and BF₃-methanol.

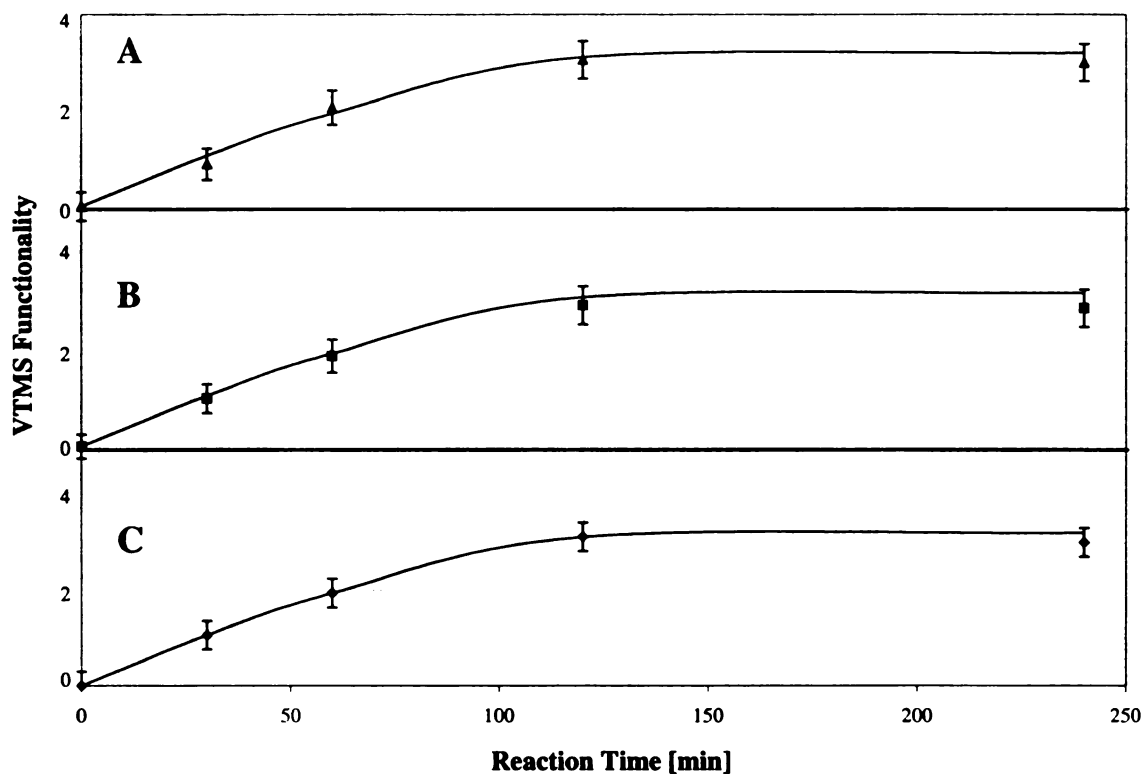


**Figure 7.2: Addition of VTMS to SO at 150C with Time
(A) no catalyst; (B) L101; (C) BF3-methanol**

Similarly, no significant differences were observed when the reaction temperature was adjusted from room temperature to 100°C, 150°C, 200°C, or 250°C for 30 minutes. Under these conditions, for reaction at 150°C and above, 1 mole of VTMS was added to SO as shown in **Figure 8.3**. In these cases the VTMS addition is kinetically controlled, as opposed to thermodynamic control.

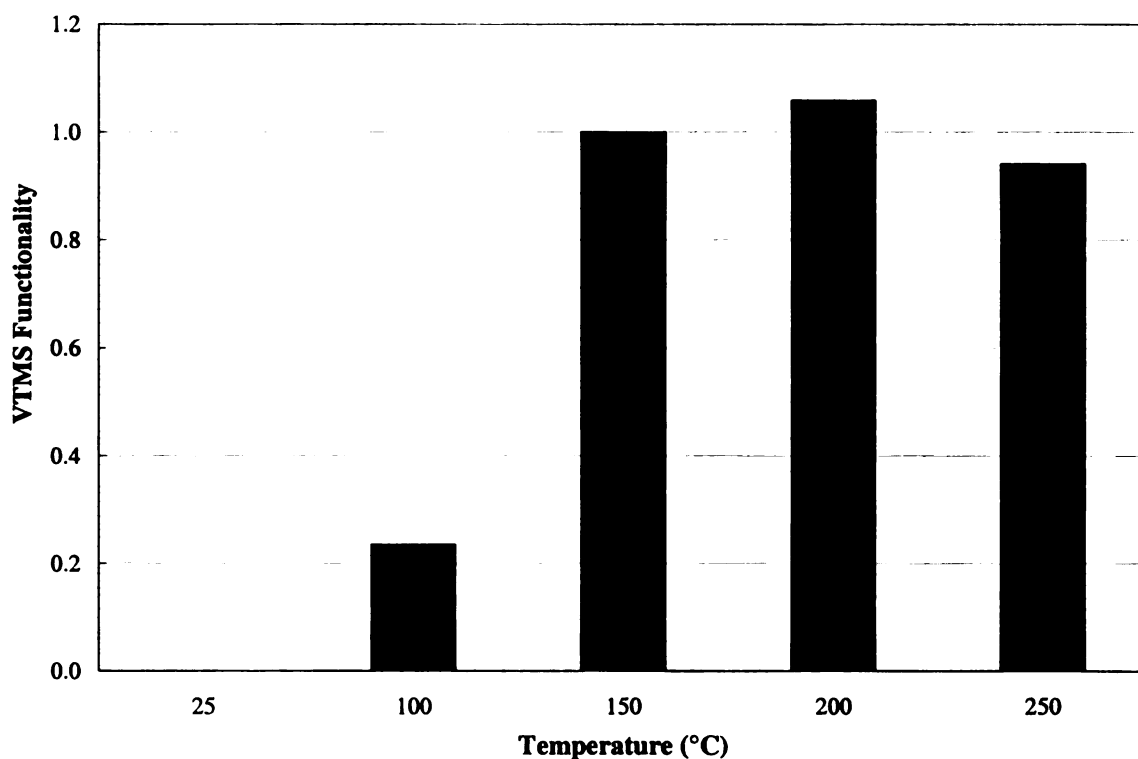


Figure 7.3: Addition of VTMS to SO with No Catalyst for 30 minutes with Increasing Temperature

Experimentally, it was observed the addition of VTMS to SO (or fatty acid residue) by an “ene” addition. In the case of the Diels-Alder adduct, there is expected to be a net reduction of 1 double bond from the unmodified soy oil (e.g. ~3.6 double bonds). This same number of double bonds suggests that reactions favor the “ene” addition over the Diels Alder addition. Further verification was done by using the fatty acid residues of SO as model compounds. In these reactions OA and LA were reacted with VTMS with and without the peroxide. Similar, to the reaction of VTMS with SO at 150 °C for 120 minutes yielded no reduction in the number of double bonds; the reactions with the model compounds also retained the original number of double bonds (Figure 7.4). Although, further addition of VTMS is theoretically possible, it was found experimentally that only

3 mole of VTMS had reacted as determined by gravimetric analysis. Although the reason for this upper limit addition of VTMS is not clear at this time, one possible explanation could be steric hindrance effects that impede further reaction of VTMS.

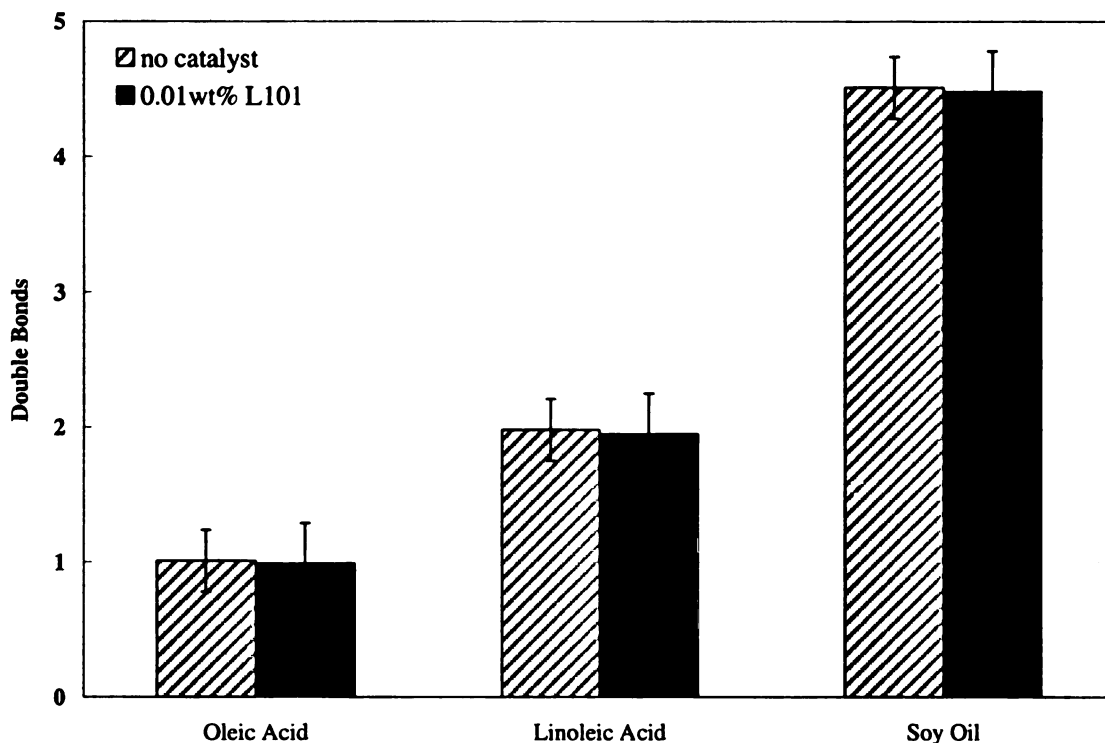


Figure 7.4: Double Bonds Remaining Following the Reactions of VTMS with SO at 150 °C for 120 minutes (and other model compounds)

7.3.2 Characterization of Silane Functionalized Soy Oil

The VTMS functionalized SO was further characterized by FTIR spectroscopy (Figure 7.5) and exhibits a splitting of the carbonyl peak at $\sim 1750\text{ cm}^{-1}$ present in neat soy oil to another peak at $\sim 1710\text{ cm}^{-1}$ not present in SO. Additionally, there are significant differences within the finger print region. Especially, noticeable is the peak at 1085 cm^{-1} and its intensity. Further verification was done using a model compound. As seen in Figure 7.6, the reaction between VTMS and LA also shows a new peak at ~ 1710

cm^{-1} and an intense peak at 1085 cm^{-1} not seen in FTIR of pure LA. The narrowing of the broad peaks of hydrogen bonded acid groups in LA to that in the silylated LA suggests there is some transesterification between the methoxy group from the silane and the carboxylic acid group of LA.

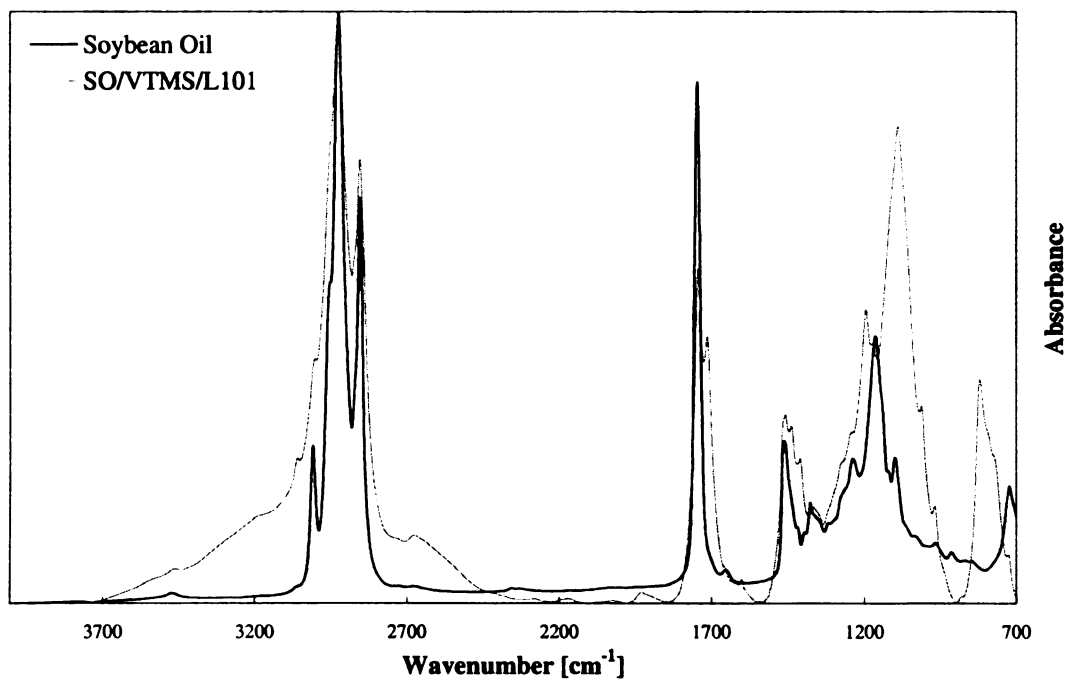


Figure 7.5: FTIR of SO and VTMS Functionalized SO

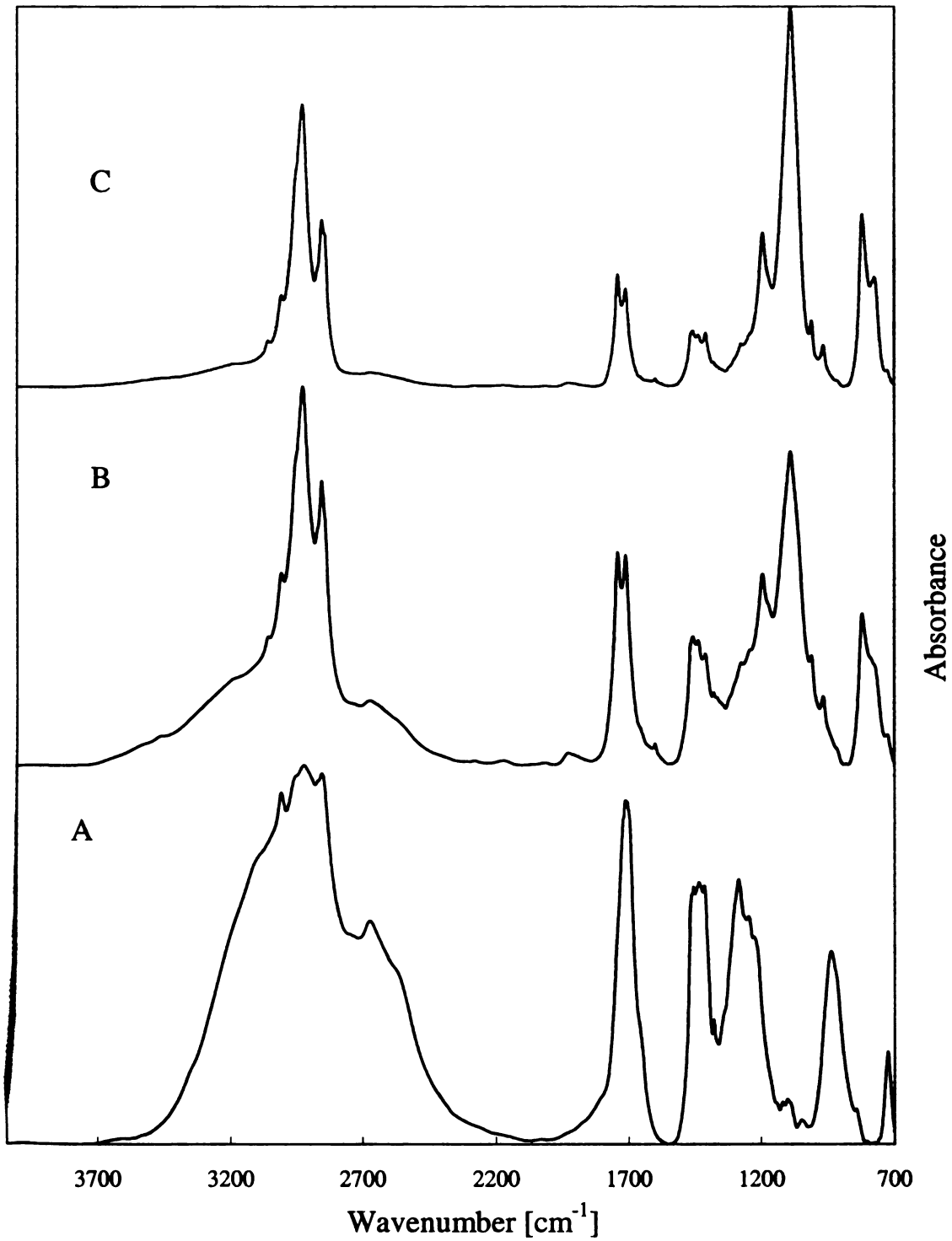


Figure 7.6: FTIR of LA (A); LA/VTMS (B); and LA/VTMS/L101 (C)

Further characterization was done using NMR using CDCl_3 as the solvent. Carbon, proton and HMBC spectra were recorded, in order to confirm the grafting of the vinyl group onto soy ester and elucidate the structure of the resulting compound. Since native soybean oil is a mixed ester of different fatty acids, the NMR spectra are complex and are not easily resolvable. The methylene protons of glyceryl backbone appear at 4.1 ppm and 4.3 ppm. The methine proton appears downfield at 5.2 ppm and the positions vary depending on the fatty acid attached to the backbone. The methyl groups on each of the fatty acids also vary in position and appear in the region 0.88 – 1.00 ppm. The double bonds in the soy fatty acids are all non-conjugated and the protons appear in the region 5.2 – 5.6 ppm. The methylene protons in the fatty acids appear over a wide range depending on their position in the acid. The methylenes adjacent to the carbonyl appear around 2.1 – 2.3 ppm, methylenes sandwiched between double bonds appear downfield at 2.6 – 2.8 ppm. Methylenes β to the carbonyl appear at 1.6 – 1.7 ppm. Methylenes on either side of double bonds (not sandwiched) appear around 2.0 ppm and the rest of the methylenes appear in the region 1.2 – 1.5 ppm.

The proton spectrum of the silane modified soy oil shows clear differences from that of native soy oil. The intense peak at 3.5 ppm is characteristic of the methoxy groups of the silane. The additional peaks at around 6.1 ppm correspond to vinyl protons. Since no such peaks are found in native soy oil, these have to result either from the residual unreacted silane in the mixture or from some bond migration due to grafting. The NMR spectrum of the pure silane does not show any peaks in this region and hence it can be indirectly concluded that these peaks are a result of grafting reactions. It is also known that conjugated double bonds appear in the 6.1 ppm region. From these results it can be

concluded that the grafting does occur and it occurs by an ene addition mentioned elsewhere in this work. Also integration of the spectrum shows the relative proton number for the 6.1 ppm peak to be around 2 (indicating at least one ene addition) and that of the methoxy peaks of the siloxane moiety to be around 18. Since each siloxane unit carries three methoxies, this corresponds to 2 moles of silane grafted onto soy. Thus it can be inferred that at least 2 moles of silane have grafted onto the backbone. The ene addition produces conjugation only in the polyunsaturated acid groups and does not affect oleic acid or the saturates. The methoxy groups are by far the best means to ascertain the extent of grafting through NMR. The absence of any broad peaks at 4.4 ppm indicates the absence of silanols which can be formed by hydrolysis of the siloxane groups. The possibility of self condensation of methoxy groups activated by heat is not ruled out and this might account for the discrepancy in grafting efficiency as ascertained by thermo gravimetric and gravimetric methods previously mentioned. **(Appendix D)**

The carbon spectra of native soy oil and silylated soy oil are also complex and were used only to confirm the methoxy carbons of the siloxane moiety. These carbons show up around 52.0 ppm as a broad peak. The vinyl carbons appear in the region 130.0 – 140.0 ppm and the carbonyls at 170.0 ppm. **(Appendix D)**

HMBC spectra were recorded in order to confirm the structure of the silylated soy molecule. Since soy oil is a mixed ester, the spectrum was complex and no significant information could be inferred from the spectrum than from the 1-D experiments. Also from the postulated mechanism (ene addition) and the resultant structure, it can be seen that the protons on the carbon attached to silicon have a 4 bond coupling to the protons on the soy carbons. Since a 4 bond coupling is very weak, it is extremely difficult to spot

on the HMBC. However the HMBC spectra do confirm the results of the 1-D experiments. The one bond coupling between the protons and carbon of the OCH₃ group is visible as doublets on either sides of the actual peak (leak through one bond coupling). The carbonyl group at 170 ppm correlates with the protons of the glyceryl backbone, indicating that the ester backbone is preserved. It is not very easy to distinguish the carbons of the vinyl group on siloxane (converted to methylenic after grafting) attached to silicon in the spectra as soy oil also has peaks in the region around 10-20 ppm corresponding to methyl groups. The new peaks at 6.1 ppm which are present in the silylated soy oil, also correlate to the vinyl carbons in the structure, which is supportive of the ene addition mechanism. From the NMR data, it can be inferred that silane does graft onto the soy backbone and there is enough evidence in favor of an ene addition mechanism operating and also the ene addition leads to conjugation in the resultant structure. (Appendix D)

7.3.3 Room Temperature Moisture Activated Cure Studies

Room temperature cure studies of the VTMS functionalized soy oil were done in a heat and moisture controlled room set at 25C and 50% relative humidity. The moisture present in the was used to promote the hydrolysis of the silicon alkoxide bonds, to form silanols which further react to form highly stable siloxane linkages. It was further observed that this process could be enhanced with a catalyst. This is particularly the case when an amine catalyst is used. As seen in **Figure 7.7**, to obtain the same sol fraction as the amine catalyzed cure, takes ~3 times as long in the absence of any catalyst under the same cure conditions. The use of a tin or titanate catalyst were effective in reducing the cure time but not as efficient as the amine catalyst.

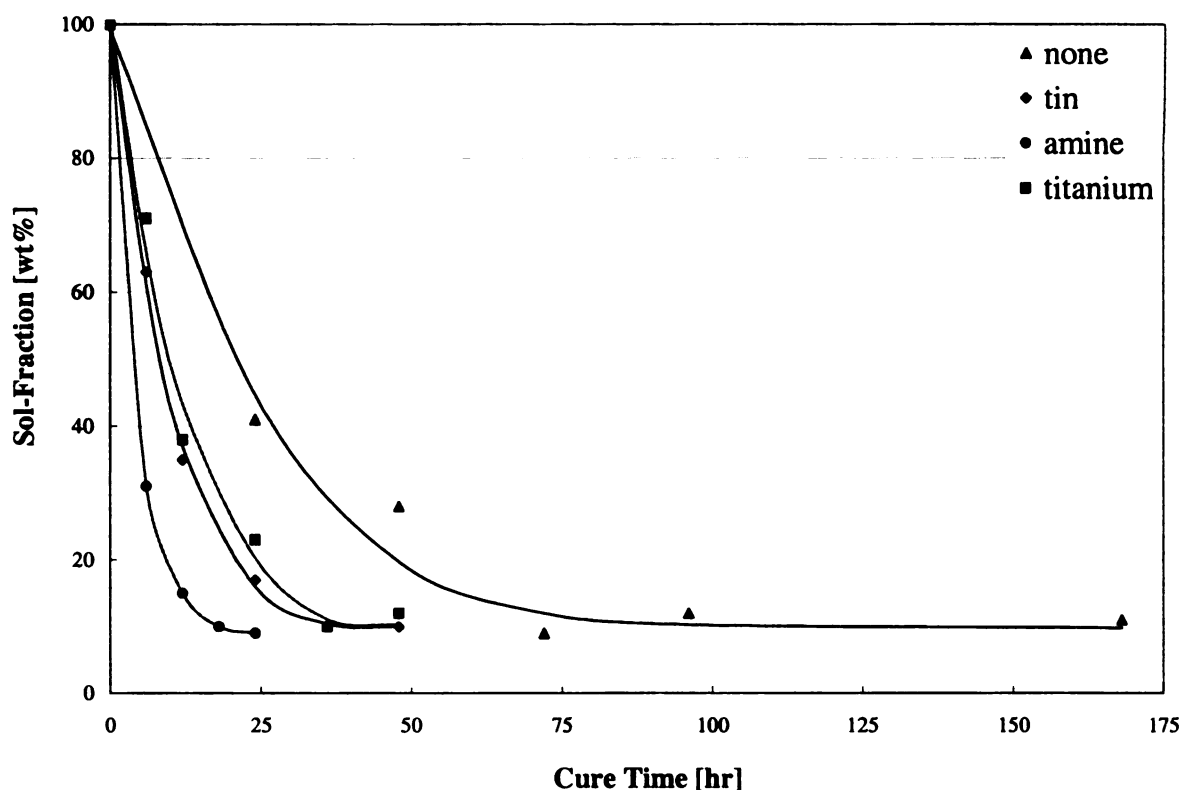


Figure 7.7: Room Temperature Cure of VTMS Functionalized Soy Oil

7.3.4 Swelling of Soybased Thermosets

The degree of swelling of the soy thermoset was determined for a series of solvents (**Table 7.1**) and plotted against the solvents' solubility parameter. Dissolution of a polymer begins with permeation of solvent molecules into the polymer's amorphous regions. The solvent breaks down intra- and inter-molecular bonds between polymer chains, increasing their mobility and free volume. This results in swelling and softening of the polymer and extraction of low molecular weight additives and polymer chains. The thermodynamically driven swelling force is counterbalanced by the retractive force of the crosslinked structure. Two forces become equal at some point and equilibrium is reached. As seen in **Figure 7.8** the greatest degree of swelling is observed for

trichloroethylene and chloroform. Interestingly, the graph shows the degree of swelling of the soy thermoset in methylene chloride is more than acetone, even though acetone has a closer solubility parameter. Theoretically, liquids with similar solubility parameter should have similar solubility characteristics, and yet the observed behavior in this instance is different. This is most likely due to the differences in kinds of polar contributions that give rise to the total cohesive energy densities in each case.

Solvent	Density (g/ml)	δ [MPa ^{1/2}]
n-Hexane	0.659	14.9
Trichloroethylene	1.463	18.7
Toluene	0.865	18.3
Methylene Chloride	1.325	20.2
Chloroform	1.492	18.7
Acetone	0.791	19.7
n-Butanol	0.81	28.7
Ethanol	0.789	26.2
Methanol	0.791	29.7
Water	1	48

$$\delta_{Total}^2 = \delta_{Dispersion}^2 + \delta_{Polar}^2 + \delta_{Hydrogen}^2$$

Table 7.1: Solubility Parameter for Various Solvents

Since, there are 3 types of polar interactions contributing to solubility: dispersion forces, polar forces, and hydrogen bonding forces. The inconsistencies observed in are mostly likely contributed to the difference in hydrogen bonding between the chlorinated solvents and the ketones. The intermolecular forces in the soy thermoset are primarily due to dispersion forces, with practically no hydrogen bonding involved. These polar configurations are perfectly matched by the intermolecular forces between chloroform molecules, thus encouraging interpenetration and swelling of the soy thermoset. Acetone, however, are more polar molecules, with moderate hydrogen bonding capabilities. Even

though the solubility parameter is more similar chloroform than methylene chloride, the differences in component forces, primarily hydrogen bonding, lead to the observed differences. Thus, acetone is attracted to each other rather than to the soy thermoset.

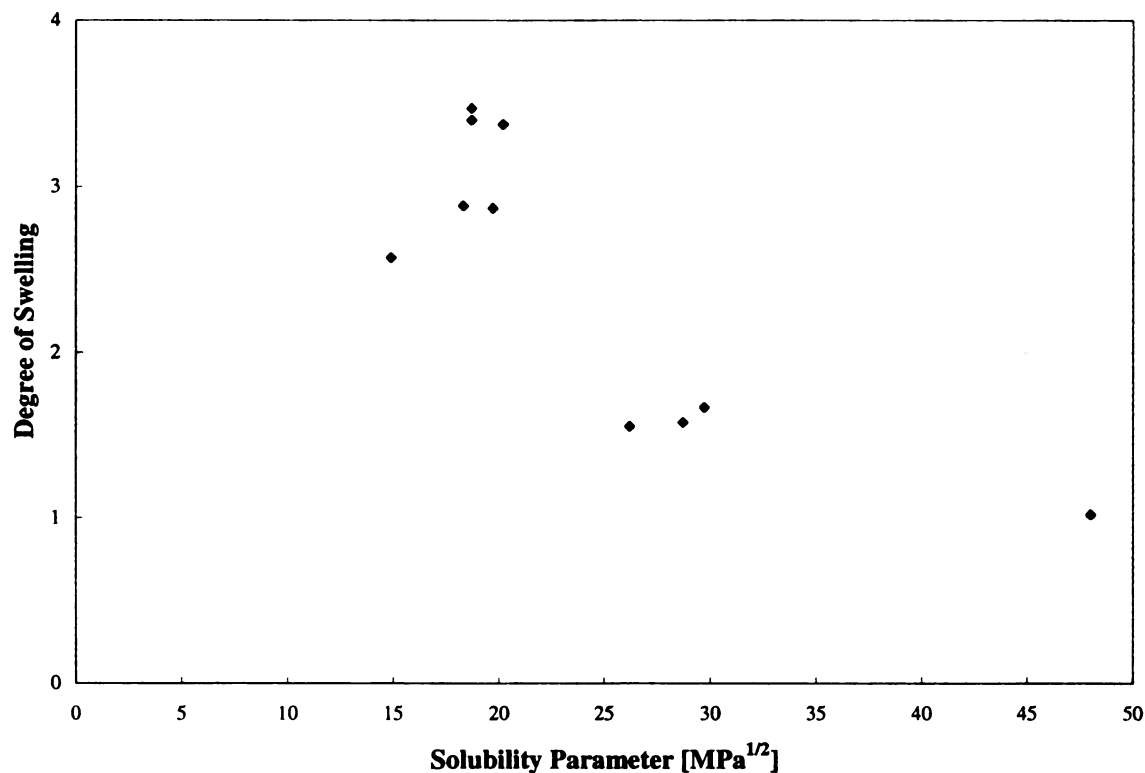


Figure 7.8: Degree of Swelling of the Soy Thermoset with Different Solvents

Thermogravimetry was carried out on the native and cured silylated soybean oils to determine their relative thermal stability in air and also evaluate the grafting efficiency of the silane (**Figure 7.9**). The results of the thermal analysis show that grafting slightly enhances the temperature stability of the soybean oil as indicated by the absence of any sharp drops in weight with temperature and also the ultimate weight after the analysis. The native soy oil degraded completely in an air atmosphere while the silylated samples still retained 15% or more of their weights. This gives an indication of the extent of grafting of silane. When the experiments involving silylation were run, a simple mass

balance around the reaction setup indicated that around 3 moles of silane were used up in the reaction. This would correspond to an ultimate weight of around 14% after the TGA run (assuming all the carbon was oxidized in the sample to leave silica). The TGA results indicate that more than 15% of the sample remains after the experiment which confirms the grafting efficiency of the silane. The onset of weight loss however is at a lower temperature for the silylated materials than for the soy oil. This is due to the fact that curing reactions with siloxane invariably lead to loss of small compounds like methanol or ethanol, which account for the early onset of weight loss. From the analysis it can also be seen that the amine catalyzed cure and plain cure have better thermal stability than the Tin catalyzed and TYZOR catalyzed cure. This could be explained on the basis that both tin and TYZOR are capable of catalyzing the hydrolysis of ester backbone in soy leading to lower degradation temperatures. This is also true for the amine catalyst, but its activity is much lesser than that of the former.

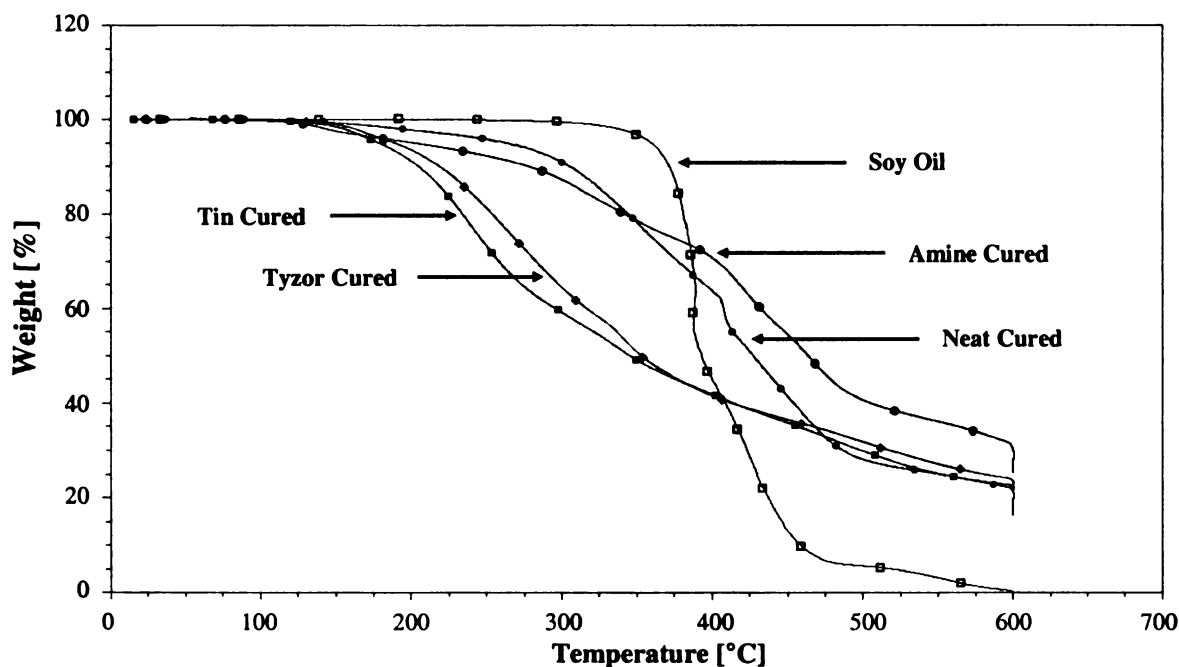


Figure 7.9: Thermal-Oxidative Stability of Soy Oil and RT Cured Silated Soy Oil

7.4 CONCLUSIONS

Silane functionalities were introduced to soybean oil for use as a chemical feedstock. The investigation and optimization of this work resulted in a single step process to react vinyltrimethoxy silane to soybean oil. Three systems were evaluated, thermal addition, a peroxide initiated addition, and a Lewis acid catalyst. The effects of reaction time, catalyst type, and reaction temperature were investigated. The silylated soybean oil was characterized using iodine value, FTIR spectroscopy, $^1\text{H-NMR}$, $^{13}\text{C-NMR}$ and TGA. Characterization suggested that 3 moles of silane were added to each TAG by an “ene” addition. Soybased thermosets were prepared using a room temperature moisture activated cure of these silane functionalized soy oils, and degree of swelling in a series of solvents was investigated.

7.5 REFERENCES

1. J. Baghdachi, J. and Li D., Soybean oil-based non-isocyanate containing moisture cure resins and coatings. Proceedings of the International Waterborne, High-Solids, and Powder Coatings Symposium (2001), 28th 231-233.
2. Reaction product of a silane and an unsaturated fatty substance and its use in coating compositions for siliceous materials. GB patent No. 1129219 (1968).

Chapter 8: Overall Conclusions and Recommendations

8.1 MALEIC ANHYDRIDE FUNCTIONALIZED SOY OIL

New value added product was developed from soybean oil for use as a chemical feedstock. The investigation and optimization of this work resulted in a simple and fast process to maleate soybean oil. Anhydride functionality was introduced to soybean oil through a free radical initiated maleation. Two initiators were evaluated, 2,5-bis(tert-butylperoxy)-2,5-dimethylhexane peroxide and di-*tert*-butyl peroxide. The effects of reaction time, initiator concentration, maleic anhydride concentration, and reaction temperature were investigated. The maleated soybean oil was characterized using acid value, iodine value and FTIR spectroscopy. The acid value was directly related to the initial concentration of maleic anhydride, whereas the concentration and type initiator had little effect on the acid value. The peroxide initiated functionalization of soybean oil with maleic anhydride in a closed vessel at elevated pressure and temperature was found to proceed by a Diels-Alder mechanism.

8.2 BIOFIBER REINFORCED SOYBEAN COMPOSITES

Composites with good mechanical properties were prepared from chemically modified soy oils and biofibers without additional petroleum-based polymers. These composites were prepared from maleic anhydride and epoxide functionalized soybean oils that were cured in the presence of various biofibers (e.g. kenaf, kayocell, protein grits, and solka-floc) by a flexible amine catalyst. Rigid thermosets characterized by high crosslink density network and a high gel fraction were obtained. FTIR was used to follow the cure reaction via the disappearance of the characteristic anhydride absorptions. Composites having high tensile strength and low elongation were obtained when kenaf

fibers were treated with (2-aminoethyl)-3-aminopropyl-trimethoxysilane and then added to the epoxidized/maleated soy matrix and cured with hexamethylene diamine. These biobased composites could provide inexpensive epoxy resin alternatives for a wide variety of industrial applications.

8.3 SYNTHESIS OF SOY POLYOLS VIA OZONE CHEMISTRY

New soy-based polyols were prepared by passing ozone through a solution of soybean oil and ethylene glycol in the presence of an alkaline catalyst. Under these conditions the double bonds in the unsaturated fatty acids are cleaved and the ozonide intermediates that are formed react with one hydroxyl group of the glycol through an ester linkage leaving the other hydroxyl group unreacted. The product of this reaction is composed of triglycerides containing primary alcohols and a mixture of low molecular weight diols and mono-alcohols. The latter are derived from cleaved fragments of the unsaturated fatty acids beyond the double bonds. Due to the position of the double bonds in the unsaturated fatty acid residues of soy oil, the primary triglyceride products contain a nonanoate ester. The composition of the soy polyols mixture was calculated based on statistical analysis and characterized by hydroxyl value, iodine value, C-NMR, and FTIR spectroscopy. The effects of experimental conditions with various catalysts were also investigated. A portfolio of soy polyols were prepared with varying hydroxyl functionalities (varying reaction time) and molecular weight (varying hydroxy compound and concentration) were prepared. Rigid soy-based polyurethanes were successfully prepared using 100% of the soy polyols. Whereas in most current commercial technologies soy polyol normally contribute 20-30 wt%, with the majority still petroleum based.

8.4 EVOLUTION SOY POLYOL PRODUCTION

There have been 4 major milestones achieved since establishment of the proof-of-concept. Initial preparation of soy polyols were done in small quantities (~20 grams) in a chlorinated solvent at low temperatures (-70°C). The solvent was used to minimize the concentration of the ozonides for safety concerns. However, use of the solvent did allow for reactions to be run at low temperatures to increase ozone solubility. Commercially, it would be beneficial to have a process which does not require solvent or low temperatures.

The first significant milestone was achieved by removal of the solvent and room temperature synthesis. Concurrently, larger batches of soy polyol were being prepared (~1000 g). It was recognized that a key variable was the mass transfer of ozone through the reaction median. A mass balance around the system showed that only 30% of the ozone fed was reacting, while the majority was exiting the system into the destruction unit. A preliminary economic evaluation showed the polyol production cost was greatly influenced by the energy associated with producing the ozone. Running reactions at low temperatures was advantageous for safety and enhanced mass transfer, since ozone solubility is inversely related to temperature. However, it was determined to be more economical running at room temperature because of the high cost of dry ice.

The second significant milestone was the successful application of a heterogeneous catalyst. Initial studies were done using NaOH as a catalyst. Some difficulties associated were the breakdown of the triglyceride backbone and difficulties removing residual NaOH. Next, different amines were considered as catalyst. Amines were selected because the target application for the soy polyols is polyurethanes, and since the amines

are also used to catalyze urethane chemistry; the goal was use the same catalyst for both applications. This would be beneficial because it completely removes a unit operation for removal of the catalyst. However, there was severe discoloration of the polyol overtime which was attributed to the oxidation of the amine. Heterogeneous catalysts were considered for ease of removal. Alkaline solids such as CaCO_3 and MgO were evaluated, and both were found to be effective at redirecting the decomposition of the ozonides to form polyols. For cost and availability CaCO_3 was determined to be the preferred catalyst.

The third milestone was the development of soy polyols applicable for use in flexible polyurethane. These polyols were developed by increasing the amount of C-C linkages, to allow for more flexibility within the molecule. This was done using 2 different approaches. The first approach involves preparing the polyols using different molecular weight PEG. These polyols were prepared using CaCO_3 , and PEG400, 500, and 600 instead of and/or in combination with ethylene glycol. When used in polyurethane synthesis, these new polyols were found to produce a more resilient and flexible foam, as apposed to those prepared using only ethylene glycol. Another scheme to increase the molecular weight of the polyols is to run the reactions near stoichiometric with ethylene glycol. Experimentally, it was found that as the reaction progressed and the concentration of ethylene glycol reduced, oligomerization reactions occur. This was found to be the preferred method because of the increased soy oil content (increased biobased content) and economically advantages since soy oil is less expensive. The newest developed polyol using this approach had a MW = 4100 g/mol and a hydroxyl value of 48. This newly prepared polyol could be a sustainable alternative to an industry

standard, DOW's Voranol 4701. Commonly used for flexible foam applications the petroleum based polyol has a MW = 4800 g/mol and a hydroxyl value of 34.

The fourth milestone is the development of the continuous production of soy polyols. A baffled CSTR with 3 impellers was designed to achieved enhance mass transfer of ozone within the system through creating turbulent flow.

8.5 MODIFIED SOY OIL BASE OIL LUBRICANT PROPERTIES EVALUATED

The oxidative stability of soybean oil was enhanced by transforming the double bonds into more oxidatively stable esters by two chemical modifications. The first modification was done by incorporation of anhydride functionality in soy oil in the presence of a peroxide, followed by an esterification using alcohol. A series of alcohols with increasing molecular weight were considered, and it was found that butanol was the most stable of the series. The second modification was done using a catalytic ozonolysis in the presence of an alcohol. A series of alcohols with increasing molecular weight were considered, and it was found that the use of methoxy-PEG350 resulted in the most stable product for the series. Both modifications were also found to reduce the tendency to form deposits and improve lubrication performance in comparison to the untreated soy oil.

8.6 SILANE FUNCTIONALIZED SOY OIL

Silane functionalities were introduced to soybean oil in a single step process by reacting vinyltrimethoxysilane with soybean oil. Three systems were studied and the effects of reaction time and reaction temperature were investigated. The use of catalyst did not greatly affect the progress of the reaction as the reaction products from thermal addition, peroxide initiated addition, and Lewis acid catalyst did not vary. The siled soybean oil was characterized using iodine value, FTIR spectroscopy, ¹H-NMR, ¹³C-

NMR and TGA. It was determined that 3 moles of silane were added to each triglyceride. A room temperature moisture activated cure of these silane functionalized soy oils were used to prepare soybased thermosets, and degree of swelling in a series of solvents was investigated.

8.7 RECOMMENDATIONS

Ozone Mediated Synthesis

- Soy polyol with reduced moisture content of soy oil.
- Prepare amine (ethanolamine) and acid (water) functionalities to soy oils
- Optimization of continuous polyol production

Application of Polyols

- Evaluation in unsaturated polyesters
- Formulation of flexible foam polyurethanes
- Evaluate in concrete preparation

Soy-based lubricants

- Formulation using additives technology.

Silated Soy Oil

- Synthesis using low sat soy oil to reduce sol content

Appendix A: Verification with a Model Compound

EXPERIMENTAL PROCEDURE

Ozonolysis of Soybean Oil

Methyl soyate (20 g), methanol (40 ml), methylene chloride (150 ml) and triethylamine (0.4 M in CH₃OH) were placed in a 500 ml gas wash bottle and cooled to -75°C in an isopropanol dry ice bath and then ozone was bubbled through the reaction mixture. Samples were taken as the reaction proceeded as noted. The product was then washed with excess distilled water 5 times in order to remove any excess methanol and catalyst. The first 2 washes were slightly acidic (0.2M HCl) to neutralize the base. A rotary evaporator was then used to strip off the solvent and residual methanol. The product was then dried over molecular sieves for 48 hours prior to testing.

Characterization Procedures

GM-MS were done at the MSU Mass Spectrometry Facility

RESULTS

The reaction products using triethylamine was similar to those formed when NaOH was used, and these products could be match to the NIST database.

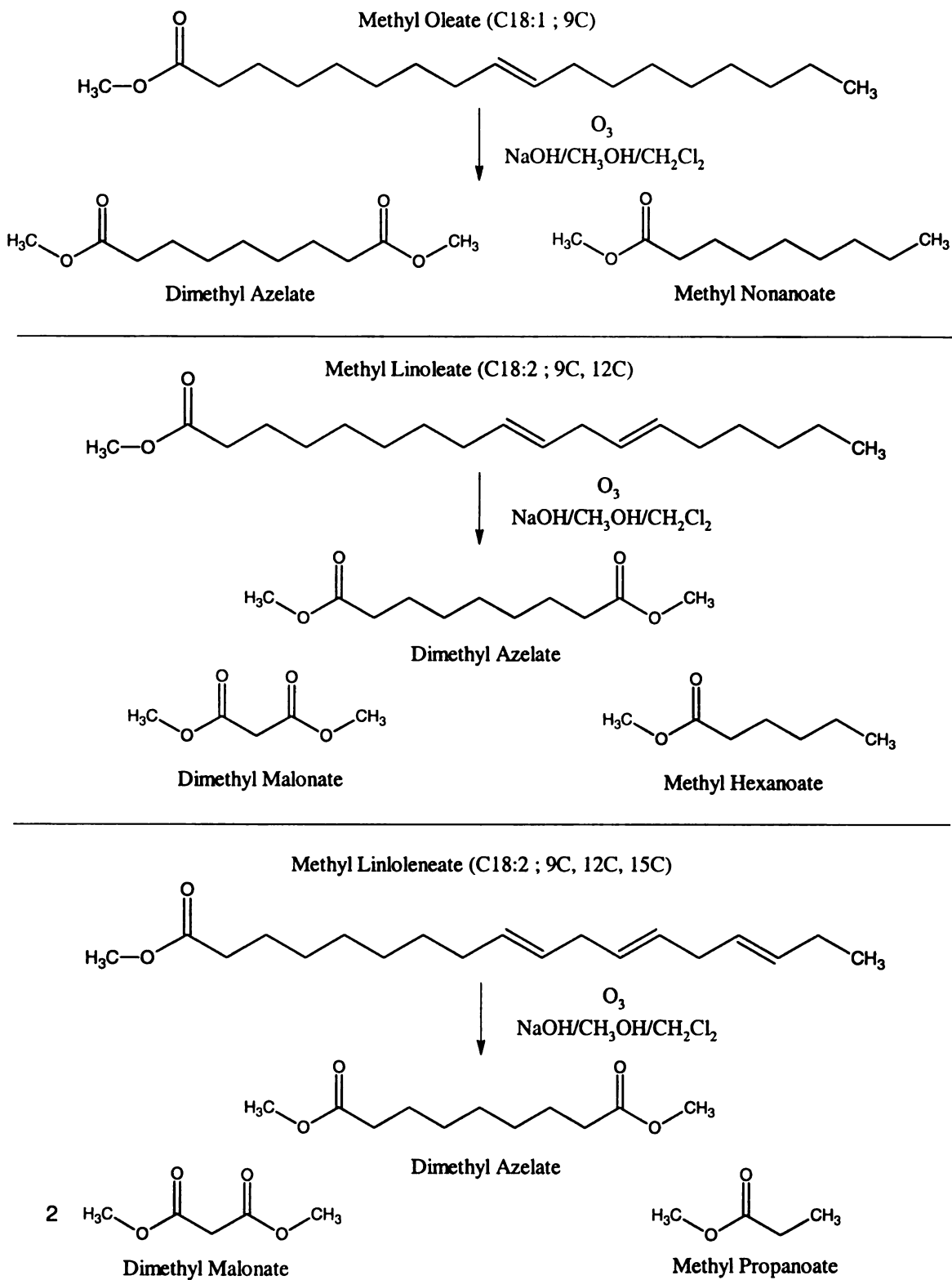


Figure A1: Ozonolysis of Methyl Soyate in Triethylamine and CH₃OH

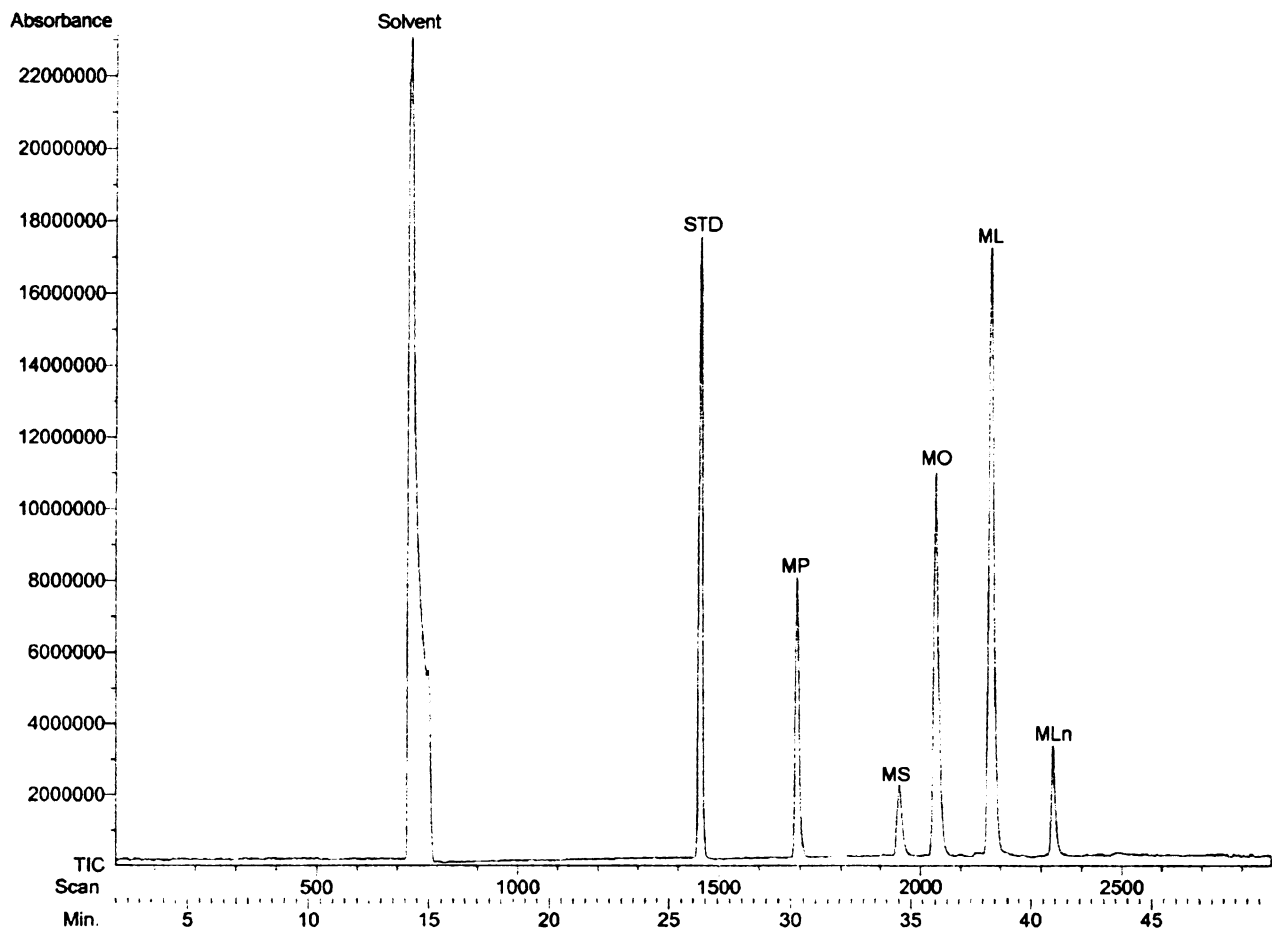


Figure A2: GC-MS of Methyl Soyate

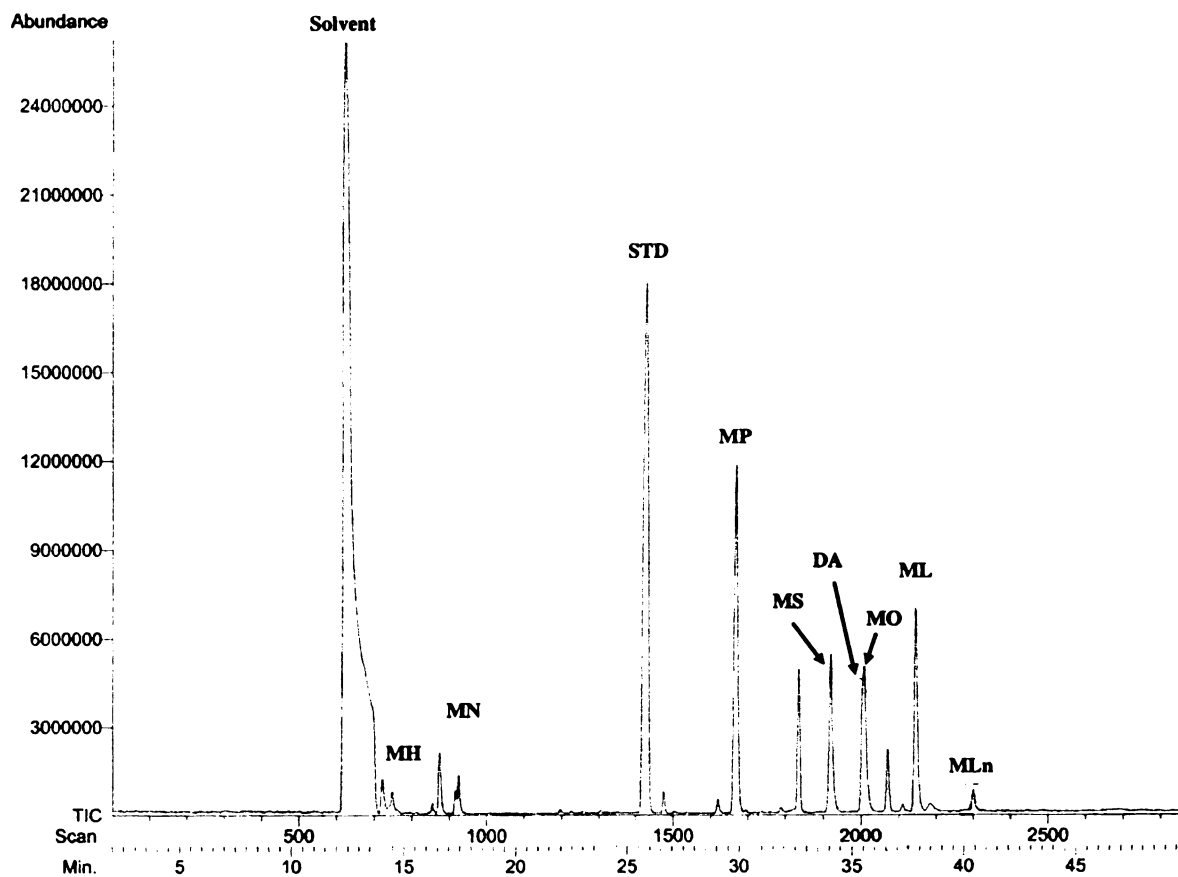
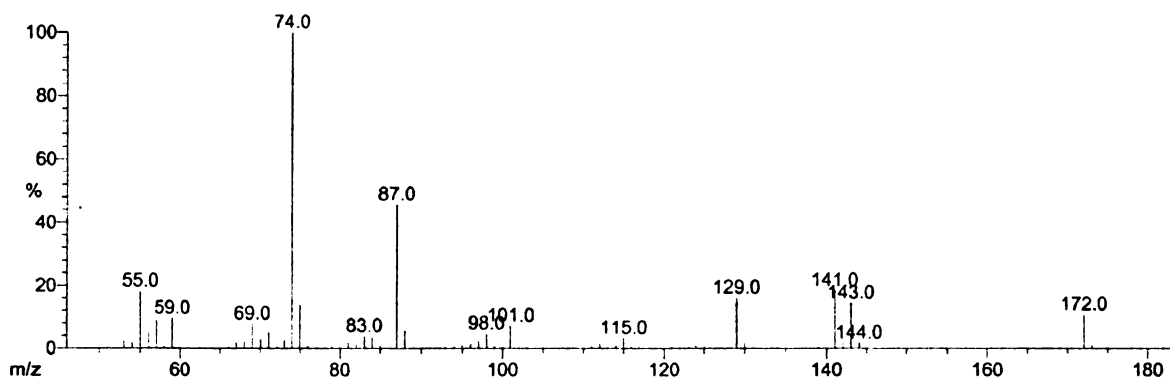


Figure A3: GC-MS of Ozonolysis Products

Scan: 926

R.T.: 17.47

Base: m/z 74; 36%



NIST MS 1 of 40 (1731-84-6)
Nonanoic acid, methyl ester

Base: m/z 74

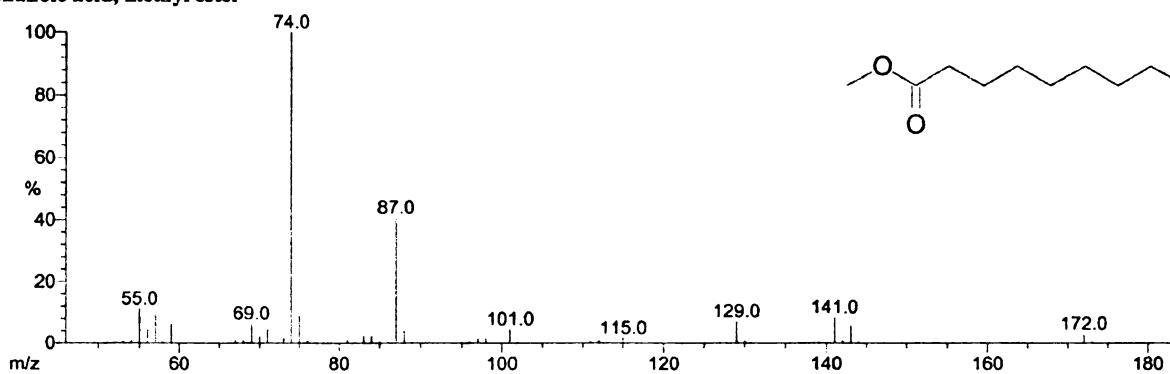
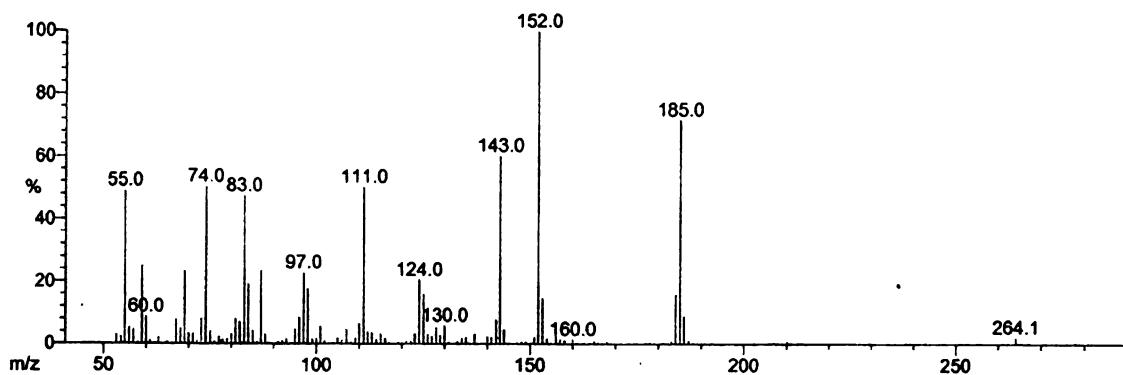


Figure A4: Mass Spectra of C₉ Ozonolysis Products

Scan: 1998

R.T.: 35.38

Base: m/z 152; 12%



NIST MS 1 of 40 (1732-10-1)
Nonanedioic acid, dimethyl ester

Base: m/z 152

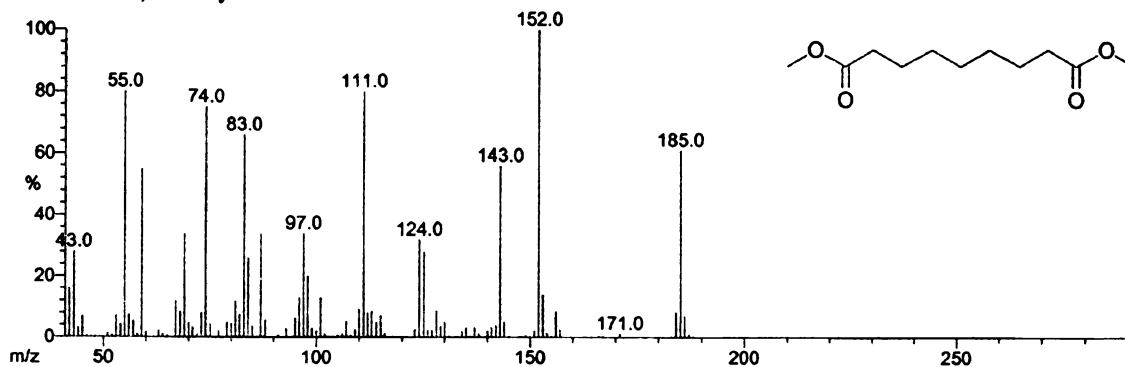
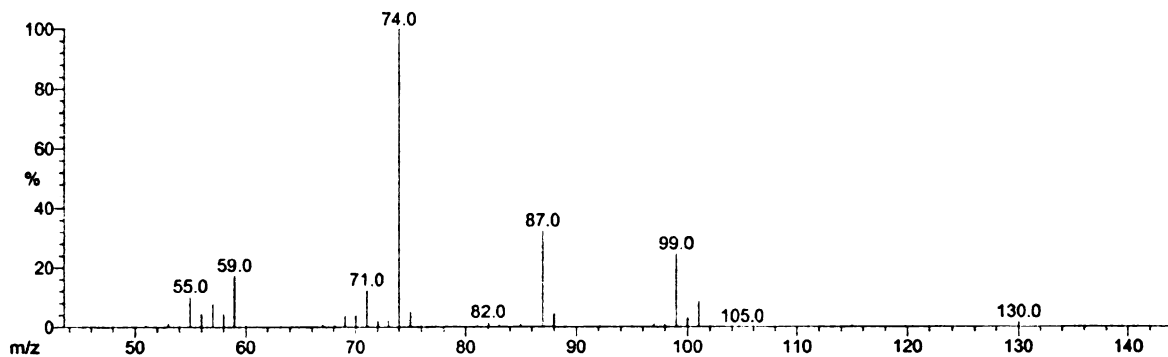


Figure A5: Mass Spectra of C, Base Fragment

Scan: 747

R.T.: 15.53

Base: m/z 74; 37.1%FS



NIST MS 1 of 40 (106-70-7)
Hexanoic acid, methyl ester

Base: m/z 74

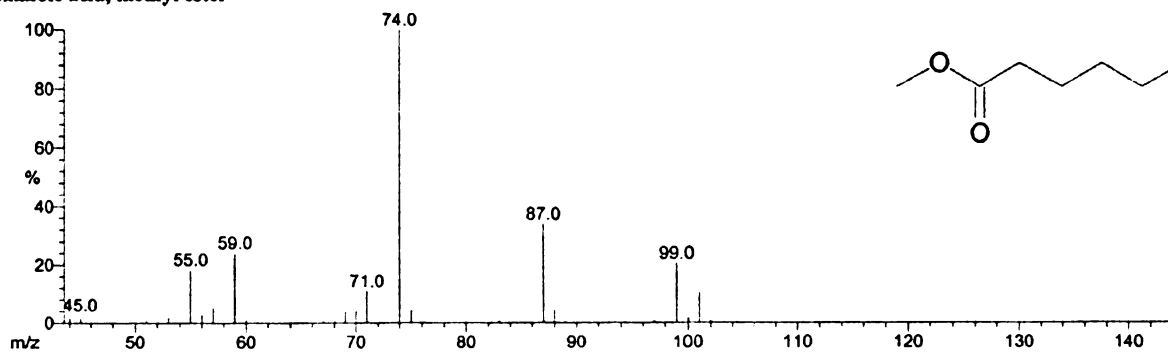


Figure A5: Mass Spectra of C₆ Fragment

Appendix B: Ozonolysis in an alkaline median

PROPOSED CHEMISTRY

Ozone reacts with double bonds such that the first step is a 1,3-dipolar cycloaddition, forming a primary ozonides (**Figure B1**).

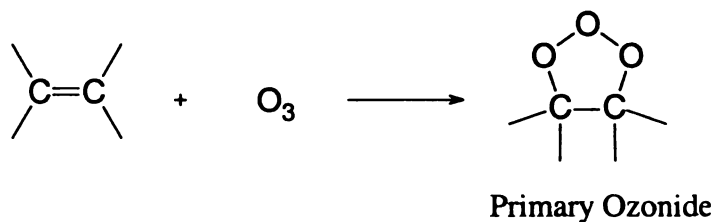


Figure B1: Formation of Primary Ozonide

The primary ozonide is a very unstable and decomposes immediately by selective cleavage of the carbon-carbon bond and one oxygen-oxygen bond leading to a carbonyl compound and a peroxidic carbonyl oxide, as a second fragment (**Figure B2**).

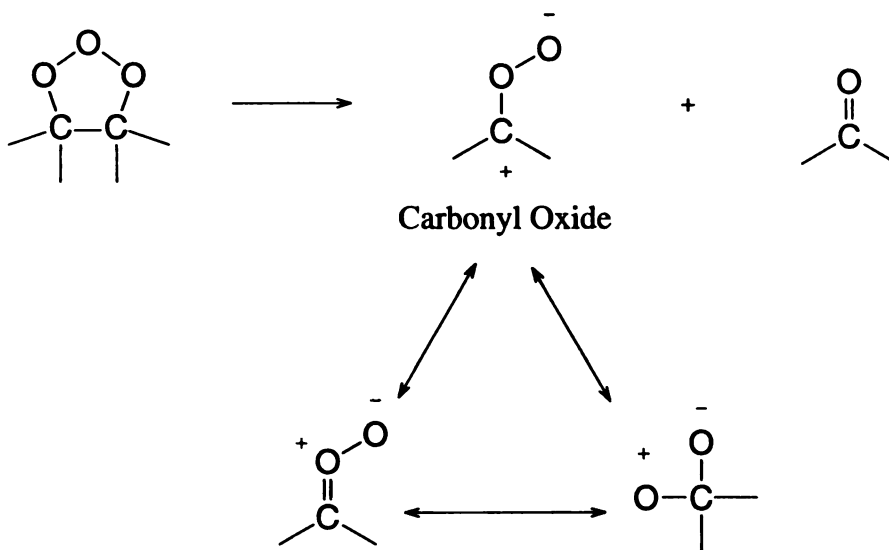


Figure B2: Ozonolysis Reaction Mechanism

This carbonyl oxide is a very reactive and can react in various routes, all of them generating peroxides. Some of the possible carbonyl oxide reactions are shown in

Figure B3.

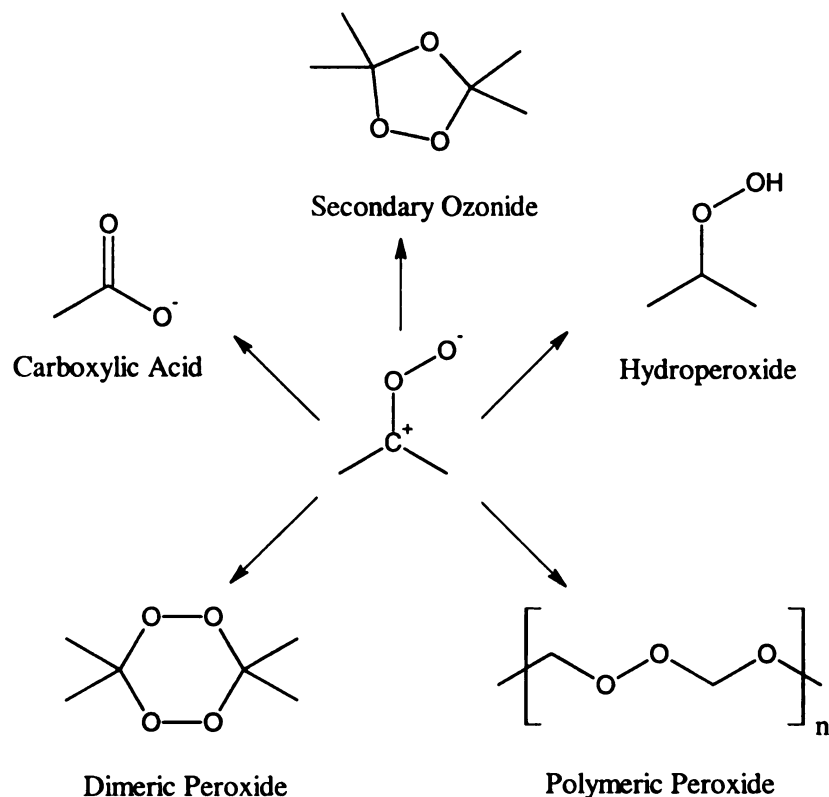


Figure B3: Possible Reactions of Carbonyl Oxides

A reaction with the carbonyl compound forms as a second fragment to yield secondary ozonides. The resulting 1,2,4-trioxolanes are more stable than the primary ozonides. Another reaction is with protic molecules (e.g. solvent) to form hydroperoxides. Also, possible is a rearrangement to carboxylates, as well as dimerization and polymerization. However, due to the large oxygen content of these molecules, the carbonyl oxide, secondary ozonides, dimeric and polymeric structures are very unstable and tend to decompose. Polymeric peroxides are of particular concern because of their low solubility and tendency to precipitate. Therefore for safety consideration maintaining low

concentrations of these species is important. This can be achieved by using a continuous process or working in diluted solutions.

Nominally, the ozonolysis of methyl oleate would lead to a mixture of aldehydes and carboxylic acids (**Figure B4**). It was proposed by Marshall and Garafalo that under basic conditions, the ozonolysis of alkenes in methanolic NaOH could redirect the decomposition to form methyl esters (**Figure B5**).

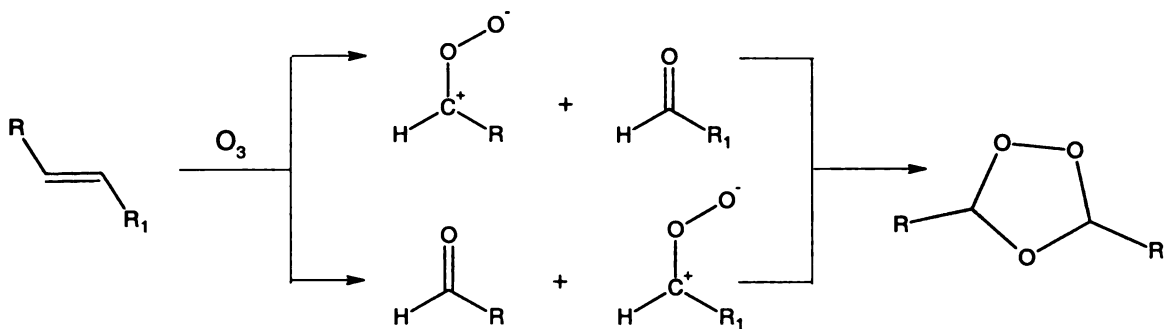


Figure B4: Ozonolysis of Methyl Oleate

The reaction pathway is hypothesized to be by formation of an aldehyde and carbonyl oxide from the primary ozonide, reacting with methoxide and methanol to form a hemiacetal and hydroperoxide. The former undergoes a base assisted hydride abstraction by O_3 and the latter dehydrates to form a methyl ester (**Figure B5**).

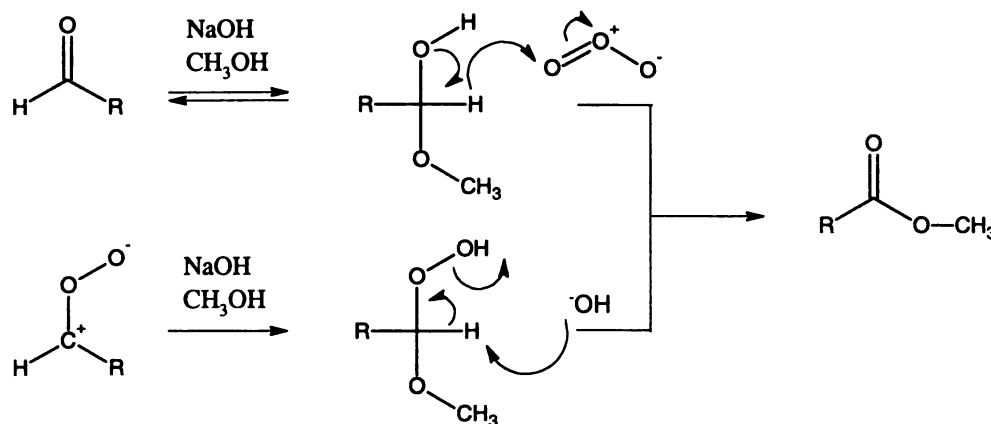


Figure B5: Ozonolysis of Methyl Oleate in the Presence of Methanolic NaOH

Appendix C: Scale-up Process Economics for Polyol Production

Reaction Stoichiometry				Polyol	
Compound	mols	MW (g)	weight (g)	weight (lb)	wt%
Soybean Oil	1	870	870	1.9162996	0.5337423
Ethylene Glycol	10	62	620	1.3656388	0.3803681
Calcium Carbonate	-	-	-	0.3281938	
Ozone	10	48	480	1.0572687	
Water	10	18	180	0.3964758	
Oxygen	5	32	160	0.3524229	
			Total	3.5903084	lbs

Raw Material				
Compound	weight (lb)	wt%	Cost (\$/lb)	Cost
Soybean Oil	0.53374233	0.533742331	0.25	\$0.1334
Ethylene Glycol	0.3803681	0.380368098	0.46	\$0.1750
Calcium Carbonate	0.1	-	0.75	\$0.0750
Oxygen	281 ft3 ~ \$4.31		-	\$0.9509
	1	lbs		\$1.3343

Manufacturing Cost	
Ozone Required (g)	122.997791 g O3 required to treat 0.58 lbs of SO
Reaction efficiency (%)	0.8
	153.747239 * g of O3 required
Time	4.1329903 hr at 0.62 g O3/min
Ozone consumes <0.07 kW per kg O3	
0.00936486	\$/hr to run the ozone generator assuming \$0.06/kWhr
0.038704876	* energy cost to operate ozone generator per hr
Ozone Generator	\$200,000
Peripheral equipment:	\$800,000
	5 years write-off, debit per year: \$200,000
Production capacity ds:	500 lb/hr
Production hours per year:	6132 hr
debit per lb ds	\$0.0652

Labor	
three shifts per day, 24 hours	
Production hours per year:	6132 hr
Personnel	\$10 per hr
	3 men
Personnel per lb	\$0.02

Per lb product			
Raw material	\$1.334	Raw material	\$0.383
Energy	\$0.039	Energy	\$0.077
Debit	\$0.065	Debit	\$0.065
Personnel	\$0.020	Personnel	\$0.020
Total	\$1.46	Total	\$0.5460

* using air
* assume doubling power to account for air compressor

Raw Data for Sensitivity Analysis

Assumptions:

- * Energy cost is \$0.06 per kWhr
- * Ozone is generated from air
- * Energy cost is doubled to account for the air compressor and heater
- * **Synthesis done in a PBR production cost ~\$0.471/lb (CaCO3 cost removed), else \$0.546/lb**

Effects of Extent of Reaction

~ Assume 80% ozone reaction efficiency

COST	Reacted Double Bonds
\$ 0.5460	4.6
\$ 0.5292	3.6
\$ 0.5124	2.6
\$ 0.4956	1.6
\$ 0.4787	0.6

Effects of Ozone Efficiency

COST	efficiency	Variation (%)
\$ 0.8726	20%	-0.333333333
\$ 0.8106	25%	-0.166666667
\$ 0.7694	30%	0
\$ 0.7399	35%	0.166666667
\$ 0.7178	40%	0.333333333

Effects of Price Fluctuation on Raw Material Cost

COST	EG (\$)	Variation (%)
\$ 0.6371	\$ 0.36	-0.2
\$ 0.6561	\$ 0.41	-0.1
\$ 0.6751	\$ 0.46	0.0
\$ 0.6942	\$ 0.51	0.1
\$ 0.7132	\$ 0.56	0.2

COST	SO (\$)	Variation (%)
\$ 0.6218	\$ 0.15	-0.4
\$ 0.6485	\$ 0.20	-0.2
\$ 0.6751	\$ 0.25	0
\$ 0.7018	\$ 0.30	0.2
\$ 0.7285	\$ 0.35	0.4

COST	CC (\$)	Variation (%)
\$ 0.6651	\$ 0.65	-0.133333333
\$ 0.6701	\$ 0.70	-0.066666667
\$ 0.6751	\$ 0.75	0
\$ 0.6801	\$ 0.80	0.066666667
\$ 0.6851	\$ 0.85	0.133333333

Appendix D: NMR for Silated Soy Oils

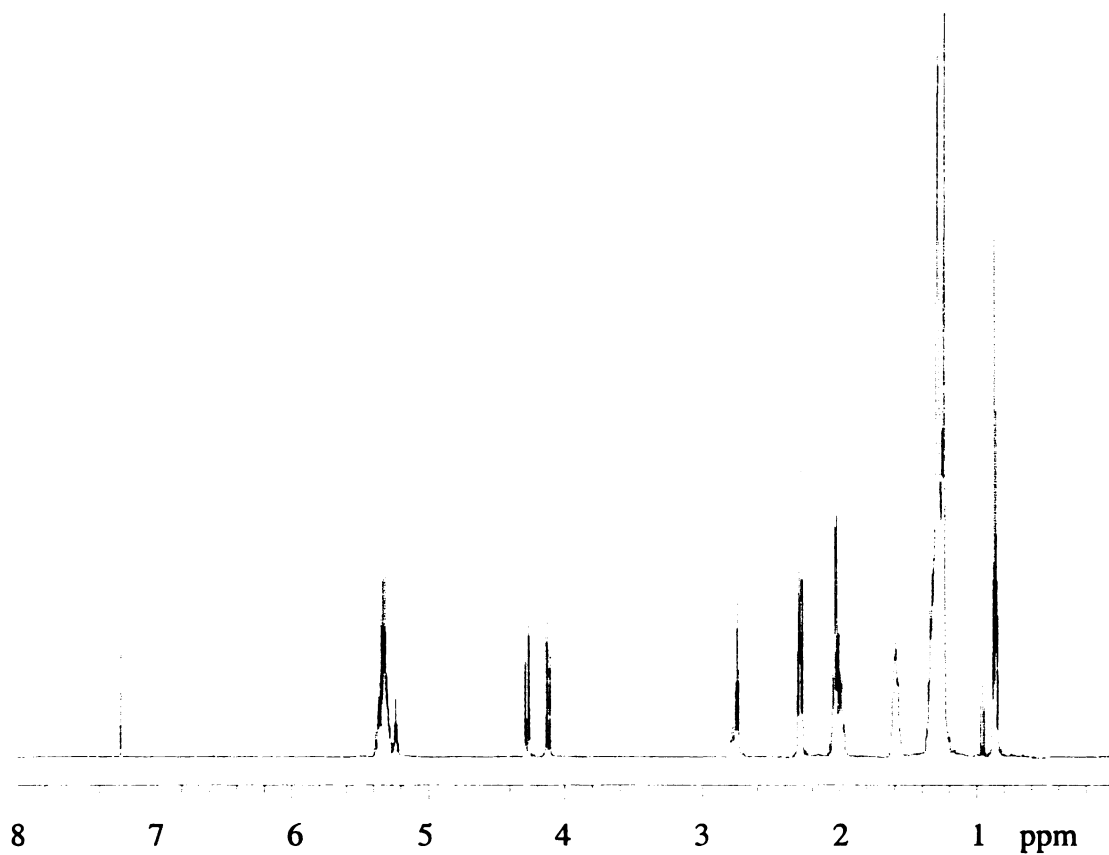


Figure D.1: ^1H – NMR Spectra of Soybean Oil

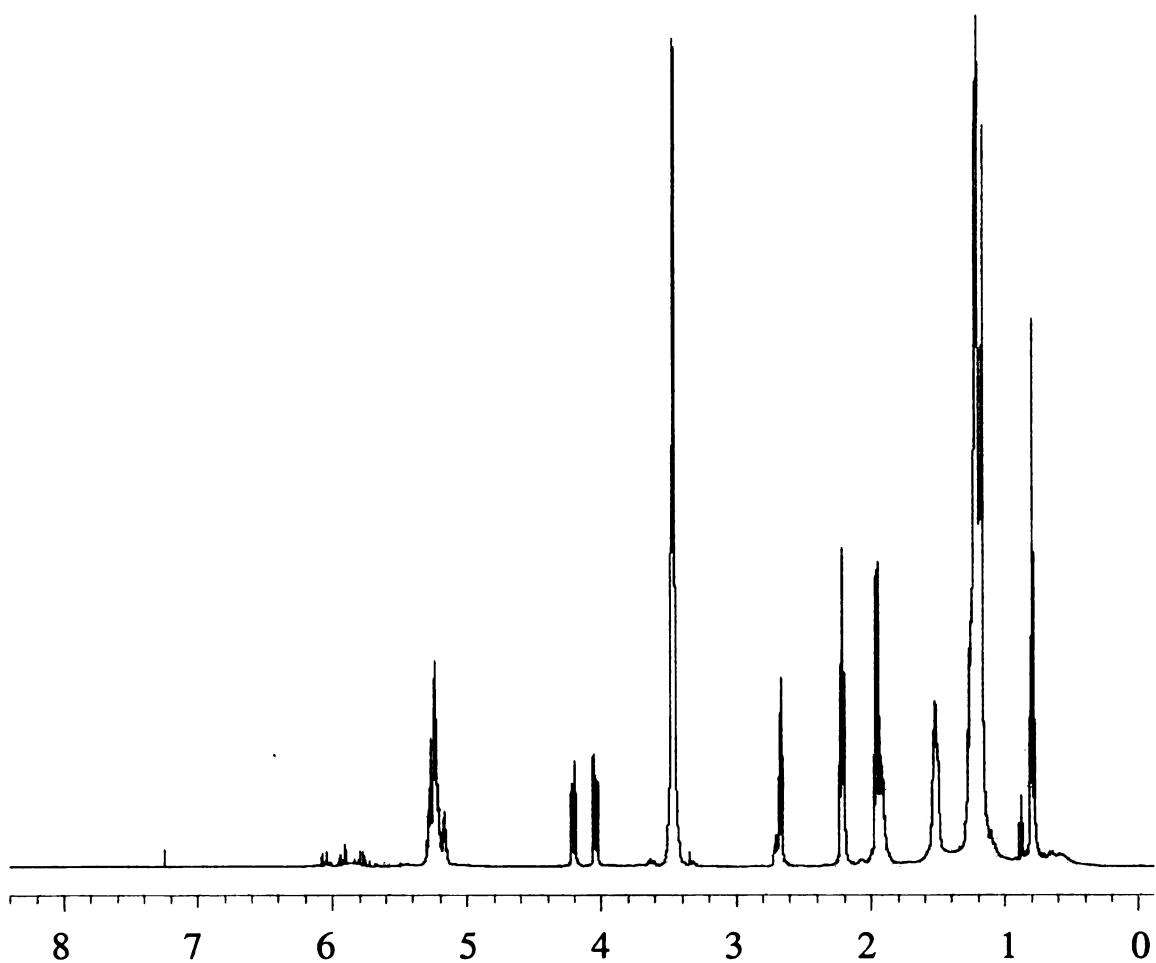


Figure D2: ^1H - NMR of Silylated Soybean Oil

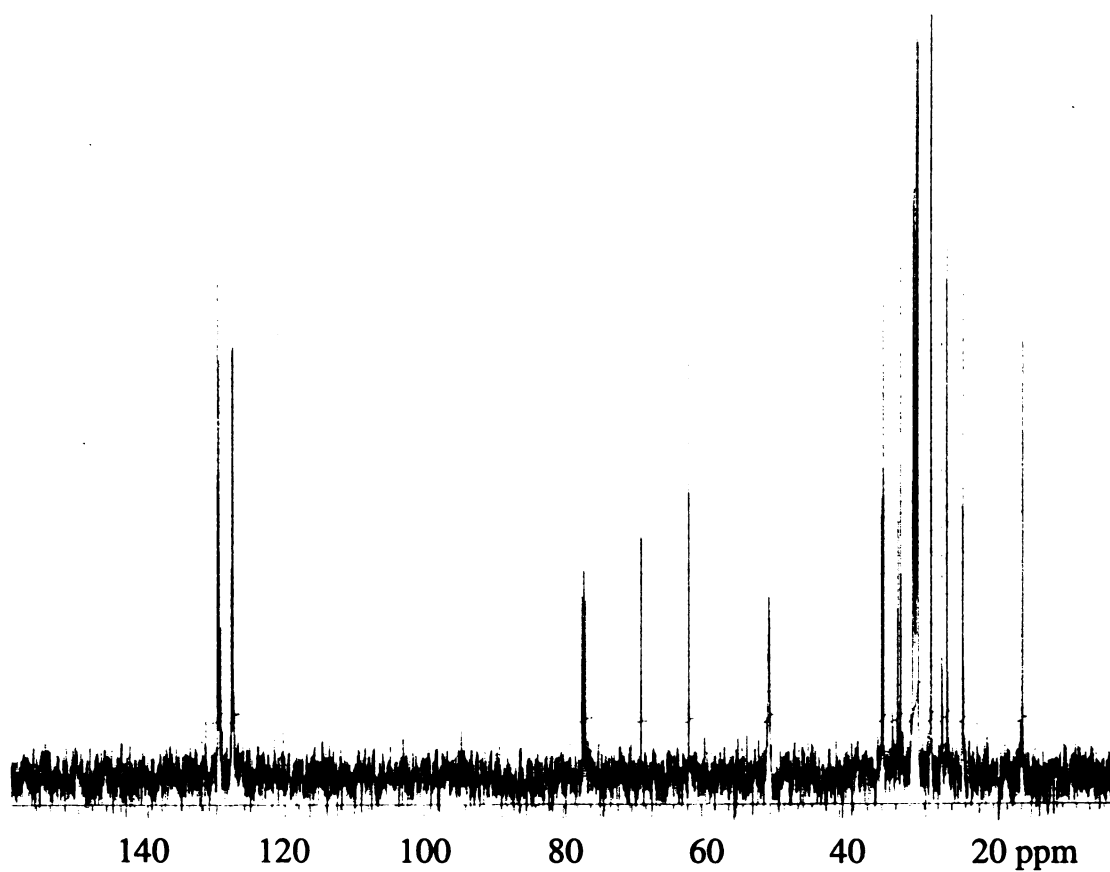


Figure D3: ^{13}C – NMR Spectra of Silylated Soybean Oil

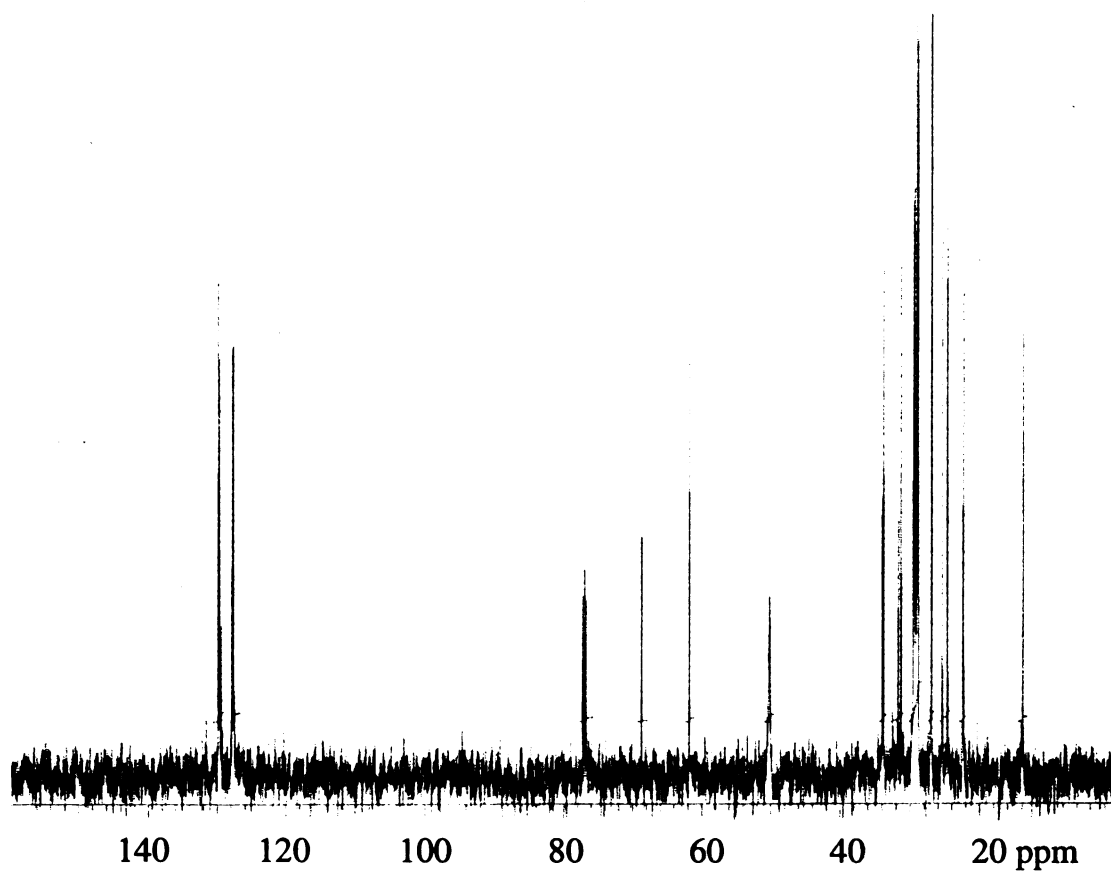


Figure D3: ^{13}C – NMR Spectra of Silylated Soybean Oil

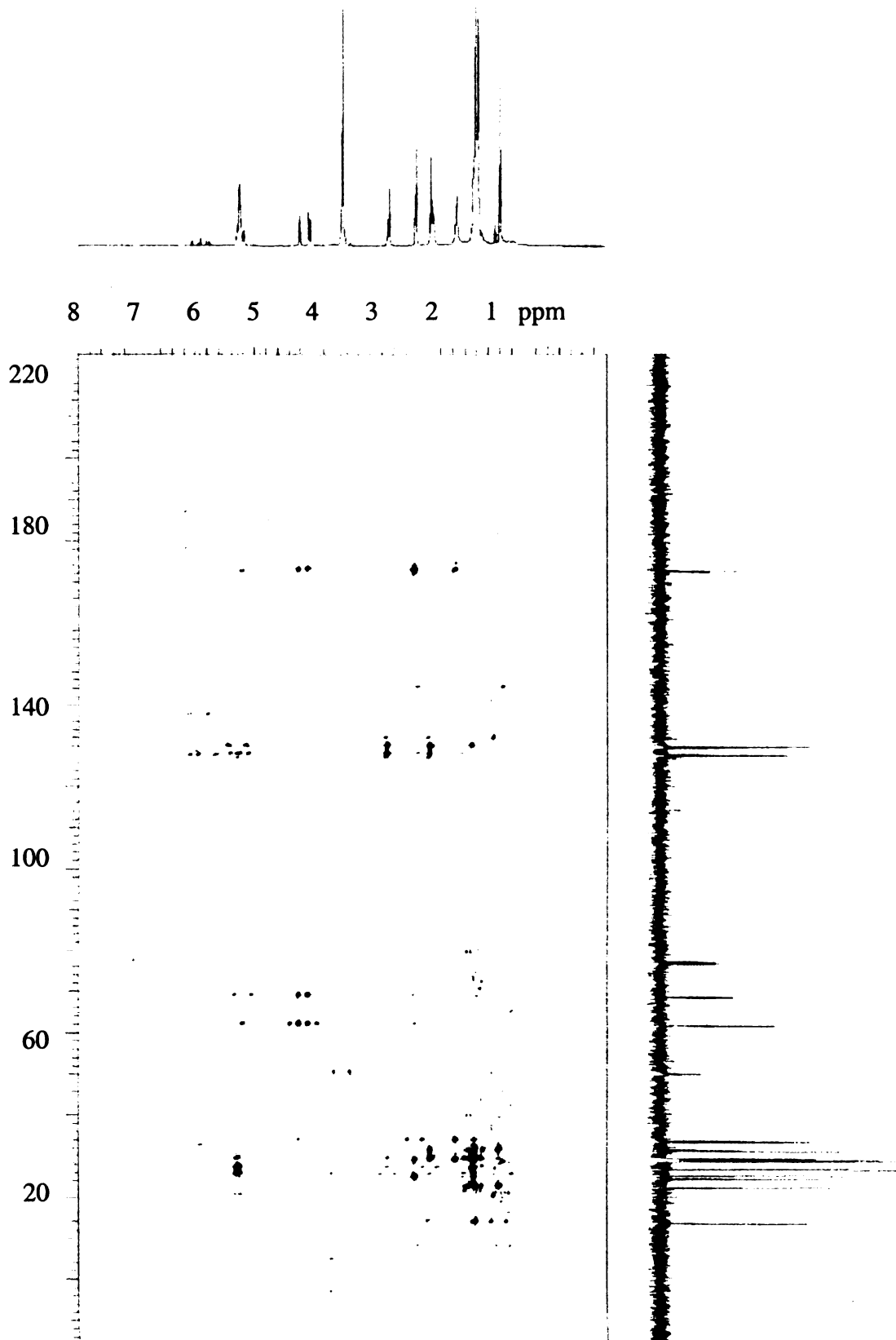


Figure D4: HMBC Correlation Spectrum of Silylated Soy Oil